# Synthesis and characterization of photosensitive ligand for copper complexation and functionalization of UiO-67 MOF

Bjørn Terjei Austenaa


MSc thesis

[60 credits]

Department of Chemistry

UNIVERSITY OF OSLO

Spring 2023

2023

Synthesis and characterization of photosensitive ligand for copper complexation and incorporation into MOFs.

http://www.duo.uio.no/

Print: Grafisk senter, Universitetet i Oslo

# Abstract

This master thesis describes the synthesis and characterization of photosensitive ligands for metal complexation and possibly incorporation into UiO-67 MOF.

It was successfully made two ligands. It was tried to make a third ligand by elongating the $\pi$-system with an alkyne in a Sonogashira reaction, but this was not successful.

The ligands and the intermediate molecules were characterized by NMR spectroscopy and mass spectrometry analysis. Melting points were also measured for most of the intermediates and ligands.

# Preface

The work with this master thesis has been done at the catalysis section at the faculty of chemistry at the University of Oslo between august 2020 and June 2023.

I will first give thanks to my supervisor Associate Professor Mohamed Amedjkouh for good discussions and helping me stay on track and giving many helpful advises and good professional insight in the topic.

I must thank the homogeneous catalysis group, headed by Professor Mats Tilset, for weekly meetings and good feedback from presentations.

I will also thank my office mates and lab coworkers Melchizedek Amoakwah, Atiqa Ambrin Ansar and Paul Arne Sagstad for good discussions and help at the lab.

A thank should also be given to Professor Frode Rise and Senior Engineer Dirk Petersen for running the NMR lab, and Engineer Erlend Steinvik and Sverre Løyland for recording my mass spectrometer analysis.

Last, but not least, I will thank my mother, three sisters and brother for encouraging me to keep going and finishing the project.

Bjørn Terjei Austenaa

Blindern, Juni 2023

# Table of Contents

# I. Abbreviations

| | |
|---|---|
| Ar | Argon |
| br | broad (NMR) |
| COSY | correlation spectroscopy (NMR) |
| d | doublet (NMR) |
| DEPT | distortionless enhancement by polarization transfer (NMR) |
| dppz: | dipyridophenazine |
| dppz-o-Br | 11,12-dibromodipyrido[3,2-a:2',3'-c]phenazine |
| EtOH | ethanol |
| h | hour(s) |
| HMBC | heteronuclear multiple bond correlation (NMR) |
| HOAc | acetic acid |
| HOMO: | highest occupied molecular orbital |
| HRMS | high resolution mass spectrometry |
| HSQC | heteronuclear single quantum coherens (NMR) |
| LUMO: | lowest unoccupied molecular orbital |
| m | multiplet (NMR) |
| min | minutes |
| MOF: | metal organic framework |
| MS | mass spectrometry |
| m.w. | microwave |
| m/z | mass to charge ratio (MS) |
| NaOAc | sodium acetate |
| NaOH | sodium hydroxide |
| NMR | nuclear magnetic resonance |
| OPD: | o-phenylenediamine |
| OPD-Tos: | N,N'-1,2-phenylenebis(4-methylbenzenesulfonamide) |
| Phen: | 1,10-phenanthroline |
| r.t. | room temperature |
| s | singlet (NMR) |
| t | triplet (NMR) |
| Tos | tosylate |
| TosCl: | p-toluenesulfonyl chloride |
| UiO | university of Oslo |

## II. Key compounds

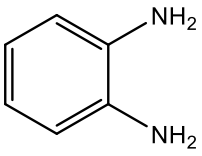


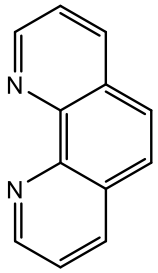


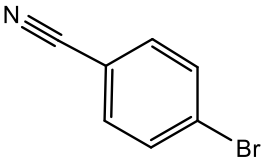


Starting materials

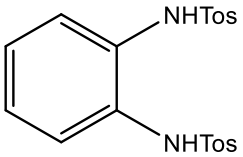


**1**

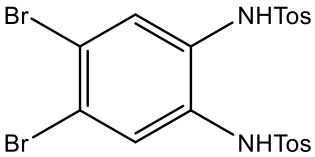


**2**

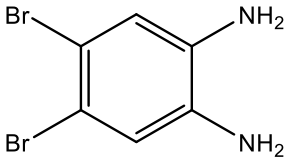


**3**

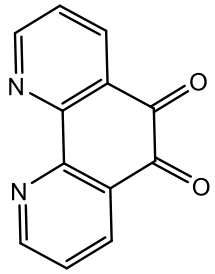


**4**

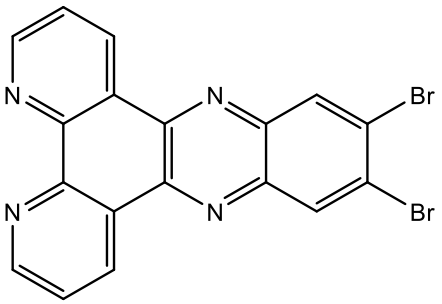


**5**

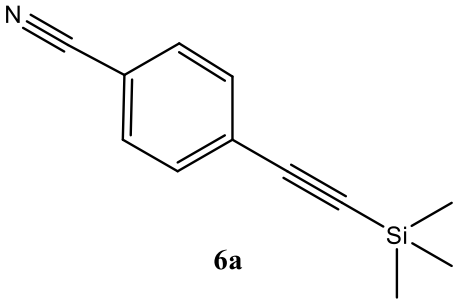


**6a**

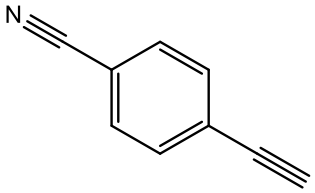


**6b**

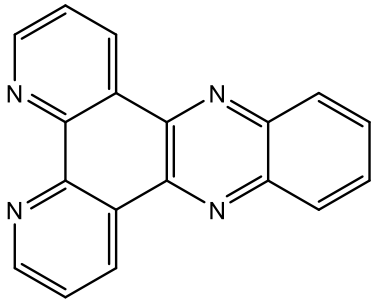


**7**

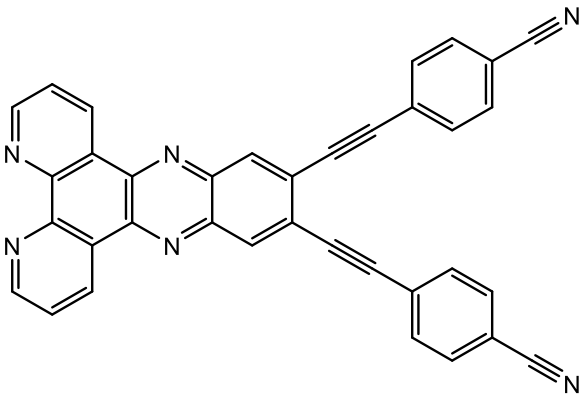


**8**

# III. The aim of the project

The aim of this project was to synthesize photosensitive ligands for copper complexation. A secondary goal was to make copper complexes with the ligands and a bipyridine linker that could be incorporated into a metal organic framework (MOF) such as UiO-67 as shown in Figure 1.

The copper complex could work as a photosensitizer, utilizing the benefits of metal to ligand charge transfer (MLCT) properties.[1] By elongating the $\pi$-system of the ligand could increase the time of the exited state and lower the HOMO – LUMO gap.[2] This could give it better photophysical properties such as greater absorption in the visible region (low energy light) of the electromagnetic spectrum.[2, 3]

A functionalized MOF would not only make the photosensitive molecule heterogeneous but could also give it better photocatalytic properties such as extending the absorption bands of these materials further into the visible region of the spectrum.[4]

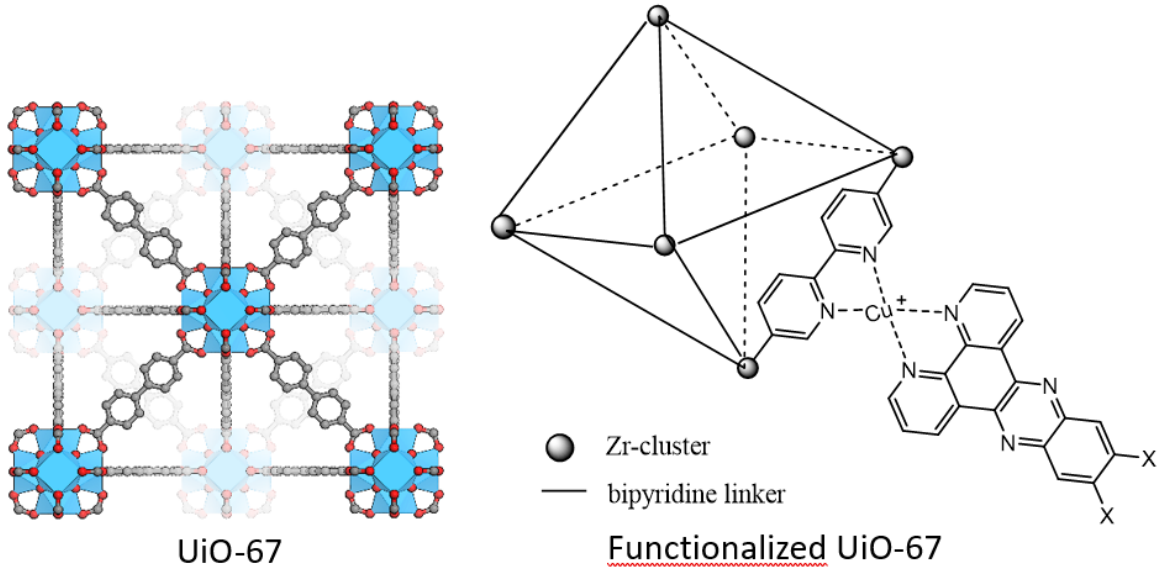


*Figure 1: Illustration of a unit cell of UiO-67 MOF and functionalized UiO-67 by making a copper complex with a photosensitive molecule, copper and a bipyridine linker. X can be an extension of the pi-system with an ethynyl-group or just H or Br for a simpler molecule.*

# 1. Theoretical background

## 1.1 Photosensitizers

Photosensitizers are compounds that absorbs light energy in the purpose of transferring this energy into a photochemical reaction and thereby altering the course of the reaction. [5]

To be able to absorb visible light with low energy it needs a large de-localized pi-system to lower the HOMO-LUMO energy gap. Photosensitizers can be organometallic compounds with electron rich metal centers like iridium[6] and ruthenium[7] complexes, rhodium nanoparticles[8], or naturally compounds like chlorophyll and dyes from plants[9]. Copper complexes are also a promising alternative to the more noble metals used as photosensitizers because they are abundant and less expensive than the more noble transition metals like Iridium and Ruthenium. It has also a stronger reducing power by photoexitation. [10, 11]

## 1.2 Metal complexes

Metal complexes are compounds with metal ions coordinated by ligands. The metals are usually transition metals with incomplete d or f shells.[12] Ligands in metal complexes are usually neutral or anionic substances. Examples of neutral ligands are ammonia, $NH_3$ and carbon monoxide, CO. They are independently stable molecules in their free states. Anionic ligands, such as $Cl^-$, $OH^-$ and $C_5H_5^-$ are stabilized only when they are coordinated to central metals.[12] According to the 18 electron rule neutral ligands are two electron donors to the metal in the complexed state and anionic ligands are one electron donor. [13]

## 1.3 Photocatalysis

In photocatalysis a photosensitive molecule (photosensitizer) or a semiconductor captures photons from UV or visible light. In a semiconductor the electrons are excited from the valence band to the conducting band of the semiconductor. In a photosensitive molecule the electrons are excited in a similar manner but now from the HOMO orbital to the LUMO orbital or a higher orbital and are then available for a reaction.

When the electron is excited to the LUMO-orbital it leaves an electron-void or electron-hole in the HOMO orbital. If the electron quickly returns to this electron-hole the electron cannot participate in any reaction. For a photosensitive molecule to be effective as a catalyst the electron must be separated from this "hole" long enough for a reactant to diffuse into the reactive cite and get the electron transferred. This is often accomplished when an inter system crossing (ISC) occur, where the electron changes spin from a singlet to a triplet state. This is illustrated in a Jablonski diagram (Figure 2) where an electron in a singlet ground state $(S_0)$ (HOMO) is excited to a higher orbital ($S_1, S_2$ or higher) in a singlet state. It then relaxes to the singlet 1 (LUMO) orbital $(S_1)$ by an internal conversion (IC). The electron can then relax to ground state by a new IC where heat is released, by fluorescence where photons are released, or it can have a spin flip to make an inter system crossing (ISC) to a triplet state $(T_1)$. The triplet state is more long lived and makes an electron transfer to a reactant possible. If the electron is not used in a reaction it will relax to ground state through a new ISC that results in phosphorescence where a photon is emitted or by heat radiation.[14]

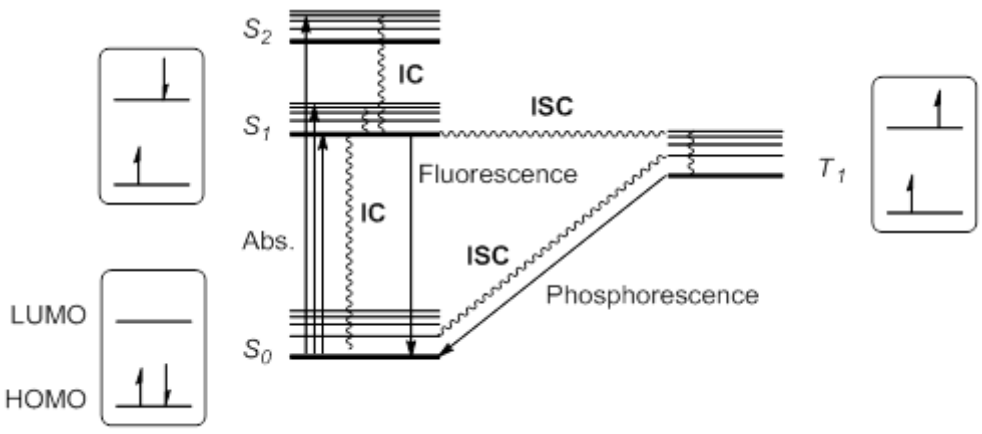


*Figure 2: Jablonski diagram: UV or visible light can excite an electron from the HOMO orbital or ground state $(S_0)$ to the LUMO orbital $(S_1)$ either directly or to a higher orbital $(S_2)$ and then relax to $S_1$ by an internal conversion (IC) where heat is radiated. It can then relax to ground state by emitting heat or fluorescence radiation, or it can have a spin flip and make a inter system crossing (ISC) to a triplet state $(T_1)$. The triplet state is long lived because the relaxation from $T_1$ to $S_0$ is spin forbidden. Because of the longer lifetime, this state can catalyze a reaction by an electron transfer to a substrate. If the electron is not used in a reaction, it will eventually relax to ground state by heat or phosphorescence radiation in a new inter system crossing.[14]*

## 1.4 Charge transfer and charge separation

When an electron is excited from the HOMO to the LUMO orbital and makes an ISC to a triplet state the electron can be transferred from either the metal to the ligand (MLCT) or from the ligand to the metal (LMCT). If the charges is also separated in space it will increase the lifetime of the excited state. For example an electron can be excited from a d- orbital on the metal and transferred to an orbital on the far end of a ligand. [15]

## 1.5 Nuclear magnetic resonance spectroscopy

Nuclear magnetic resonance spectroscopy (NMR) is a valuable tool for structure elucidation in chemistry. It utilizes the spinning property of nucleus with a magnetic moment. Only the nucleus of some isotopes of atoms have a magnetic moments such as $^{1}$H, $^{13}$C, $^{19}$F, $^{31}$P and $^{15}$N. The magnetic moment makes them into tiny magnets and can therefore interact with an external magnetic field.

When an external magnetic field ($B$) is applied to a molecule, the nucleus aligns themselves either parallel or antiparallel to the magnetic field. The parallel orientation has a slightly lower energy than the antiparallel orientation, so most nuclei align themselves in this way. The stronger the magnetic field the larger the energy gap between the orientations will be.

When the nuclei in a magnetic field are irradiated with electromagnetic radiation with a frequency that corresponds to the energy difference between the orientations, the nuclei will absorb the energy and a spin-flip from the parallel to the antiparallel orientation will happen.

Nuclei in different chemical environment will experience different amount of shielding from the electron cloud surrounding them. The electrons functions as tiny magnets that works opposed to the applied magnetic field. This local magnetic field causes the effective magnetic field the nuclei experiences to be lower than the applied magnetic field. This can be shown with the equation:

$$B_{effective} = B_{applied} - B_{local}$$

Because of different electron density around nuclei in different chemical environment, the nuclei will spin-flip at different frequencies. This makes it possible to make a absorption spectrum. The frequencies applied are converted into the unit Chemical shift ($\delta$).[16]

### 1.5.1 Spin – spin Splitting

Neighboring nuclei that are not in the same electronic identical environment will give a perturbation in the chemical shift. For example for a proton that can have two different spins, one aligned with the applied field and one against. A neighboring nuclei wil then experience either an increased magnetic field or a decreased magnetic field. This gives two signals in the spectrum. WE say that the signal has been split into two peaks or a doublet (d). In the same way signals can be split into three, a triplet (t), four - a quartet (q) and so on. More complex splitting patterns are usually called a multiplet (m).[16]

### 1.5.2 Isotopes of elements to use in NMR

The most common isotopes to use in NMR in organic chemistry are $^{1}$H, $^{13}$C, $^{19}$F and $^{31}$P because of their usefulness in structure elucidation and their relative abundance. Nitrogen is more difficult to use in NMR, because the most common isotope $^{14}$N with 99.6 % abundance is not NMR active. The NMR active $^{15}$N isotope has a relative abundance of only about 0.4 % and in combination with other properties gives it a very low signal to noise ratio in NMR and a very long sampling time even in a high magnetic field. To use nitrogen in NMR effectively it is usually necessary to enrich the molecules with $^{15}$N.

The carbon NMR active isotope $^{13}C$ has also a low relative abundance of only 1.1 % compared to $^{1}H$, $^{19}F$ and $^{31}P$ with almost 100 % relative abundance. This means to get a good signal from $^{13}C$ in NMR it is needed longer sampling time (1 hours, 1024 scans, 400 MHz) and more sample than with $^{1}H$, $^{19}F$ and $^{31}P$ (2 minutes, 16 scans, 400 MHz

### 1.5.3 Two-dimensional (2D) NMR

2D NMR spectra measure the coupling between two nuclei at the same time. This can be nuclei of the same type or different type. Some common 2D NMR techniques are $^{1}H$ – $^{1}H$ COSY, $^{1}H$ – $^{13}C$ HSQC, $^{1}H$ – $^{13}C$ HMBC, $^{1}H$ – $^{1}H$ NOESY.

### 1.5.4 Distortions Enhancement by Polarization Transfer (DEPT)

DEPT NMR distinguishes $^{13}C$ atom according to how many protons are attached. There are different types of DEPT techniques. DEPT 90 shows CH up and C down, and cancels $CH_2$ and $CH_3$. DEPT135 shows CH and $CH_3$ up and C and CH down.[17]

### 1.5.5 Correlation Spectroscopy (COSY)

COSY is a 2D NMR technique to determine $^{1}H$ - $^{1}H$ correlations. The two axes in the spectrum shows identical proton 1D spectra. The peaks at the axes are also shown on the diagonal as diagonal peaks. The peaks of interest are those off the diagonal, called the cross peaks. They come in pairs one above and one below the diagonal symmetrically. The cross peaks shows correlations between protons of usually two or three bonds distance, but can be longer also. [18]

### 1.5.6 Heteronuclear Single-Bond Correlations (HSQC)

HSQC is a 2D NMR technique to show one-bond correlations between two attached heteronuclei, usually $^{1}H$ to $^{13}C$ or $^{15}N$. Each correlation shows a crosspeak in the 2D spectrum. For example with a $^{1}H$ - $^{13}C$ HSQC spectrum proton signals can be assigned to carbon signals. Geminal protons can easily be identified because they will show a cross peak to the same carbon. This can be difficult with a COSY spectrum. It can also help resolve overlapping proton signals by dispersing them over the carbon spectrum. This is especially useful for larger molecules such as proteins where both $^{1}H$ – $^{13}C$ and $^{1}H$ – $^{15}N$ HSQC is used. [19]

### 1.5.7 Heteronuclear Multiple-Bond Correlations (HMBC)

HMBC shows a 2D spectrum of the couplings between two heteronuclei, as for HSQC, but with a distance of two or three bonds. It is usually used for proton-carbon correlations and is a very useful tool for elucidating the structure of a molecule. [19]

### 1.5.8 Nuclear Overhauser Effect Spectroscopy (NOESY)

NOESY shows through-space correlations in contrast to COSY, HMBC and HSQC which shows correlations through bonds. NOESY can be very useful in determining stereochemistry in molecules that have two or more stereoisomers.[20]

## 2. Results and discussion

Two ligands were successfully synthesized (5, 7) while a third (8) were attempted. The synthesis routes are shown in Figure 3. A discussion of each reaction and characterization by NMR follows below.

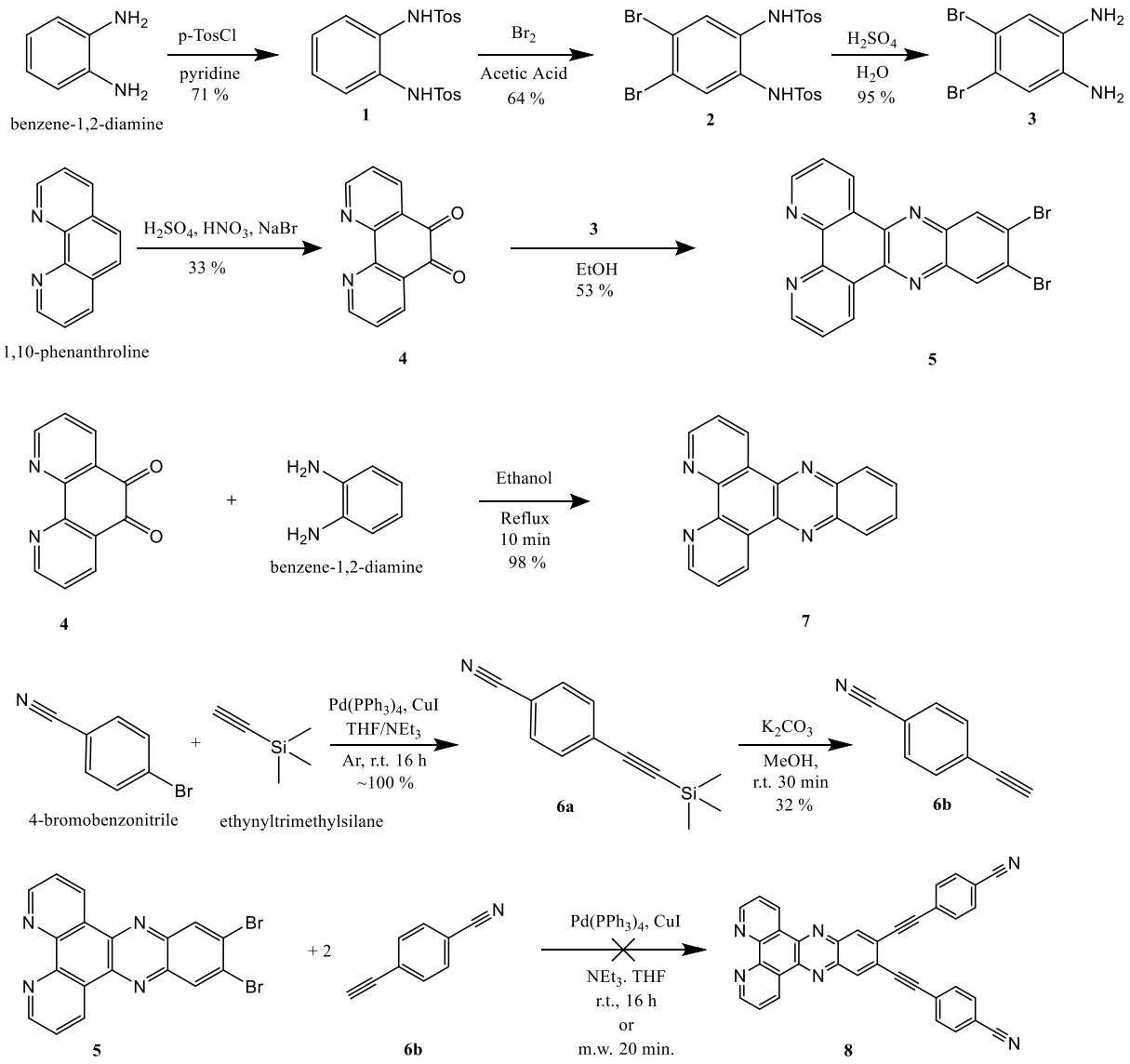


*Figure 3: Synthesis route to make the ligands **5**, **7** and **8**.*

## 2.1 Synthesis of N,N'-1,2-Phenylenebis(4-methylbenzenesulfonamide) (**1**)

The first reaction was to add protecting groups to the amino groups. The reaction scheme for synthesizing **1** is shown in Figure 4. The numbering indicates positions of carbons and protons used in characterization of NMR peaks of **1**.

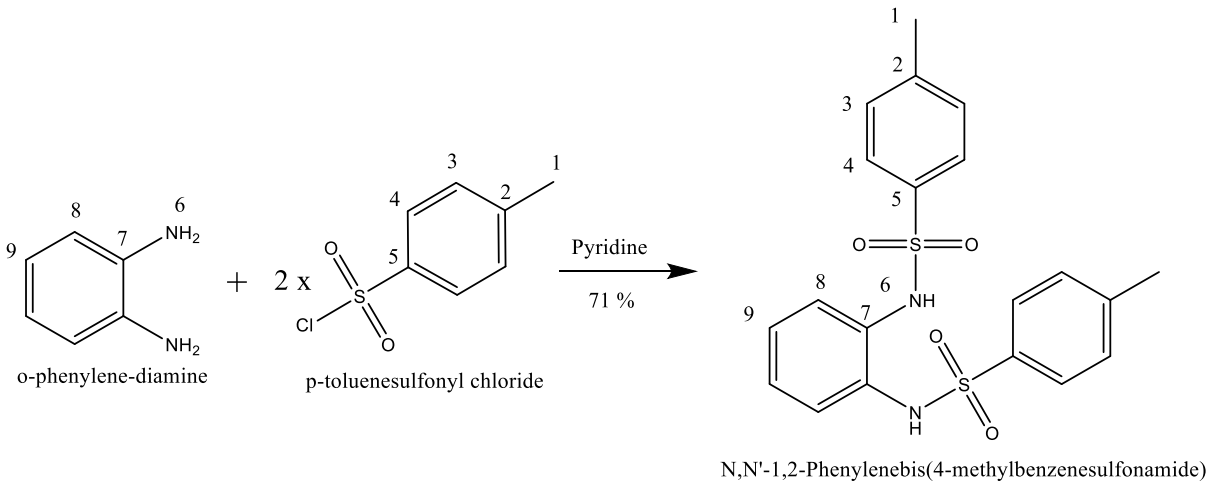


*Figure 4: Reaction scheme with reactants, product and numbering of positions with carbons and protons.*

The reaction was done according to two protocols found in literature by Oloyede et al. and Shao et al.[21, 22] with some modifications. In the first protocol the reaction was done in a microwave while in the second protocol the reaction was accomplished at room temperature by stirring for 18 hours. The microwave reaction was done mostly according to literature[21] but had to be done in two batches because of the small size of the microwave vial. It was also necessary to add more pyridine to avoid precipitation before transferring the second batch to the microwave vial. When the reactants were added to the pyridine it became very hot so it should probably have been cooled on ice-bath, as was done in [22]. The filtering on silica gel was not very successful. Too much of the product got stuck on the silica and clogged the column. Only 0.3 g and a yield = 2 % of product was isolated from the white cloudy eluate that was able to pass through before it was clogged. The filtration could probably have gone better if the crude had been dissolved in more eluent, but this was not tried. To isolate more of the product stuck on the column, we added vacuum suction to pull the rest of the eluent through the silica gel. We added also more eluent to get as much as possible through the clogged column. Then another work up protocol from literature [22] was used. This consisted of adding HCl that made a precipitate, dissolving in ethanol and filtering off the product. This gave an extra 6.0 g (yield = 36 %) of product, and a total of 6.3 g (yield = 38 %). Because we found the workup reported for the microwave reaction a bit difficult and the limited amount that could be synthesized in each batch in the microwave, we chose to use the 18 hours stirring method reported by Shao et al.[22] for a second larger batch. This worked very well and gave a yield of 71 %.

## Characterization of 1

A comparison of the $^{1}$H NMR spectra of the two reactants OPD and TosCl, and the product OPD-Tos (Figure 5) show that the peaks in the spectra from the reagents appear in the product spectra with some change in position. The methyl group (1) and the aromatic protons (3,4) on TosCl moves a bit upfield, and the aromatic protons (8,9) and amino protons (6) on OPD move downfield. The amino protons (6) are visible as a singlet at the upfield side of the multiplet.

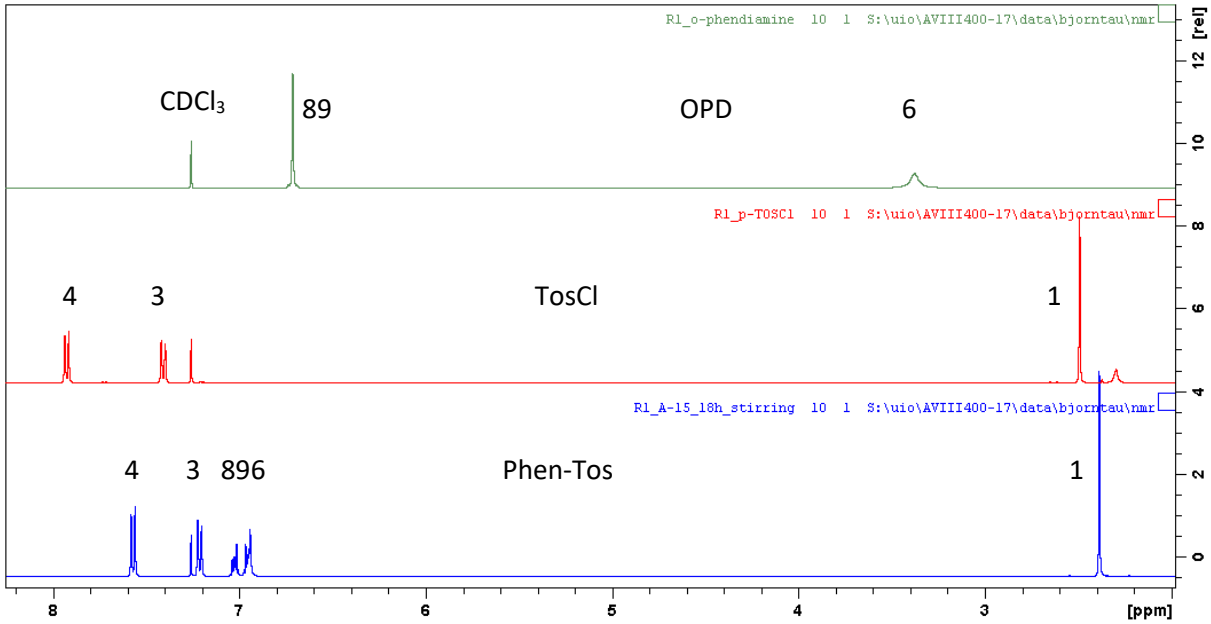


*Figure 5: $^1$H NMR (400 MHz, CDCl3) of the two reactants OPD and TosCl, and the product OPD-Tos.*

Figure 6 shows a closer look at the proton spectrum with the peaks assigned to the different protons in the product. It is only one peak in the aliphatic region which integrates to 6H. This agrees with the two equivalent methyl groups at 1. The two "doublets" from protons 3 and 4 agrees with an AA'XX'-spin system of a para di-substituted benzene ring according to Pople notation for second-order spin coupling systems [23]. The doublet most low field is assigned to 4 because this is closest to the electron withdrawing $SO_2$-group and resonance indicates a positive charge on carbon 4 (and 2) and negative charge on the oxygen. The two multiplets at 7.05 – 6.05 and 6.98 – 6.92 ppm looks like a complex AA'BB' system and must belong to the protons at 8 and 9. The signal have changed from something that resembles a singlet to a complex multiplet. The integral and form of the most upfield multiplet indicates that it contains a singlet of 2H at 6.94 ppm that can correspond to the amino proton at 6. It is not possible to decide which multiplet proton 8 and 9 belongs to, but 8 is chosen to be most downfield because it is closer to the nitrogen atom than the proton at 9.

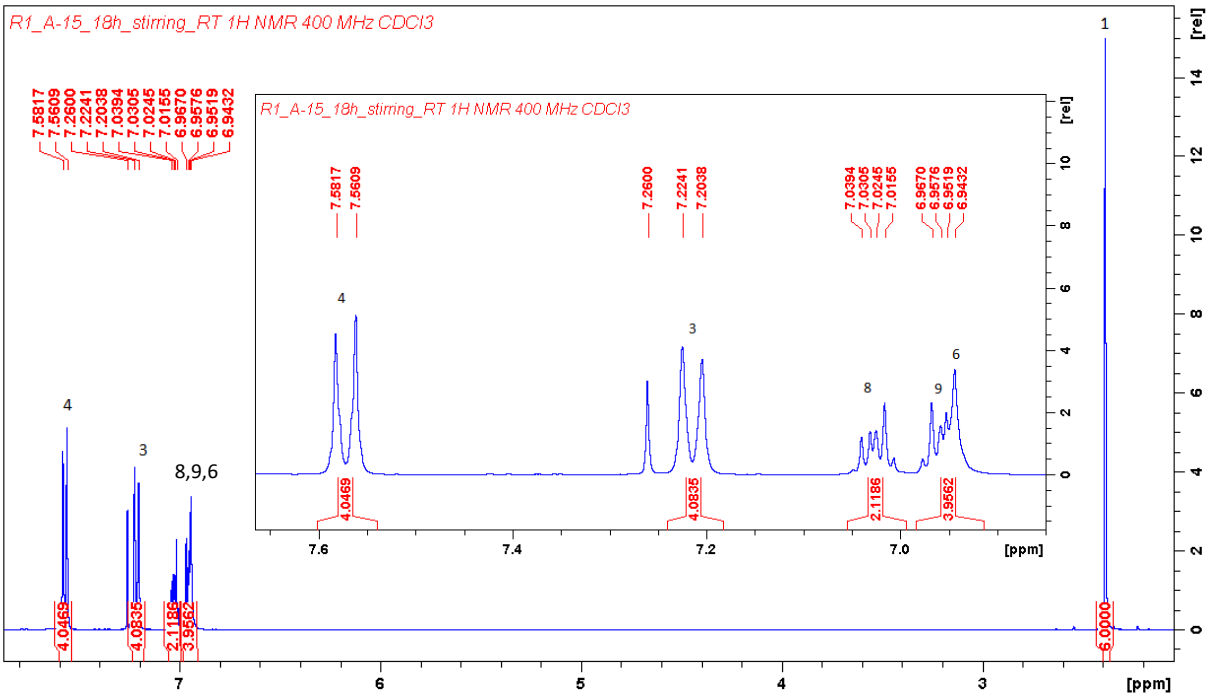


*Figure 6: 1H NMR (400 MHz, CDCl3) of OPD-Tos with inserted excerpt of the aromatic region. δ ppm = 7.57 (d, J = 8.3 Hz, 4 H), 7.21 (d, J = 8.1 Hz, 4 H), 7.05–6,05 (m, 2 H), 6.95–6.92 (m, 2H), 6.94 (s, 2H), 2.39 (s, 6 H).*

The COSY spectrum (400 MHz, CDCl3) (Figure 7) shows the $^{1}H$-$^{1}H$ correlations: 1,3 and 3,4 and 8,9. This confirms the assignment of peaks 1, 3 and 4 to TosCl and 8 and 9 to OPD.

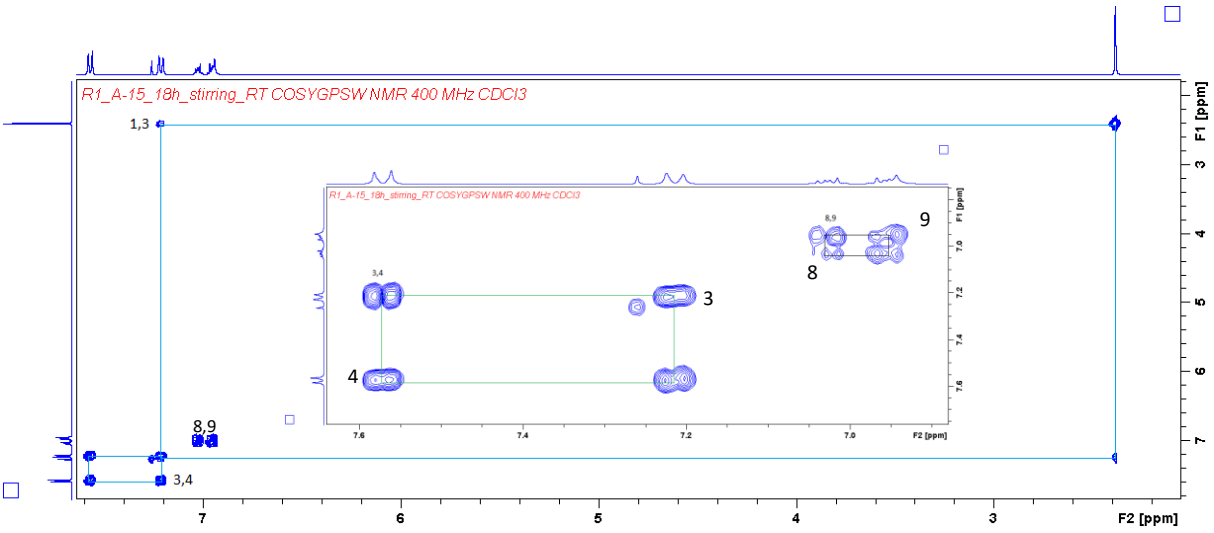


*Figure 7: COSY NMR (400 MHz, CDCl3) with $^{1}H$-$^{1}H$ correlations: 1-3, 3-4 and 8-9 with excerpt of the aromatic region.*

HSQC of **1** (Figure 8 and Figure 9) shows one bond correlations between protons and carbons. This identifies the signals for carbons (ppm) 1 (21.58), 3 (129.60), 4 (127.52), 8 (127.31) and 9 (126.09).

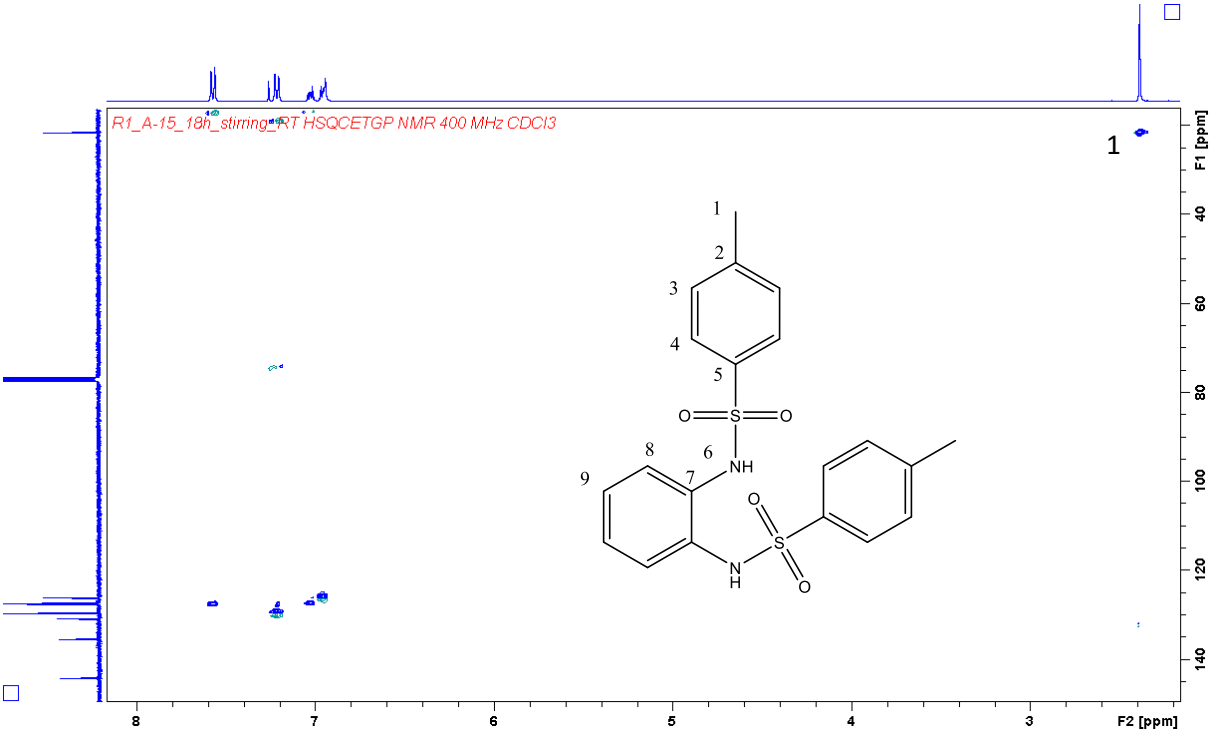


*Figure 8: HSQC $^{1}H$ - $^{13}C$ NMR (400MHz - 100 MHz, $CDCl_3$) of **1**.*

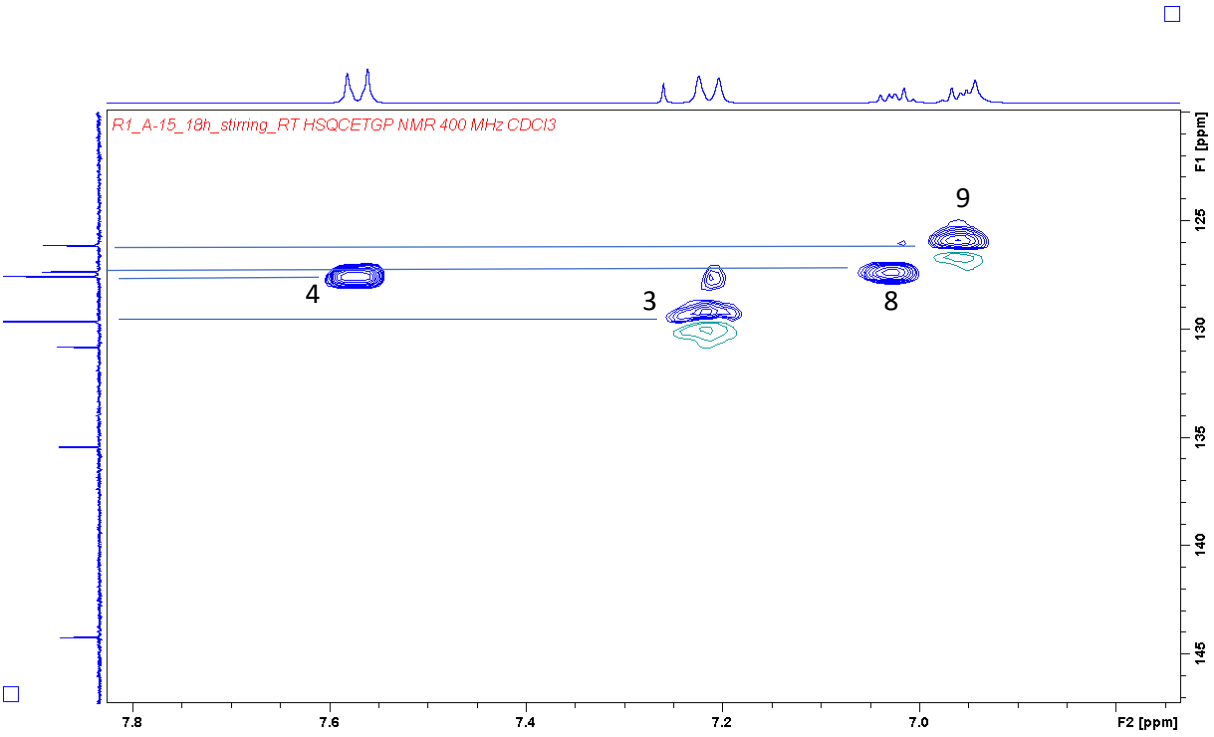


*Figure 9: HSQC $^{1}H$ - $^{13}C$ NMR (400MHz - 100 MHz, $CDCl_3$) of aromatic region of **1**.*

$^{1}H$ - $^{13}C$ HMBC (Figure 10 to Figure 12) shows two- and three-bond correlations. Figure 10 shows a three-bond coupling from $H^3$ to $C^1$ (21.58 ppm). This confirms the earlier assigned order of $H^3$ more upfield than $H^4$ in the proton spectrum. Figure 12 shows a closer look at the aromatic region, and

reveals couplings from $H^4$ to $C^3$ and $C^5$, $H^3$ to $C^4$ and $C^2$, $H^8$ to $C^9$ and $C^7$ and $H^9$ to $C^8$. This completes the assignments of the $^{13}C$ peaks to positions in **1** shown in Figure 13.

A summary of the assignments of $^1H$ and $^{13}C$ NMR peaks to positions in **1** are shown in Table 1**.**

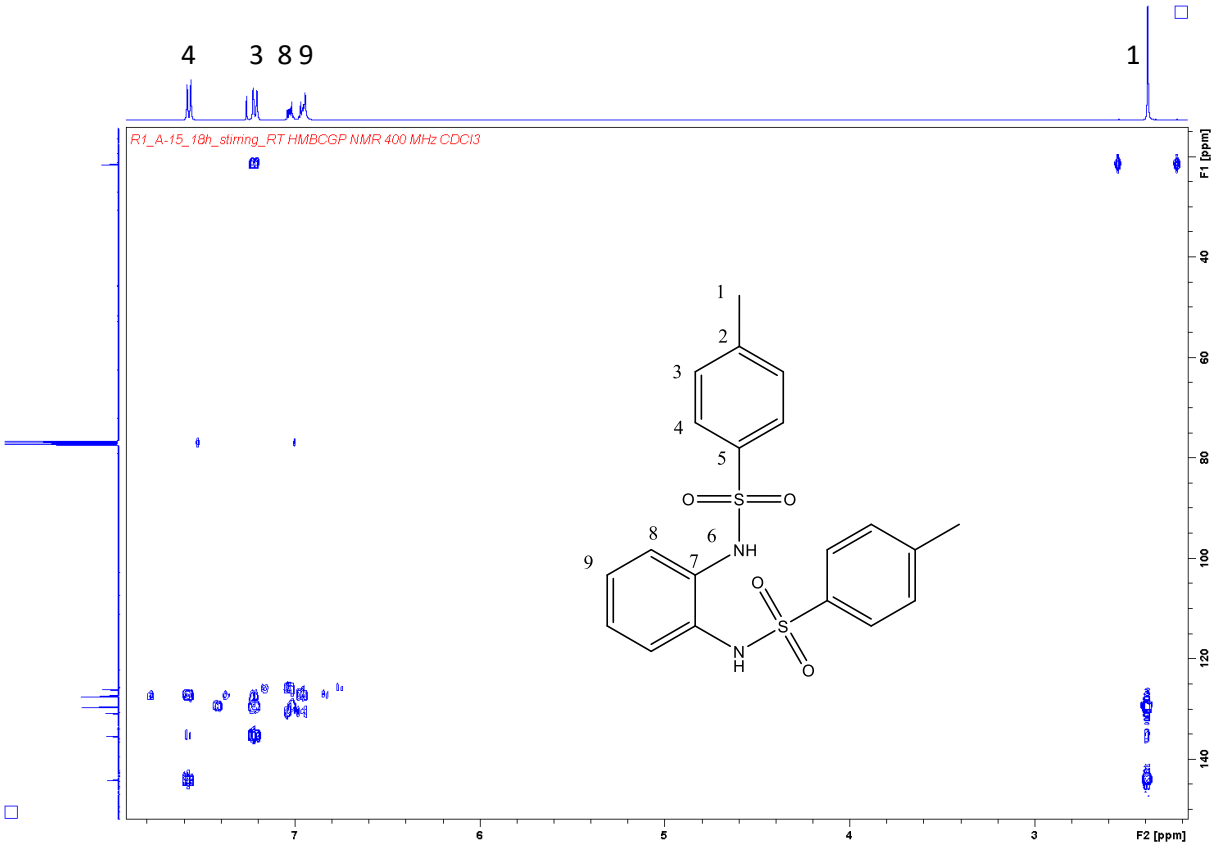


*Figure 10: $^1H$ - $^{13}C$ HMBC (100 / 400 MHz, $CDCl_3$) of **1**.*

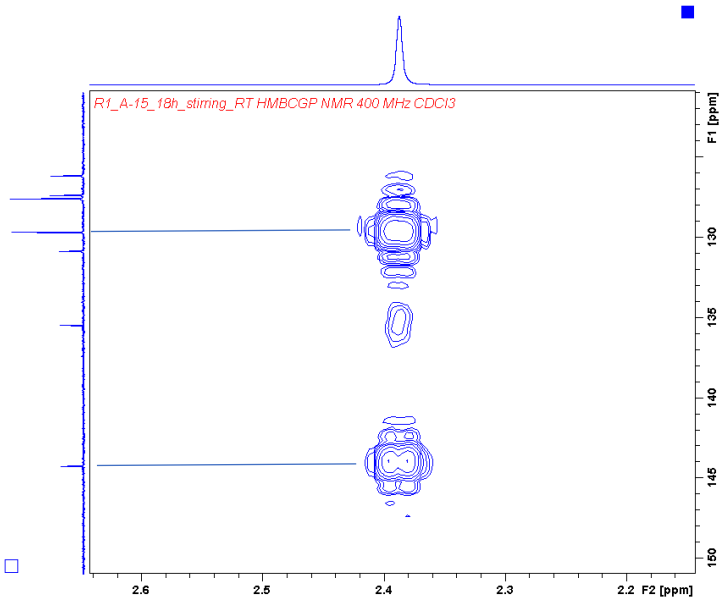


*Figure 11: The HMBC of **1** shows correlations for $H^1$ to $C^4$, $C^2$ (weak) and $C^5$.*

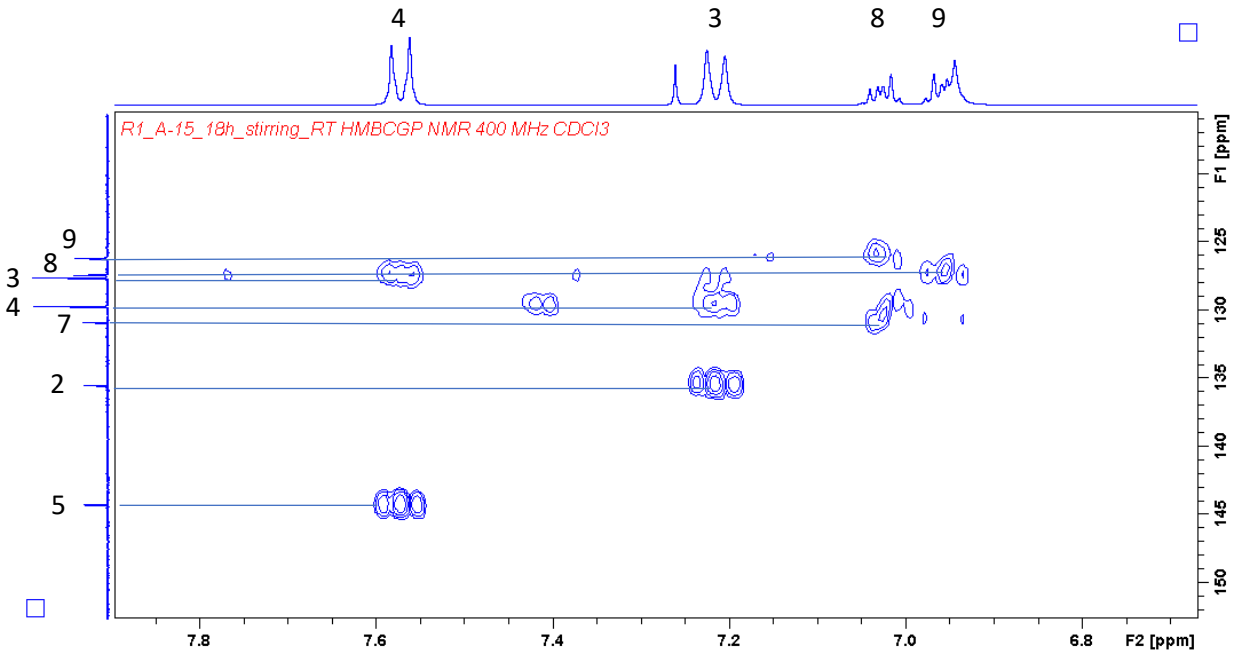


*Figure 12: $^{1}H$ - $^{13}C$ HMBC (100 / 400 MHz, $CDCl_3$) of aromatic region (weak) of **1**.*

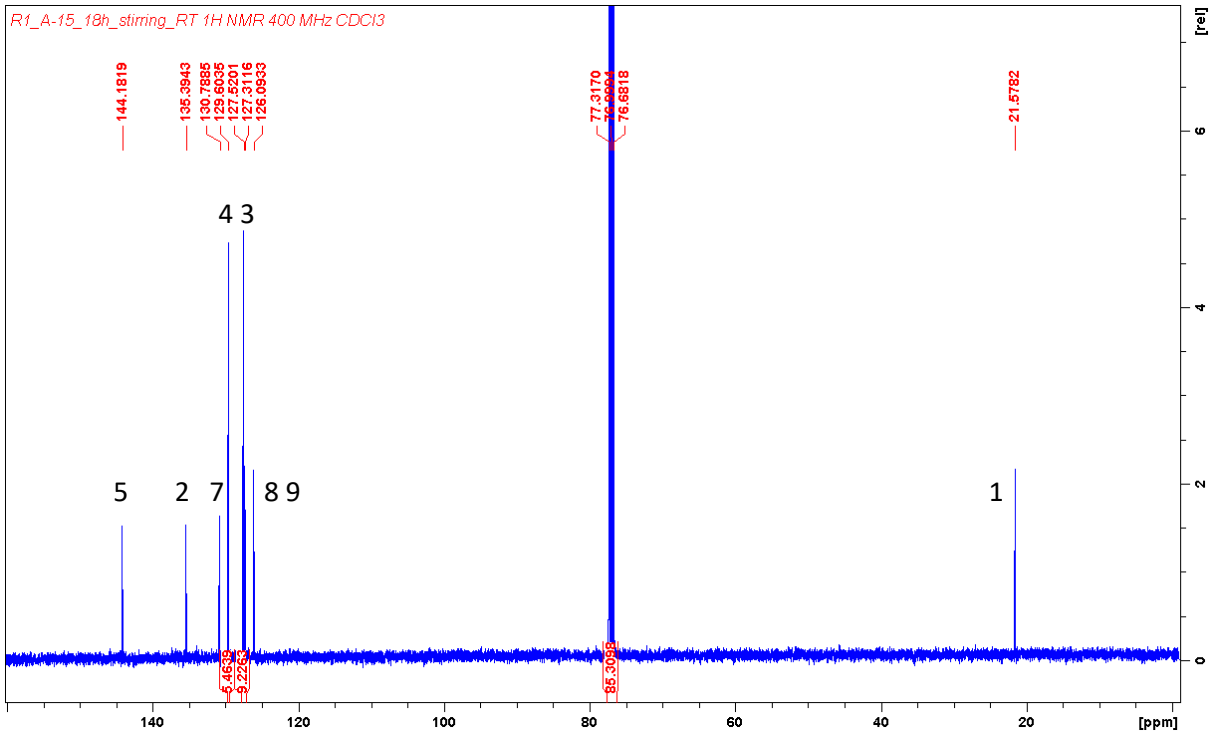


*Figure 13: $^{13}C$ NMR (100 MHz, $CDCl_3$) of **1** δ ppm = 144.18, 135.39, 130.79, 129.60, 127.52, 127.31, 126.09, 21.58.*

*Table 1: Assignments of $^{1}H$ and $^{13}C$ peaks to positions in **1**.*

| Position | $^{1}H$ (ppm) | $^{13}C$ (ppm) |
|---|---|---|
| 1 | 2.39 (s, 6 H) | 21.58 |
| 2 | | 135.39 |
| 3 | 7.21 (d, J = 8.1 Hz, 4 H) | 127.52 |
| 4 | 7.57 (d, J = 8.3 Hz, 4 H) | 129.60 |
| 5 | | 144.18 |
| 6 | 6.94 (s, 2H) | - |
| 7 | | 130.79 |
| 8 | 7.05–6,05 (m, 2 H) | 127.31 |
| 9 | 6.95–6.92 (m, 4 H) | 126.09 |

## 2.2 Synthesis of N,N′-(4,5-Dibromo-1,2-phenylene)bis(4-methylbenzenesulfonamide) (**2**)

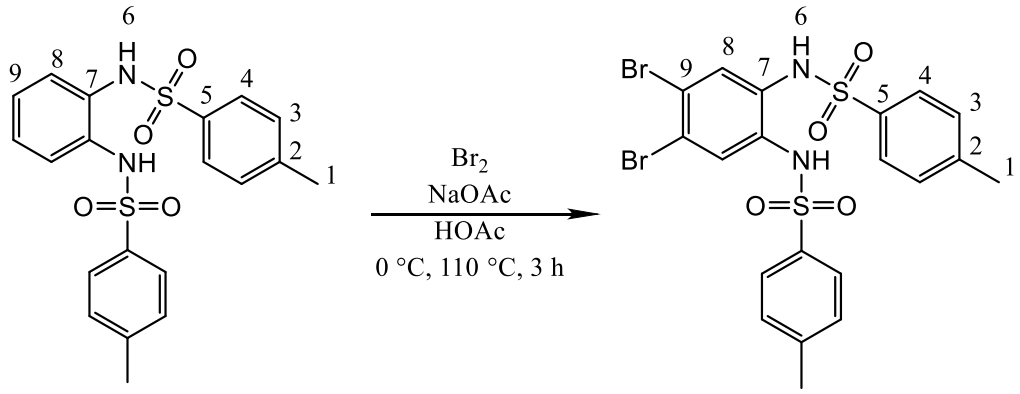


*Figure 14: Reaction scheme for **2** with bromine.*

The product was synthesized with two methods. The first method followed procedure to Shao et al. [22] with bromine. This worked well when the bromine was transferred dropwise with a syringe. Because of its volatile property using a syringe was an effective way to transfer bromine to the reaction without losing amounts in the process. It was also helpful to keep the bromine cool in the fridge. A yield of 64 % was achieved. Characterization of this product is shown below in Figure 18 to Figure 24.

Because of bromines toxicity and volatility we tried out a method based on Khrustalev et al. [24] with the salts NaBr and $KBrO_3$ as substitutes for bromine. The reaction was done in glacial acetic acid without the base NaOAc as shown in Figure 15.

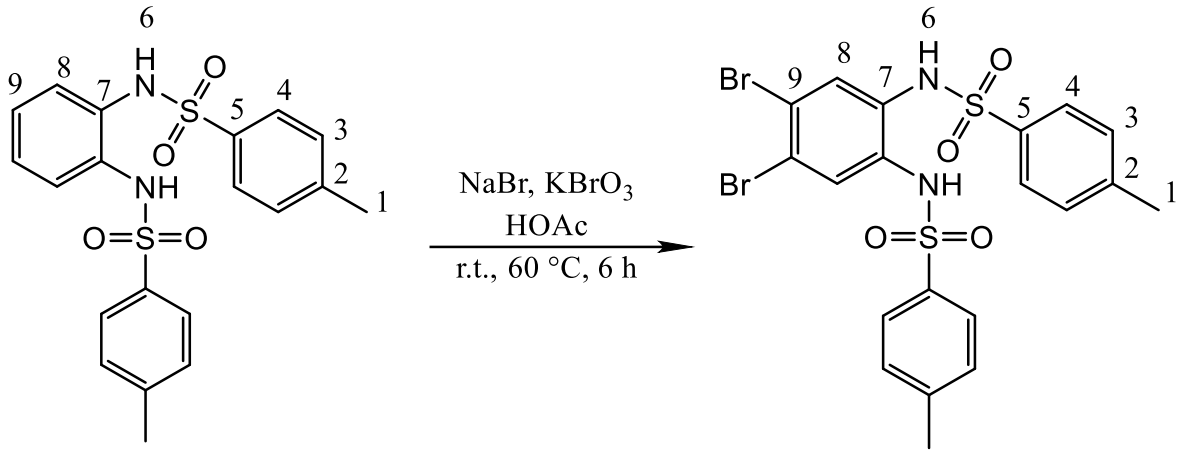


*Figure 15: Alternative reaction scheme for **2** with NaBr and $KBrO_3$.*

This method gave a partial conversion with a side product in addition to the desired product. The reaction is analyzed for conversion in Figure 16. From bottom and up it shows $^1$H NMR peaks for the starting material **1**, then the conversion after 4 h, 6 h and 8 h reaction time. On top is the desired product **2** from the reaction with bromine. We can see that after 4h the side product **x** is formed and the peaks for 1 at about 6.25 to 7.5 ppm is gone. The peak from **1** at about 7.2 is reduced but not completely gone. After 6 h the peaks for **2** are formed fully but the peaks for the side product were still there. After 8 h it was no change from 6 h. The conversion ratio of product to side product is 5 : 1 calculated from the integrals of the peaks at b and a.

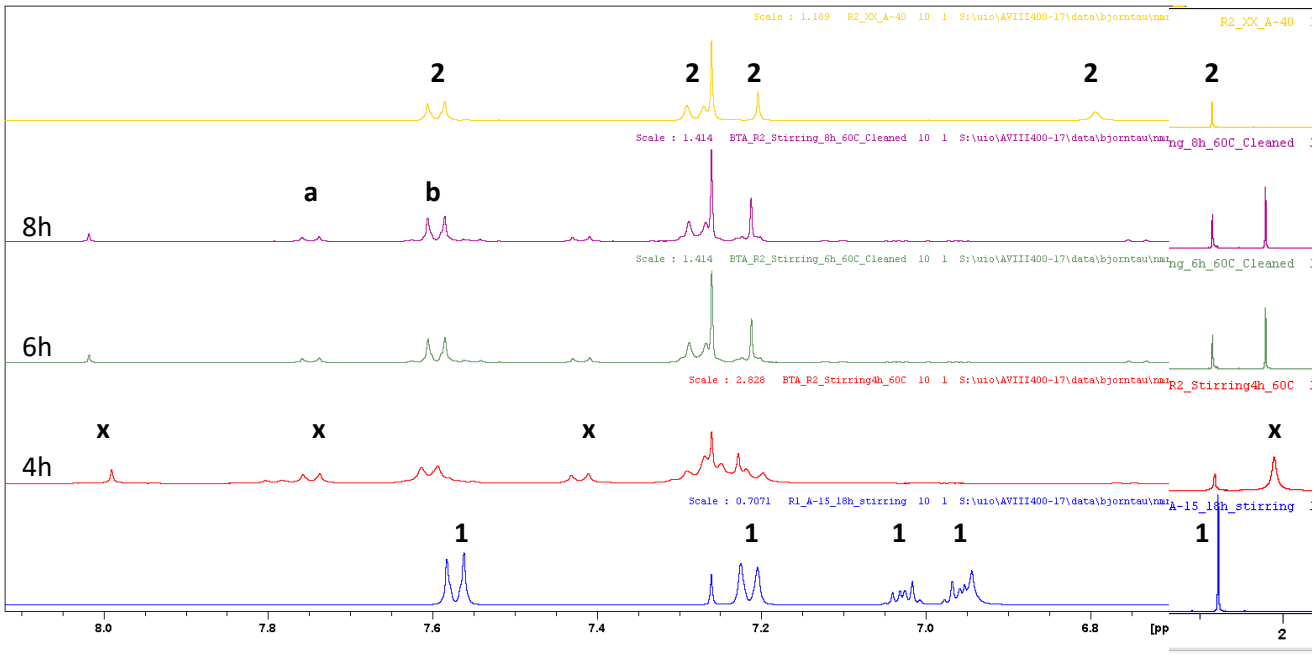


*Figure 16: The spectra shows the $^1$H NMR (400 MHz, $CDCl_3$) of the aromatic region and aliphatic region for the conversion of **2** for the method with NaBr and $KBrO_3$. From bottom: starting material **1**, after 4 h, 6 h, 8 h and top compound **2** from the reaction with $Br_2$. Full spectra is shown in Figure 67 in the appendix.*

The method NaBr and $KBrO_3$ could be developed further by tuning the reaction conditions for getting a more selective conversion. For example, using a lower temperature while adding the reagents in small portion and adding the weak base NaOAc could be tried to see if this would reduce the

formation of the side product. This would also make the conditions more similar to that used by Shao et al [22] in the first method.

## Characterization of 2 from the first method with bromine

Molecule **2** with numbered positions is shown in Figure 17.

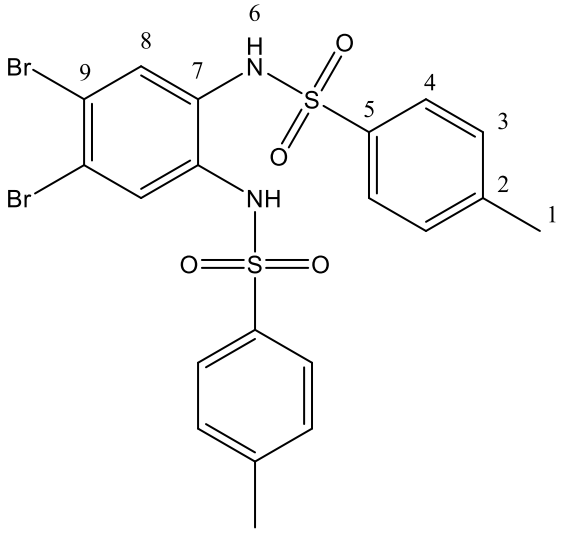


*Figure 17: N,N'-(4,5-Dibromo-1,2-phenylene)bis(4-methylbenzenesulfonamide) with numbered positions.*

The determination of the peaks from $^{1}$H NMR (Figure 18) is very similar to **1** but the multiplet for proton 8, 9 and 6 have been changed to a singlet for proton 8 at 7.20 ppm (2H) and a broader singlet for 6 at 7.79 ppm (2H). The singlet at 2.42 ppm integrates to 6 and must be the two methyl groups at position 1.

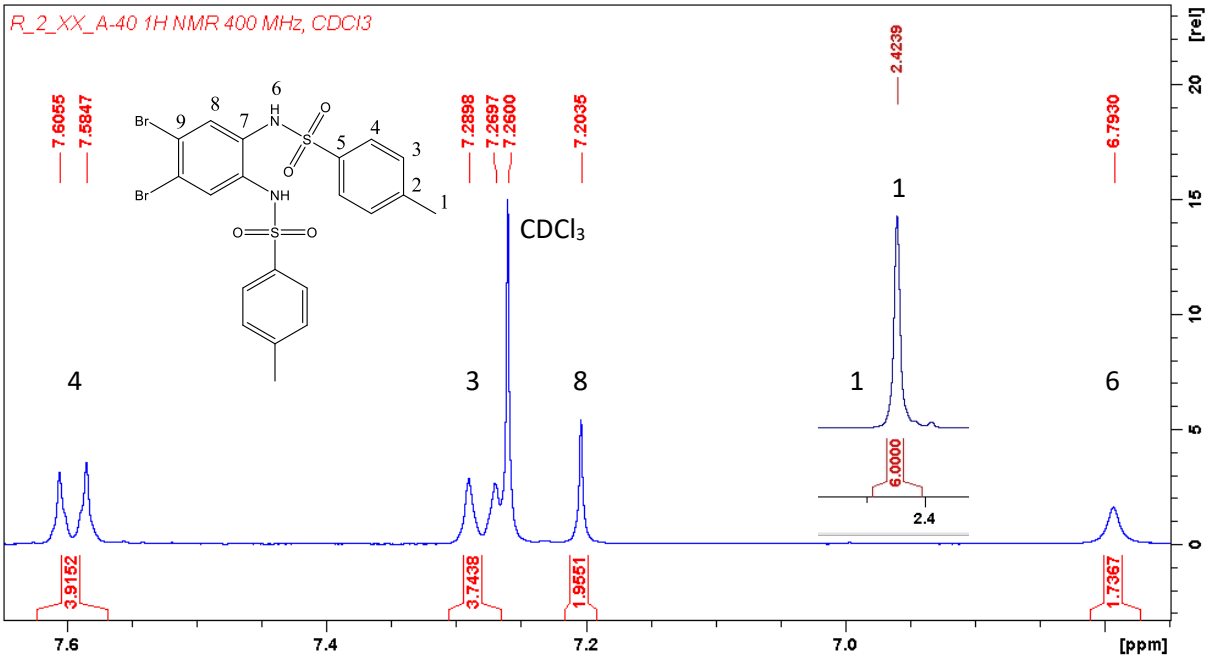


*Figure 18: 1H NMR (400MHz, CDCl3): 1: methyl group on 4-methylbenzenesulfonamide; 3,4: AB system, 8: proton on 4,5-Dibromo-1,2-phenylene; 6: N-H.*

$^{1}$H-$^{1}$H COSY spectrum (Figure 19 and Figure 20) shows $^{3}$J and $^{4}$J correlation. The singlet at 2.42 ppm is coupled to the doublet at 7.28 ppm so this must be $H_3$. It further shows a coupling between the

doublet at 7.28 ppm and 7.60 ppm so the latter must be $H^4$. There is no couplings for $H^8$ and $H^6$ as expected since they have no neighbor protons.

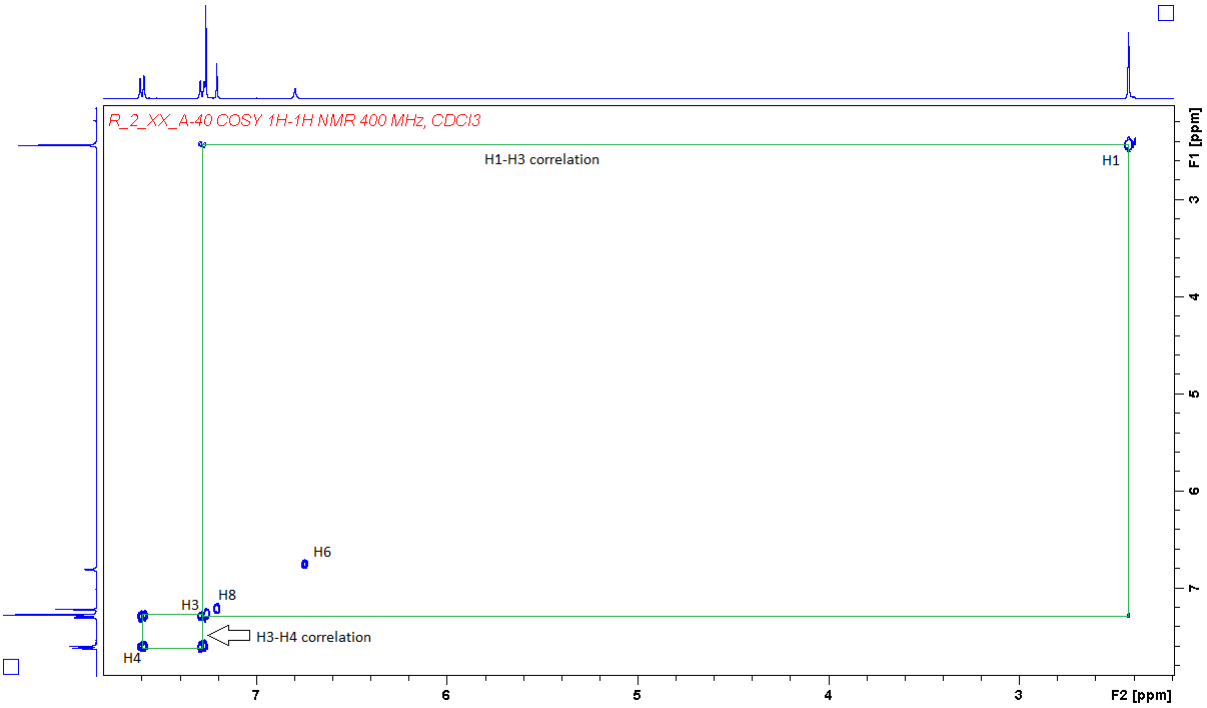


*Figure 19: $^1$H-$^1$H COSY shows correlations between $H^1$ and $H^3$, and $H^3$ and $H^4$.*

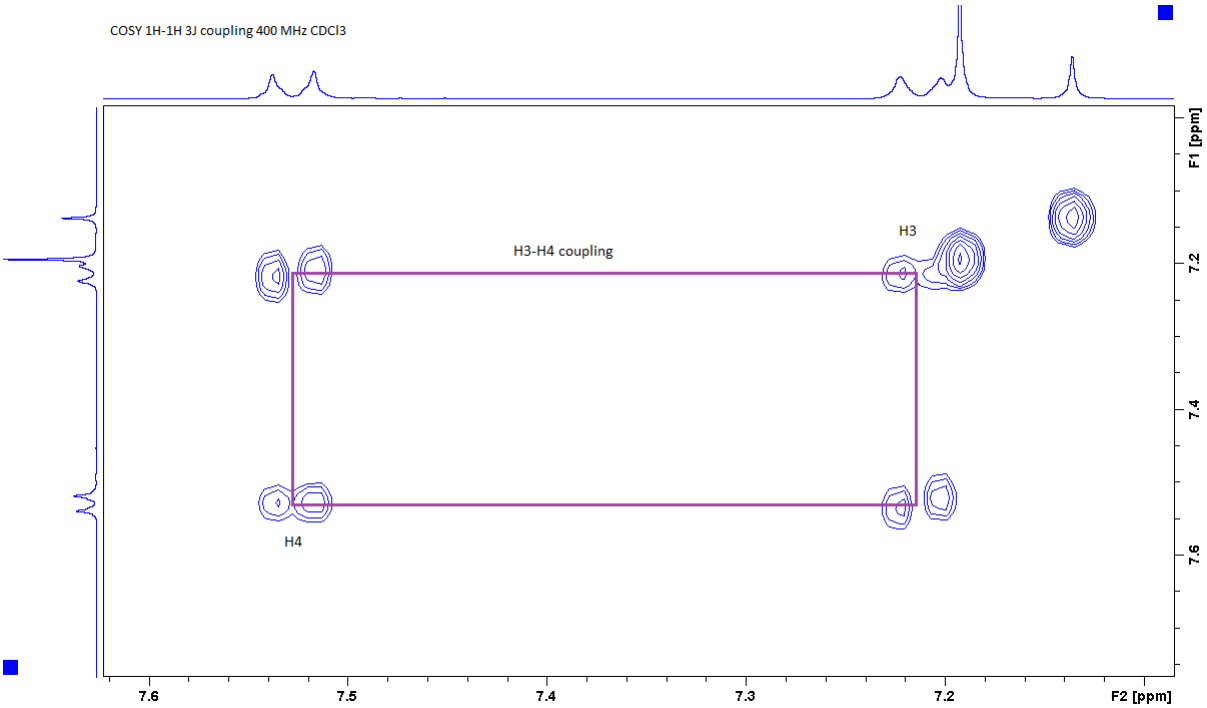


*Figure 20: Zoom in on $H^3$-$H^4$ coupling in COSY.*

$^{13}$C NMR shows eight peaks as expected for **2**. The carbon from the methyl groups must be at 21.63 since this is the only aliphatic carbon. The two large peaks 129.88 and 127.55 must be carbon at 3 and 4 since those corresponds to 4 equivalent carbons each and will give a stronger signal than the other 2 equivalent carbons. Carbon at 3 are most likely more up field than carbon at 4 because it is

further away from the more electronegative and electron-withdrawing groups (-SO2NH-). By same reasoning the peak at 122.63 ppm must be carbon at position 2.

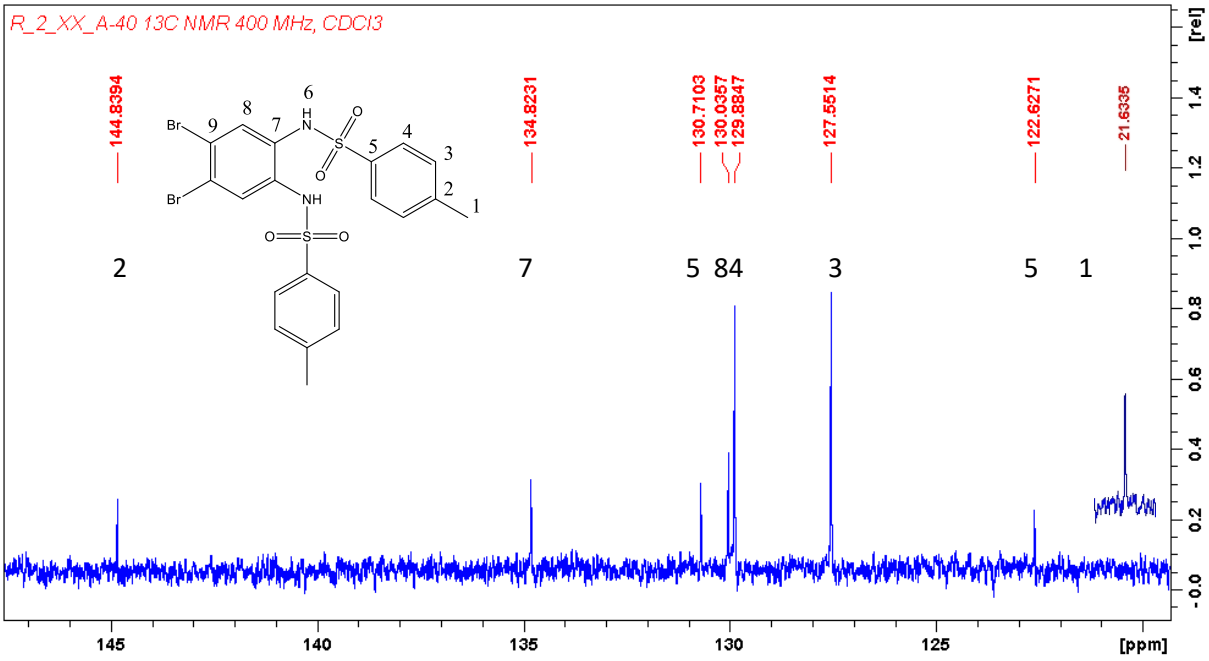


*Figure 21: $^{13}C$ NMR (100 MHz, $CDCl_3$): ppm = 144.84, 134.82, 130.71, 130.04, 129.88, 127.55, 122.63, 21.63*

The $^{1}H$ - $^{13}C$ HSQC spectrum with $^{1}J$ couplings for **2** is shown in Figure 22, and the correlations are listed in Table 2. The spectrum shows correlation ($^{1}H$ - $^{13}C$ ppm) for the methyl protons $H^1$ (2.42-21.63), $H^8$ (7.20 - 130.04), the "doublet" for $H^3$ (7.28 - 129.88) and $H^4$ (7.60 - 122.63). It is difficult to decide if the peak from $H^8$ at 7.20 correlates to 130.04 or 129.88 ppm in the $^{13}C$ spectrum. It is most reasonable to assign $H^8$ to the smaller peak at 130.04 ppm because it comes from two carbons while, the carbons at $H^3$ and $H^4$ have both a multiplicity of 4 equivalent carbons, so these should be equally large and larger than the other $^{13}C$ signals. The proton at 6.79 ppm does not show coupling to any carbon. This is consistent with the proton being bond to nitrogen.

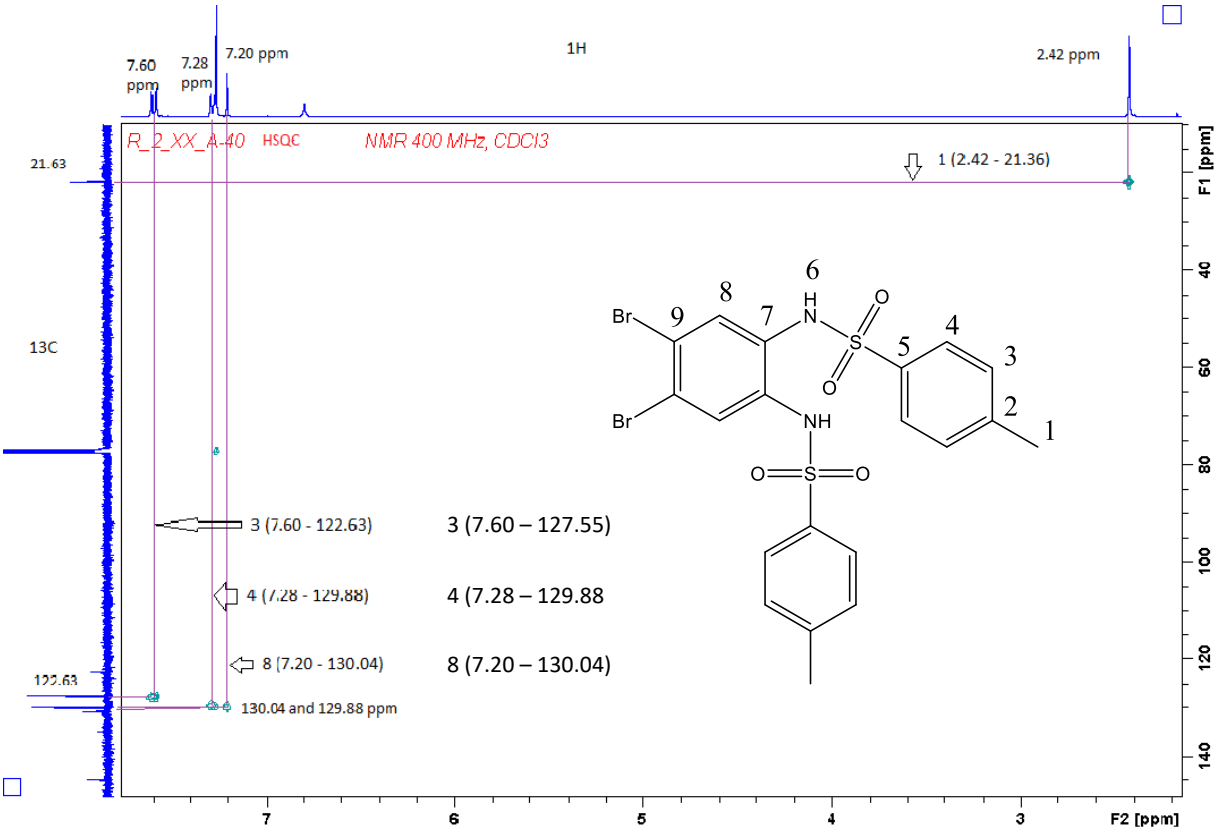


*Figure 22: $^{1}H$ - $^{13}C$ HSQC (400/101 MHz, $CDCl_3$) spectrum for **2.***

*Table 2: $^{1}H$ - $^{13}C$ HSQC correlations for **2.***

| Position | $^{1}H$ (ppm) | $^{13}C$ (ppm) |
|---|---|---|
| 1 | 2.42 | 21.36 |
| 4 | 7.60 | 127.55 |
| 3 | 7.28 | 129.88 |
| 8 | 7.20 | 130.04 |

$^{1}H$ - $^{13}C$ HMBC (Figure 23 and Figure 24) shows long range $^{1}H$ - $^{13}C$ couplings ($^{2}J$ - $^{4}J$), but $^{1}J$ couplings can also be seen as two dots (satellites) at equal distance to each side of the proton peak. For example, the two satellites at equal horizontal distance from the peak at 2.42 ppm in Figure 23 indicates a $^{1}J$ correlation to $C^{1}$ at 21.63 ppm.

Figure 23 shows the aliphatic region of the proton spectrum with a $^{4}J$ coupling to 129.88 ppm and a $^{2}J$ coupling to 144.84 ppm peak must be $C^{5}$ because of its large ppm-value and $C^{5}$ is next to the electron withdrawing S-atom and not the electron donating methyl group.

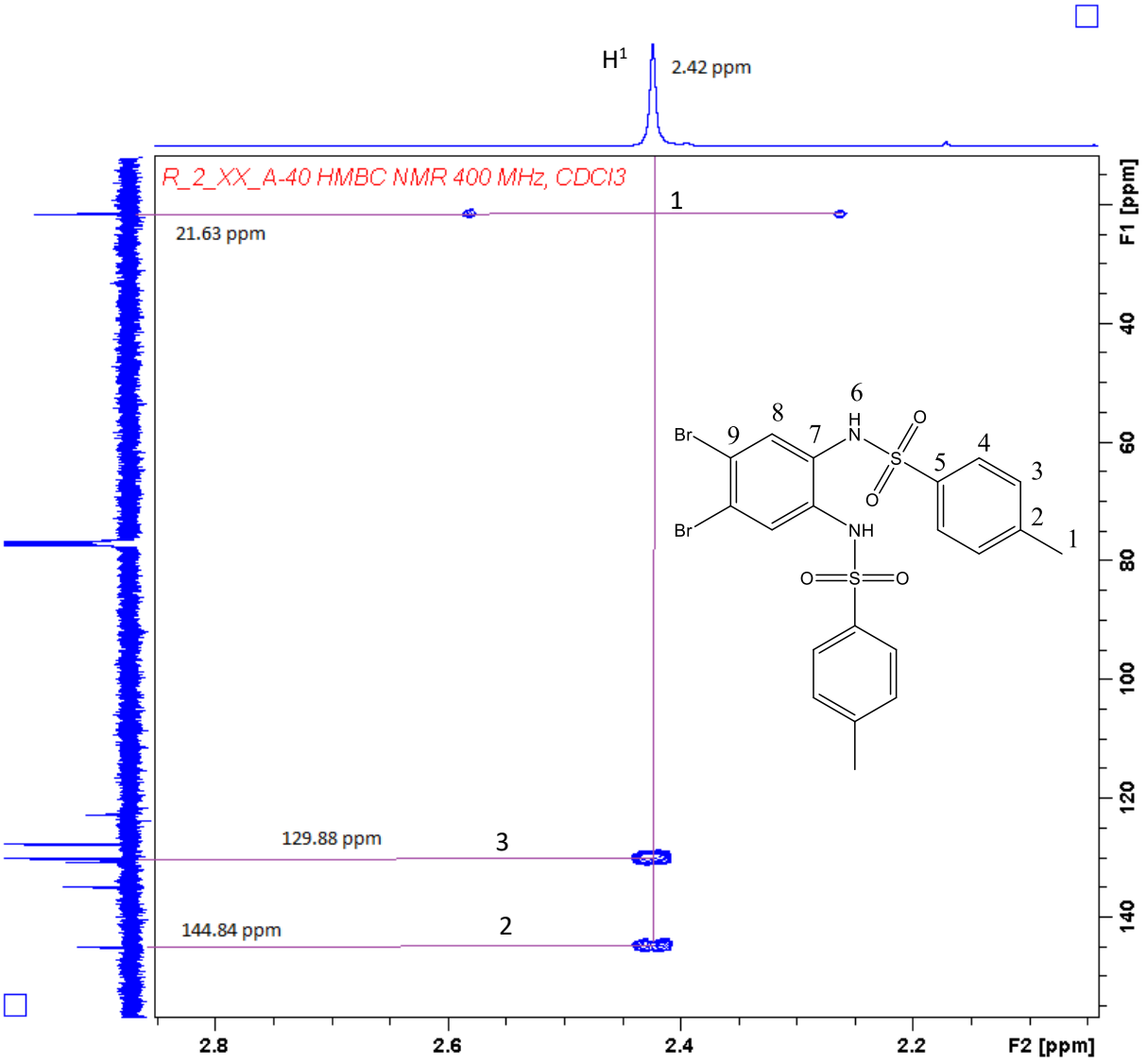


*Figure 23: $^{1}H$ - $^{13}C$ HMBC ($^{2}J$ to $^{4}J$ couplings) for proton at 2.42 ppm. It shows long range couplings to 129.88 and 144.84, and the two satellites indicate a $^{1}J$ coupling to 21.63 ppm.*

Figure 24 shows the aromatic region of the $^{1}H$ - $^{13}C$ HMBC of **2**. The singlet at 7.20 ppm peak shows $^{2}J$-$^{4}J$ coupling to 122.63 ppm and 130.04 ppm. This suggest that 122.63 ppm and 130.04 ppm peaks correspond to $C^{7}$ and $C^{9}$. Because bromine has a shielding effect and nitrogen have a deshielding effect on the ipso carbon, $C^{9}$ must be at 122.63 ppm and $C^{7}$ at 130.04 ppm. The 7.28 $^{1}H$ doublet shows $^{2}J$-$^{4}J$ coupling to peaks 21.63 ppm, 129.88 ppm (small) and 130.71 ppm.

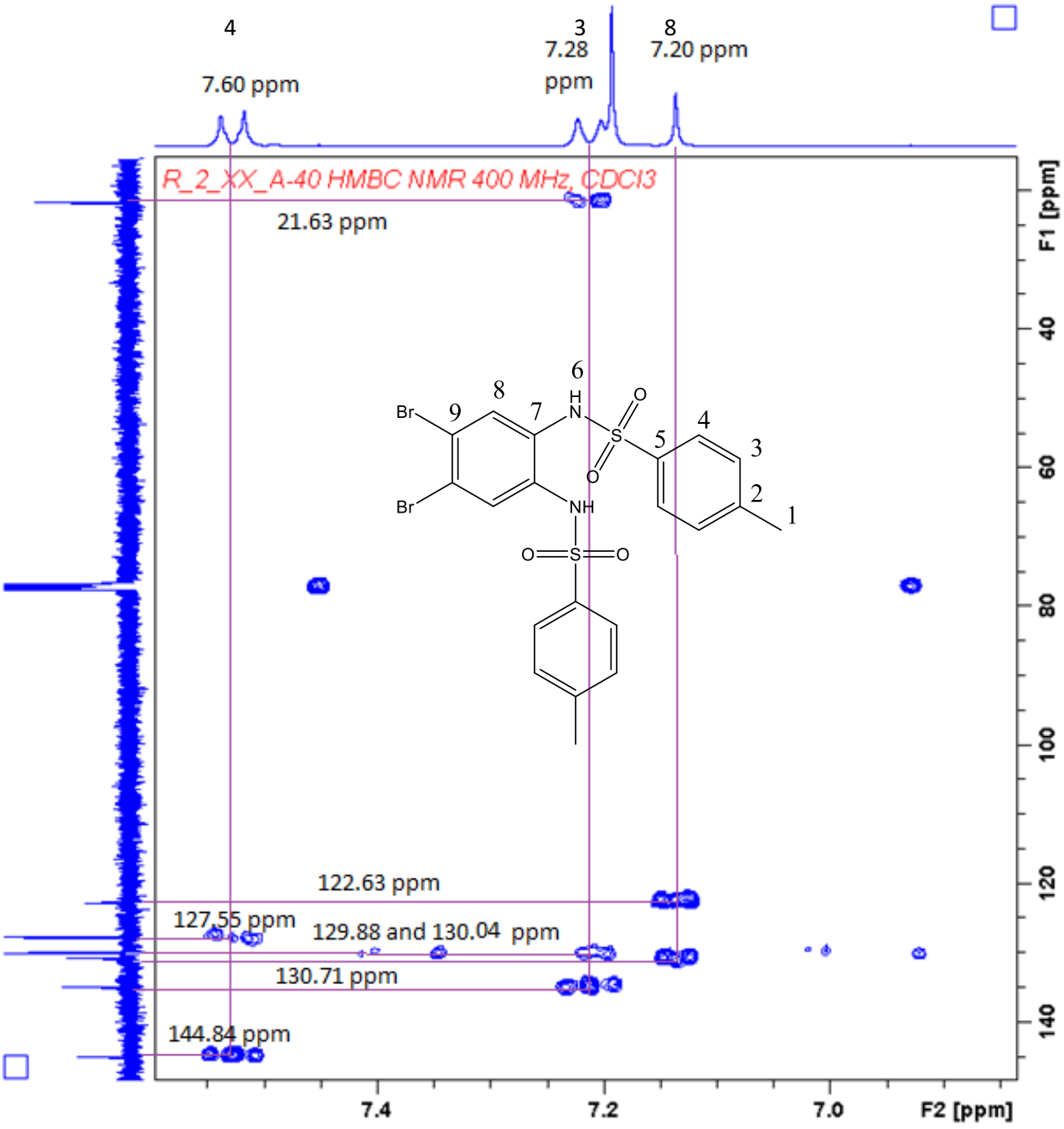


*Figure 24: $^{1}H$ - $^{13}C$ HMBC ($^{2}J$ to $^{4}J$ couplings) for proton at 7.60 (d, J=8.3, 4H), 7.28 (d, J=8.0, 4H), 7.20 (s, 2H), 6.79 (br, 2H). It shows long range couplings to 130.04 and 144.84, and the two satellites indicate a $^{1}J$ coupling to 21.63 ppm.*

A tabulated version of the characterization NMR spectra for **2** is shown in Table 3.

*Table 3: Tabulation of elucidation of **2**.*

| Position | $^1$H (ppm) | HSQC 13C coupling partner to 1H. (ppm) | Description | HMBC – 1H-13C 2J – 4J coplings | 13C |
|---|---|---|---|---|---|
| 1 | 2.42 (s, 6H) | 21.63 | 2*CH3 | 129.88<br>144.84 | |
| 2 | | 122.63/130.71/144.84 | | | |
| 3 | 7.28<br>(d,J=8.0,4H) | 129.88 | | 129.88 (weak)<br>130.71 | |
| 4 | 7.60<br>(d,J=8.3,4H) | 127.55 | | 127.55 (weak)<br>144.84 | |
| 5 | | 122.63/130.71/144.84 | | | |
| 6 | 6.79 (br, 2H) | - | 2*N-H | | |
| 7 | | | | | |
| 8 | 7.20 (s, 2H) | 130.04 | | 122.63<br>130.04 | |
| 9 | | | | | |

## 2.3 Synthesis of 4,5-dibromobenzene-1,2-diamine (3)

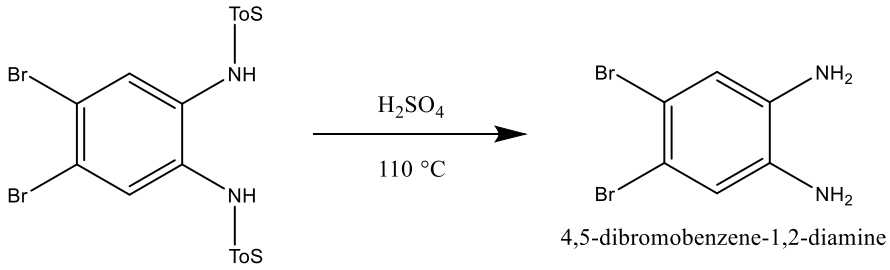


4,5-dibromobenzene-1,2-diamine

The reaction was done according to litterature[22]. It was important to use an oil bath to have temperature control and rinse with a good amount of water to get a pure product.

### Characterization of 3.

$^1$H NMR (400 MHz, $CDCl_3$, Figure 25) shows two peaks as expected. The singlet at 6.93 ppm that integrates to 2H must be the aromatic proton, while the broad peak at 3.40 that integrates to 4H must be from the protons in the $NH_2$ groups.

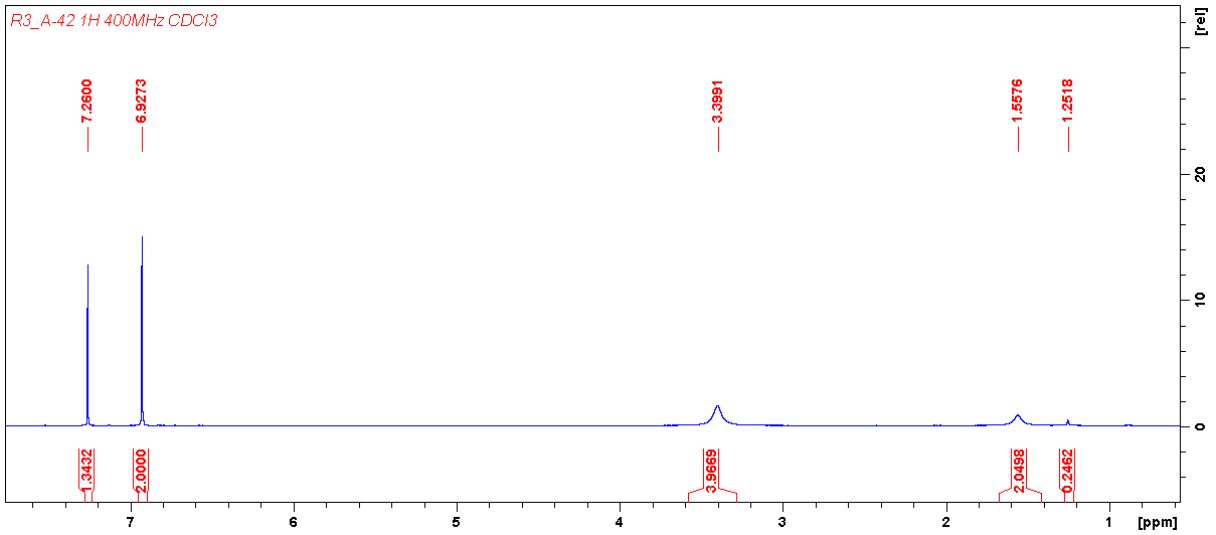


*Figure 25: $^{1}H$ NMR (400 MHz, $CDCl_3$) of **3** (4,5-dibromobenzene-1,2-diamine). ppm = 6.93 (s, 2H), 3.40 (br, 4H).*

The : $^{1}H$ - $^{1}H$ COSY (400MHz, $CDCl_3$, Figure 26) shows no correlations between the aromatic proton and the $NH_2$ signal as expected.

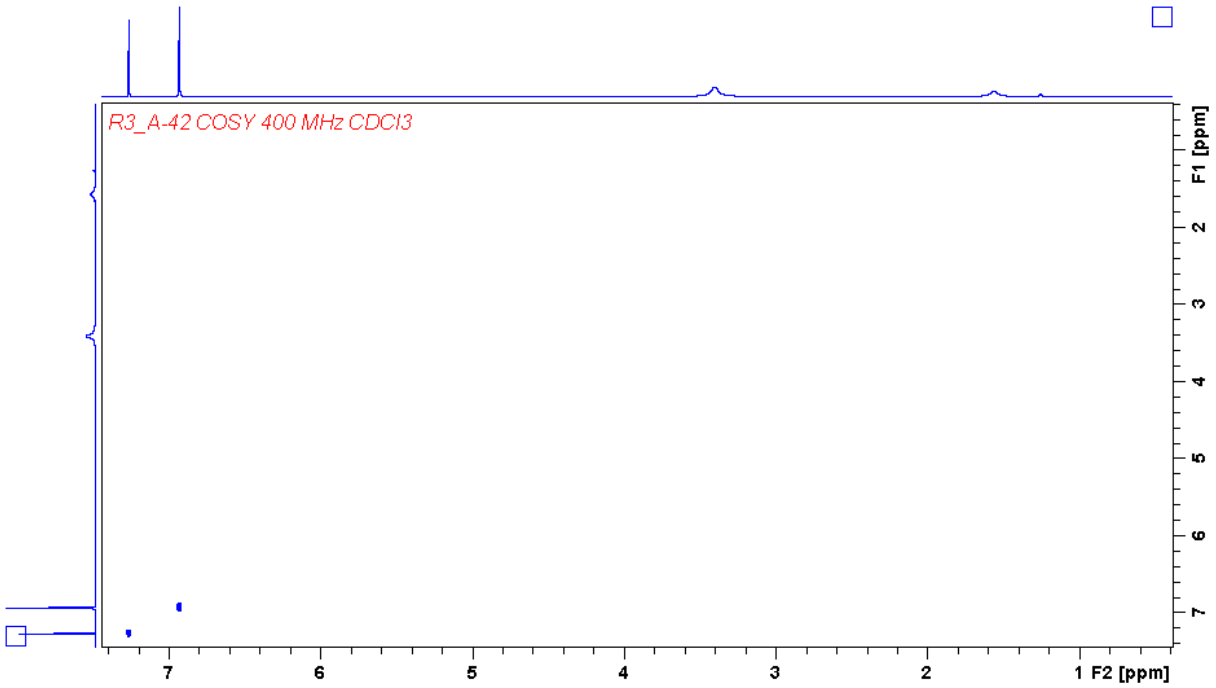


*Figure 26: $^{1}H$ - $^{1}H$ COSY (400MHz, $CDCl_3$) NMR spectrum of **3** shows no correlating peaks as expected.*

The $^{13}C$ NMR spectrum (101 MHz, CDCl3, Figure 27) shows three peaks, where the largest one at 120.46 ppm must be from the **C**-H carbon, the one with largest chemical shift at 135.35 ppm must be from the **C**-$NH_2$ carbons and the last most upfield at 113.49 ppm must be from the **C**-Br carbons. This classification is based on Br having a shielding effect and $NH_2$ has an deshielding effect on the ipso carbon.

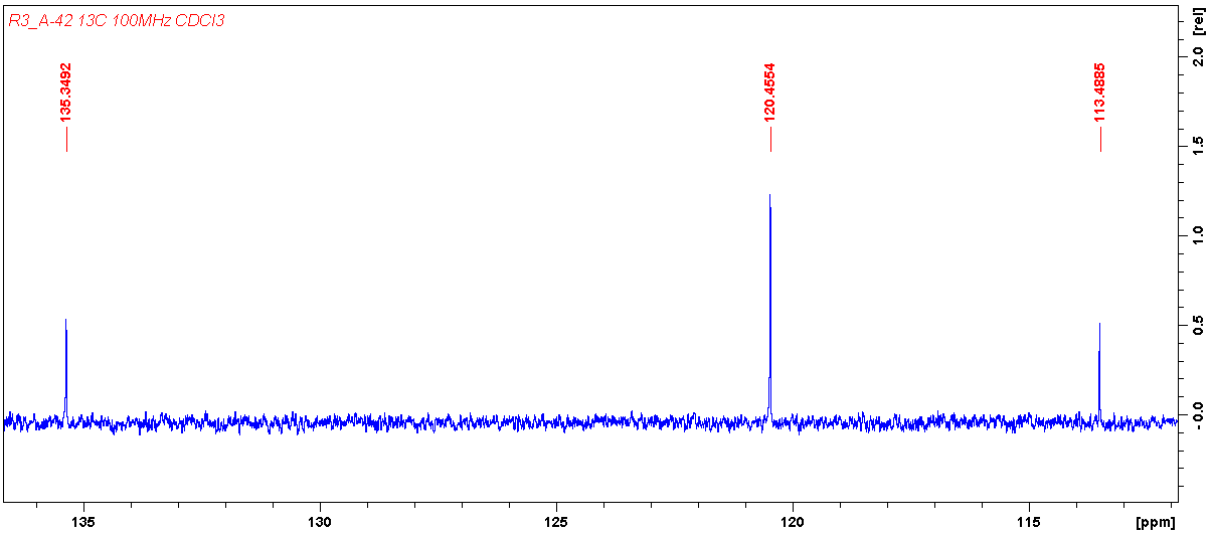


*Figure 27: $^{13}C$ NMR (101 MHz, $CDCl_3$) of **3.** ppm = 135.35, 120.46, 113.49.*

The : $^{1}H$ – $^{13}C$ HSQC (400/101 MHz, $CDCl_3$, Figure 28) confirms that the peak at 120.46 is from the **C**-H carbon.

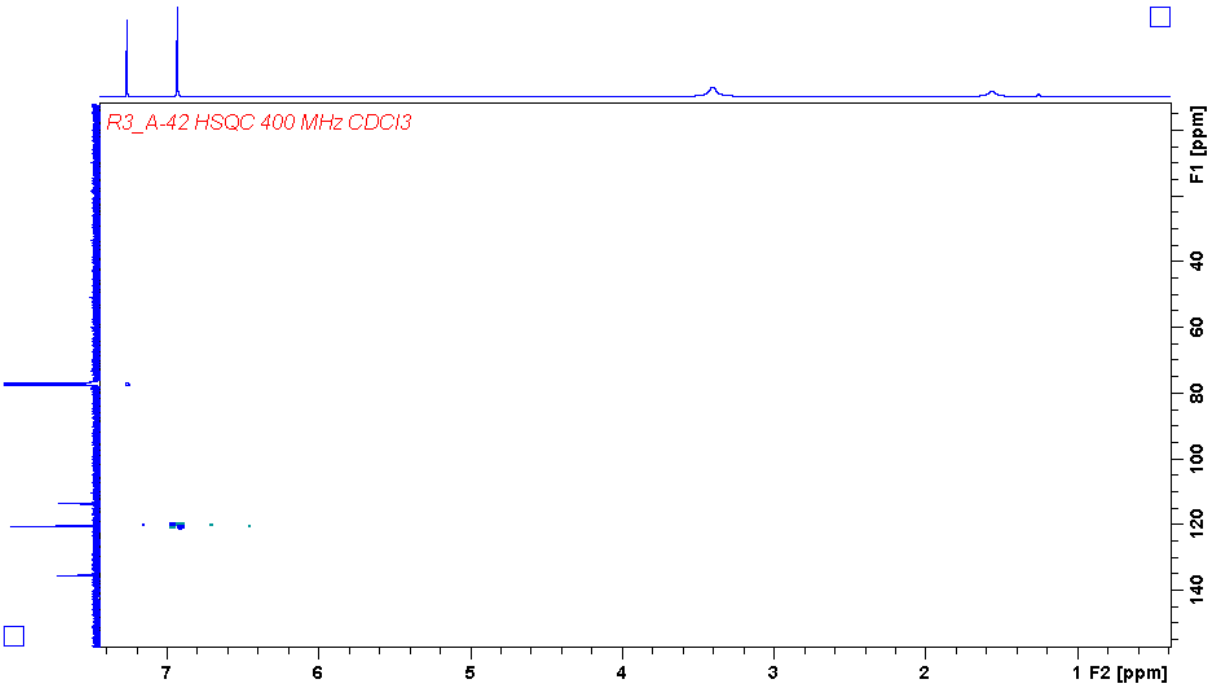


*Figure 28: $^{1}H$ – $^{13}C$ HSQC (400/101 MHz, $CDCl_3$) NMR spectrum of **3**. $^{1}H$ - $^{13}C$ correlation between 6.93 ppm $^{1}H$ peak and 120.46 ppm $^{13}C$ peak.*

The $^{1}H$ – $^{13}C$ HMBC (400/101 MHz, $CDCl_3$, Figure 29) shows $^{2}J$ couplings from the **C**-H signal to the signals at 135.35 ppm and 113.49 ppm. This gives that all the carbon peaks are from the same pi-system.

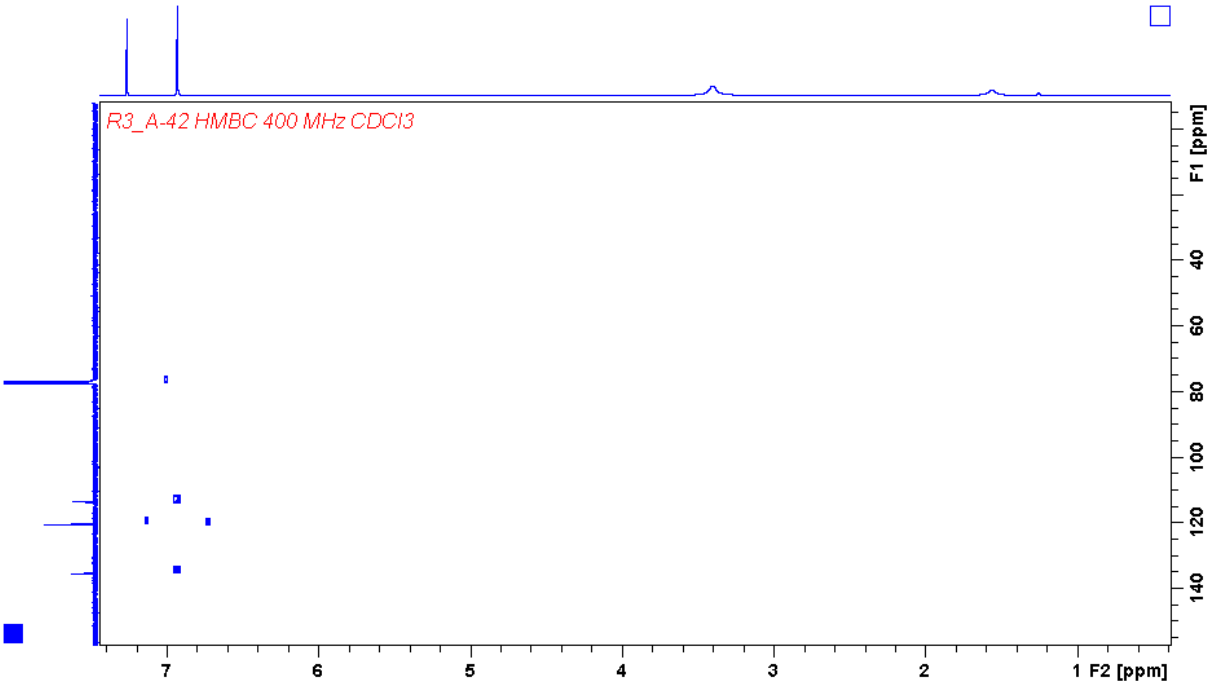


*Figure 29: $^{1}H$ – $^{13}C$ HMBC (400/101 MHz, $CDCl_3$) spectrum of **3** shows long range couplings ($^{2}J$ - $^{4}J$) from 6.93 ppm $^{1}H$ peak to 135.35 and 113.49 13C peaks. It also shows satellite peaks for a $^{1}J$ coupling from 6.93 $^{1}H$ peak to 120.46 $^{13}C$ peak shown in the HSQC spectrum.*

## 2.4 Synthesis of 1,10-phenanthroline-5,6-dione **(4)**

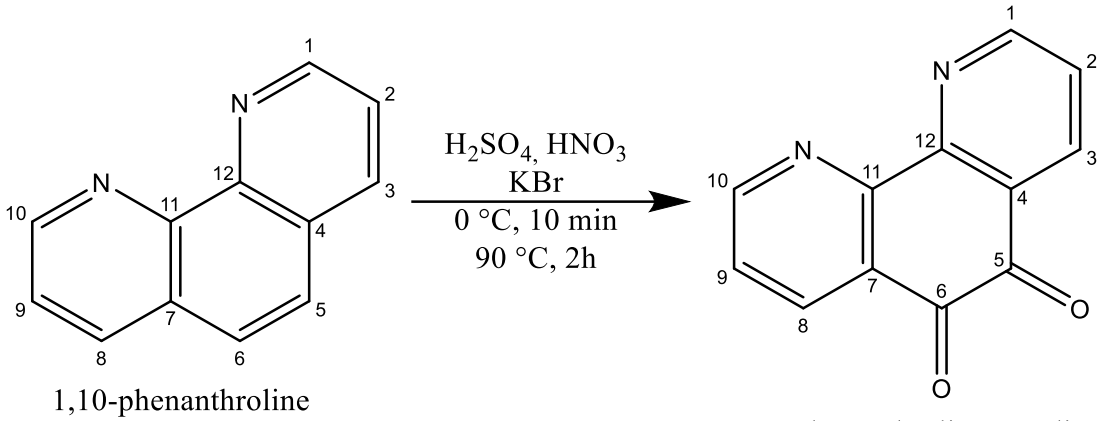


1,10-phenanthroline

1,10-phenanthroline-5,6-dione

The reaction was done according to literature[25]. In the work up it was important to do a proper recrystallisation in EtOH to get yellow needles and not only a precipitate to get a pure product. By doing several recrystallizations the amount of reactant was reduced to 2 %, with a "yield" of 52 %. A small amount of the reactant might not be a problem in further reactions, because it most likely would not do any harm to the reaction to make **5** and **7** for example. It would also be much easier to separate it from a larger molecule such as **5** or **7**.

### Characterization of *4*.

The $^{1}H$ NMR (400 MHz, $CDCl_3$,Figure 30) of **4** shows three double doublets as expected: ppm = 9.12 (dd, J=4.7, 1.8 Hz, 2H, 1-**H**), 8.51 (dd, J=7.9, 1.8 Hz, 2H, 3-**H**), 7.59 (dd, J=7.9, 4.7 Hz, 2H, 2-**H**). The assignments of the peaks are based on 2-**H** has a $^{3}J$ coupling to both 1-**H** and 3-**H** so these coupling

constants should be large. 1-**H** and 3-**H** has both one $^{3}J$ coupling and one $^{4}J$ coupling so they should have one large and one small coupling constant. **4** has a resonance form (Figure 31) that deshields 1-**H** which gives this proton a lower ppm value than for 3-**H**. The low $^{3}J$ value of 4.7 Hz from 1-**H** to 2-**H** could be because of a through space interaction of 1-**H** to the electron pair on N.

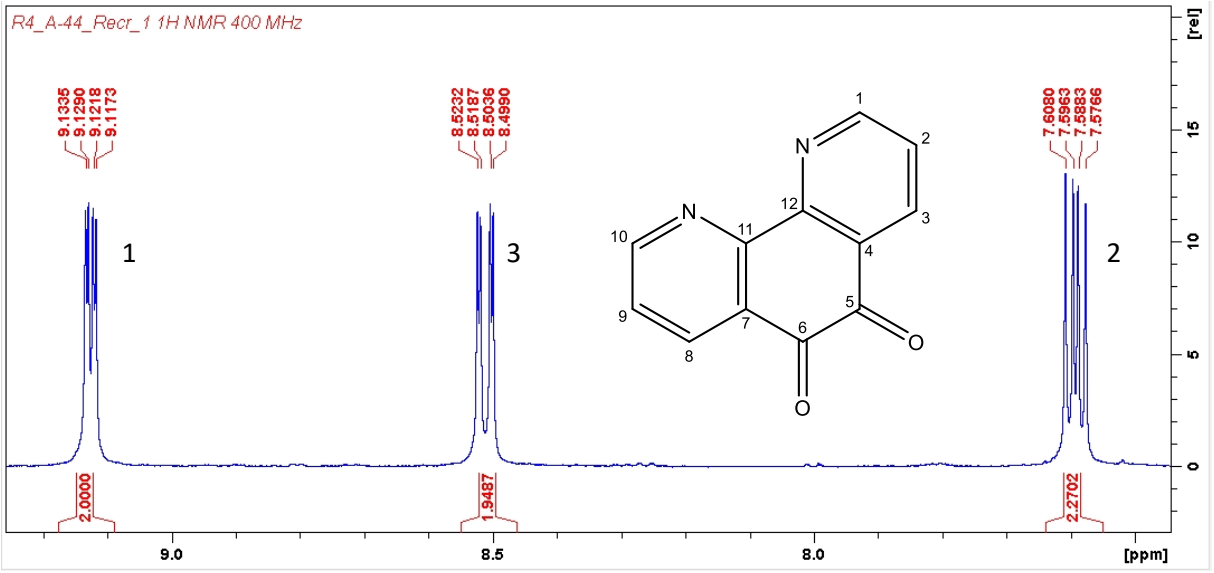


*Figure 30: $^{1}H$ NMR (400 MHz, CDCl3) of 1,10-Phenanthroline-5,6-quinone excerpt of region with product peaks. ppm = 9.12 (dd, J=4.7, 1.8 Hz, 2H), 8.51 (dd, J=7.9, 1.8 Hz, 2H), 7.59 (dd, J=7.9, 4.7 Hz, 2H).*

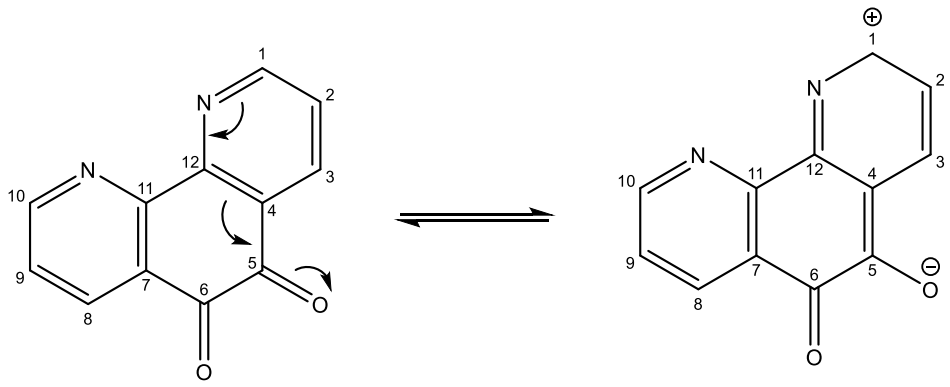

*Figure 31: Resonance form of 4 that gives a negative charge on oxygen and a positive charge on 1.*

The $^{1}H$-$^{1}H$ COSY (400 MHz, $CDCl_3$, Figure 32) of **4** shows three correlations (off diagonal peaks) 1,2 1,3 and 2,3. This shows that the three signals all correlate to each other and are therefore in the same $\pi$-system which was expected for **4**.

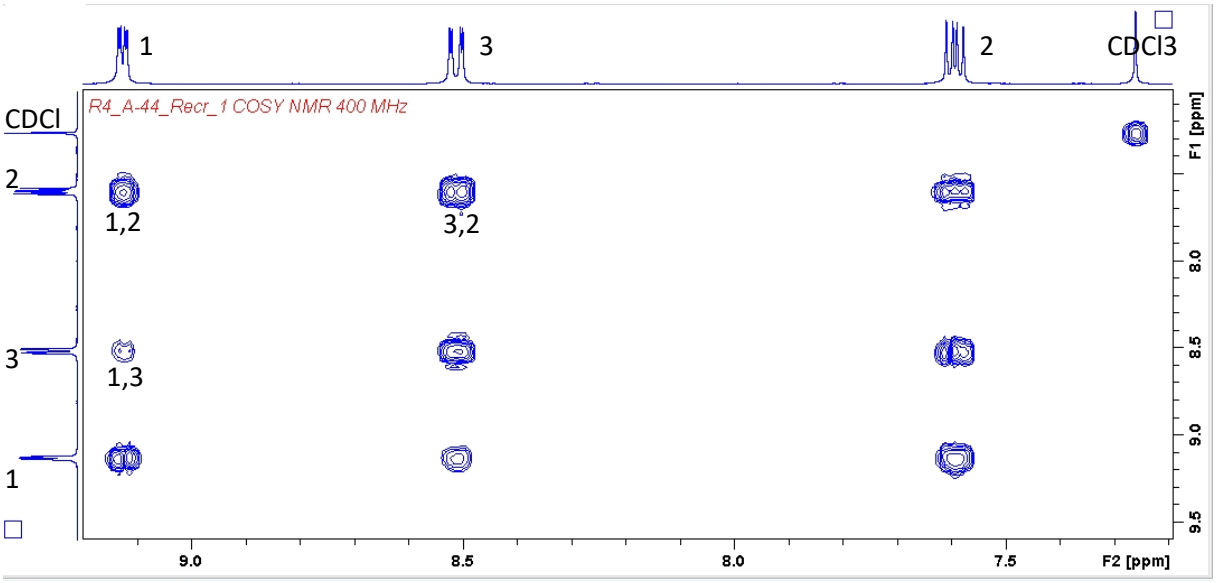


*Figure 32: $^{1}H$-$^{1}H$ COSY (400 MHz, CDCl3) of 1,10-Phenanthroline-5,6-quinone.*

The $^{13}C$ NMR (101 MHz, $CDCl_3$) of **4** shows six peaks of which three are larger: ppm = 178,67, 156.42 (l), 152.91, 137.32 (l), 128.08, 125.60 *(l)*.

The three larger peaks correspond to the three chemically unequivalent **C**-H carbons

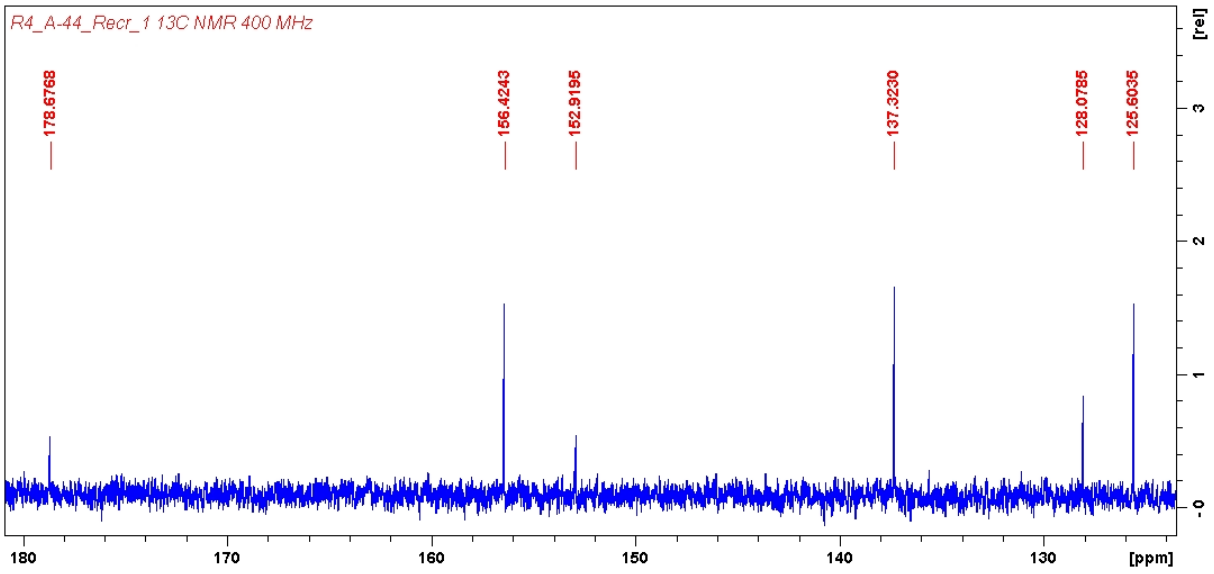


*Figure 33: $^{13}C$ NMR (101 MHz, $CDCl_3$) of 1,10-Phenanthroline-5,6-quinone: ppm = 178,67, 156.42, 152.91, 137.32, 128.08.*

## 2.5 Synthesis of 11,12-dibromodipyrido[3,2-a:2',3'-c]phenazine (dppzBr$_2$, **5**)

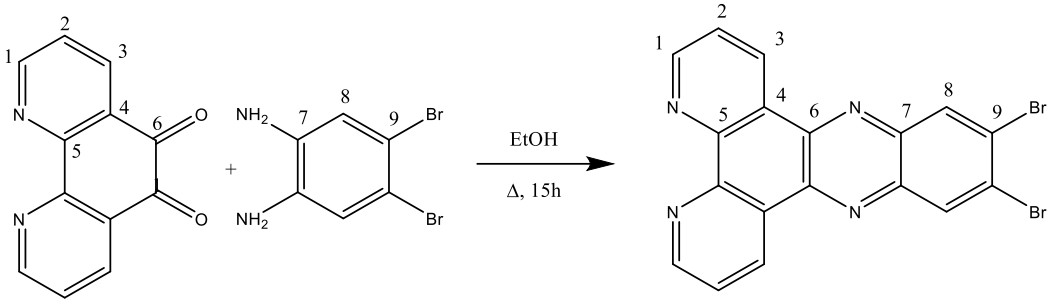


*Figure 34: R5: 11,12-dibromo.dipyrido[3,2-a:2',3'-c]phenazine (dppz-o-Br)*

The reaction was done according to literature[26]. It was a simple condensation reaction that worked well. The workup in the literature said to reduce the amount of solvent to 1/6 and then collect the product by filtration. We found this a bit difficult because the product went easily through the filterpaper. Because we used

### Characterization of *5*

$^1$H NMR spectrum (Figure 35) shows peaks that matches what is reported. It shows three double doublets for protons at 1, 2 and 3, and a singlet for 8. The signal at 7.78 must be 2-**H** because it has two $^3$J couplings (8.1 and 4.4), while the signals at 9.49 and 9.27 has both one $^3$J coupling and one $^4$J coupling so they must be 1-**H** and 3-**H**. The small $^3$J coupling af 4.4Hz indicates that the bond length of 1-**H** could be longer because of an interaction with the electron pair on the nitrogen. This could also give a through-space shielding effect and therefore a lower shift. It will be shown later from HMBC spectrum that it is correct to assign 1-**H** to 9.27 peak and 3-**H** to 9.49.

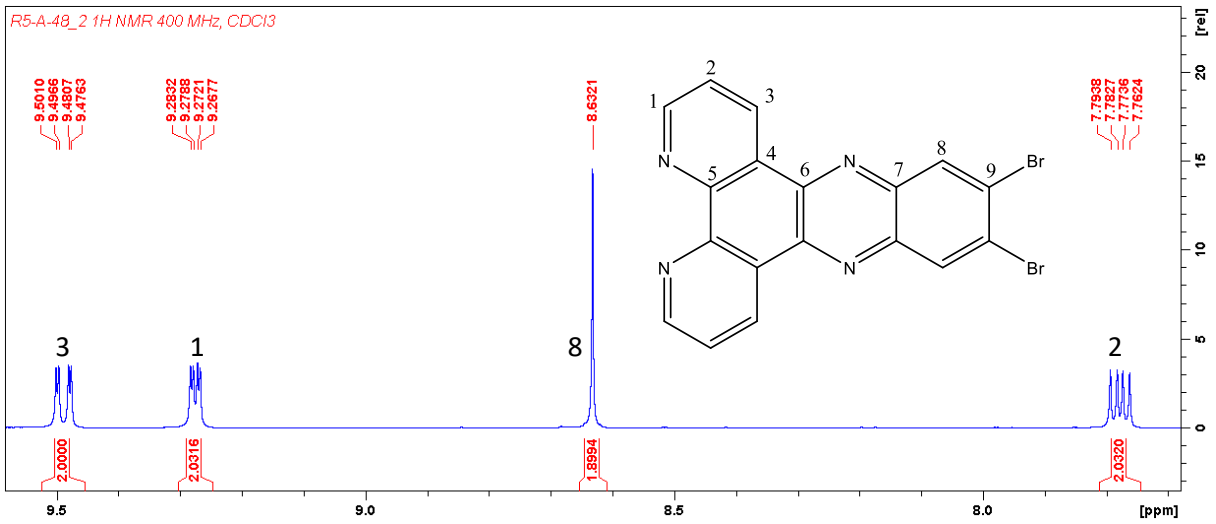


*Figure 35: $^1$H NMR (400 MHz, $CDCl_3$) of **5**: ppm = 9.49 (dd, J=8.1, 1.7, 2H), 9.27 (dd, J=4.4, 1.7, 2H), 8.68 (s, 2H), 7.78 (dd, J=8.1, 4.4, 2H).*

The $^1$H – $^1$H COSY spectrum (Figure 36) shows correlation peaks between 1-**H**, 2-**H** and 3-**H** which indicates that they are in the same pi-system and confirms the previous assignments**.**

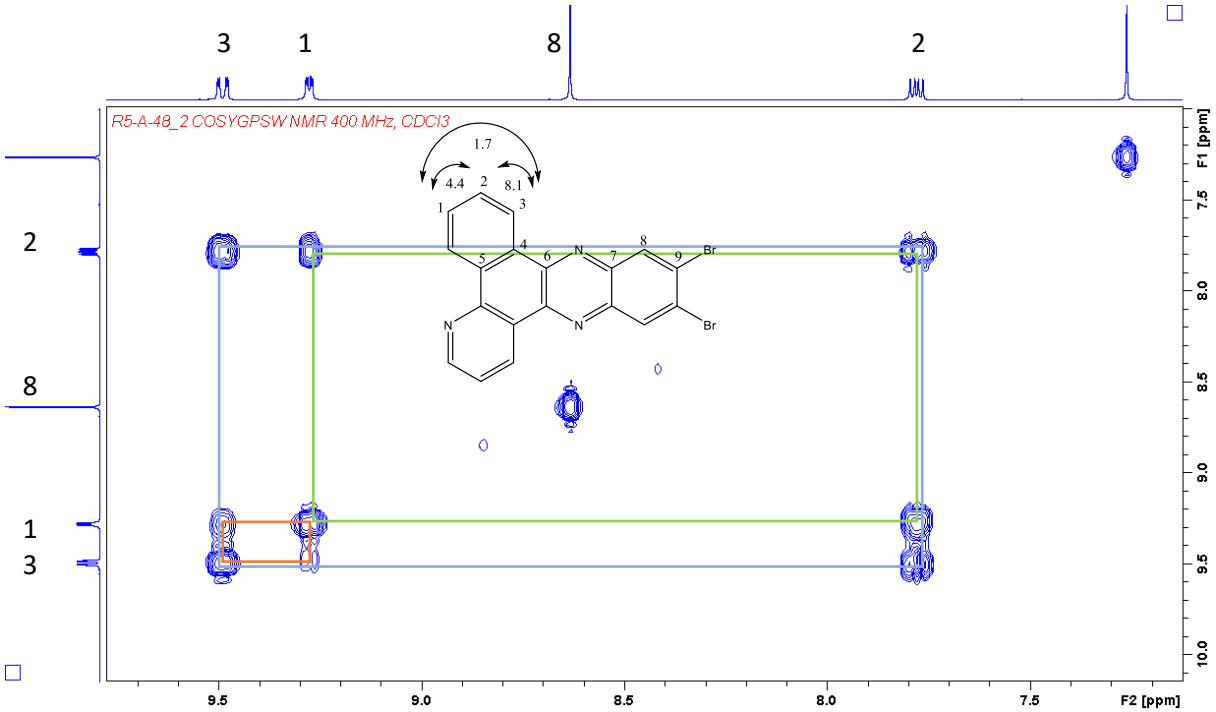


*Figure 36: Excerpt of $^{1}H$ – $^{1}H$ COSY spectrum of **5** (400 MHz, $CDCl_3$). Correlations: 1-**H** - 3-**H**, 1-**H** - 2-**H** and 2-**H** - 3-**H**.*

The carbon spectrum (101 MHz, $CDCl_3$, Figure 37) shows nine peaks that corresponds to the nine chemically different carbons in **5**. Four of the peaks are larger and possibly C-H. This is confirmed by the DEPT135 spectrum (Figure 38) and the $^{1}H$ – $^{13}C$ HSQC spectrum (400-101 MHz, $CDCl_3$, Figure 39) where also the assignments of carbon 1, 3, 8 and 2 are done.

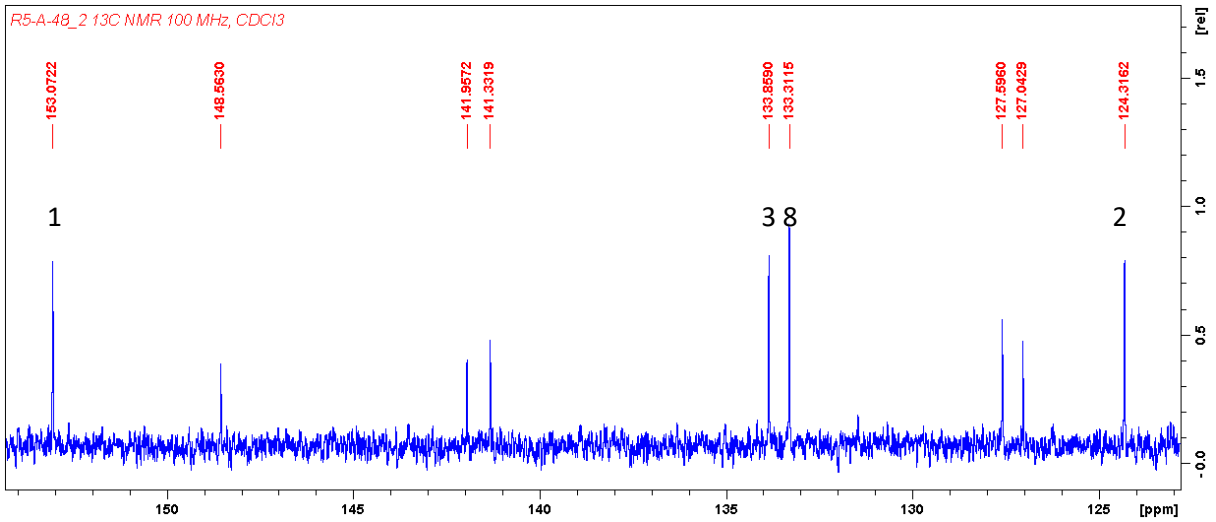


*Figure 37: Excerpt of region with peaks for **5** from $^{13}C$ NMR (100 MHz, $CDCl_3$) ppm = 153.07 (**1**), 148.56 (**5**), 141.96, 141.33, 133.86, 133.31, 127.60, 127.04, 124.31.*

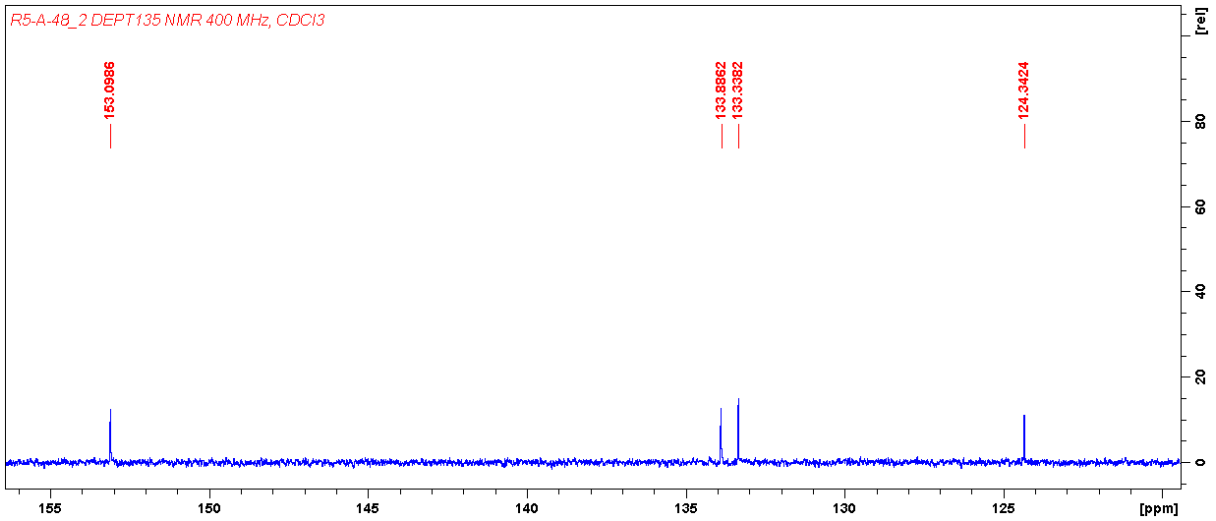


*Figure 38: Excerpt of DEPT135 of **5** (100 MHz, CDCl3). Only positive peaks are shown at ppm = 153.10, 133.89, 133.34 and 124.34.*

The $^{1}H$ – $^{13}C$ HSQC spectrum (400-101 MHz, $CDCl_3$, Figure 39) shows $^{1}J$ proton – carbon correlations for **5**. It assigns the following carbons to peaks (ppm): **3** to 133.89, **1** to 153.10, **8** to 133.34 and **2** to 124.34.

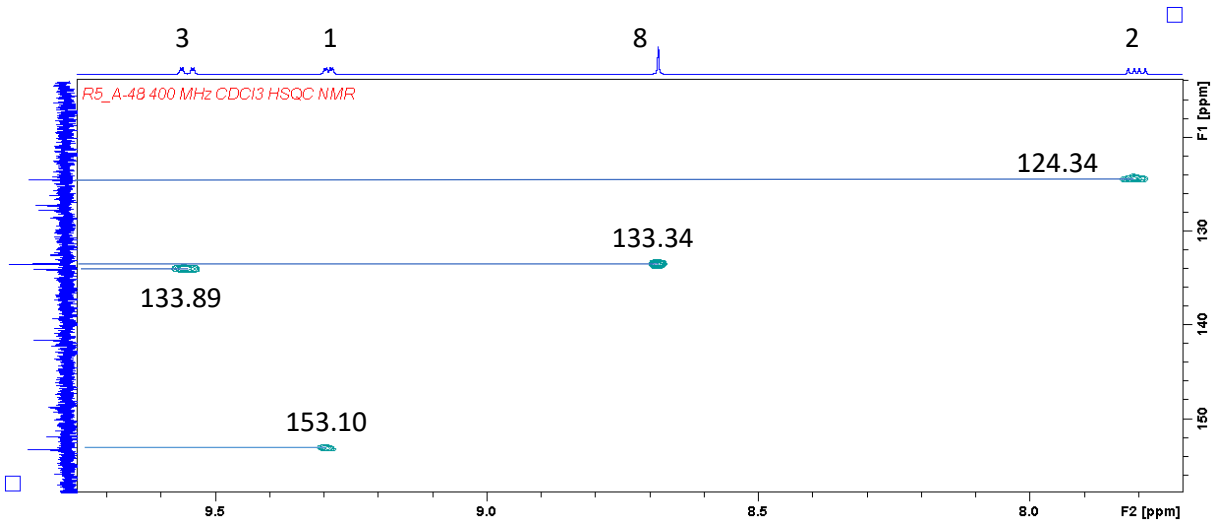


*Figure 39: $^{1}H$ – $^{13}C$ HSQC spectrum (400-101 MHz, CDCl3) assigns the carbons (ppm) **3** to 133.89, **1** 153.10, **8** to 133.34 and **2** to 124.34.*

The $^{1}H$ – $^{13}C$ HMBC spectrum (400 – 101 MHz, $CDCl_3$,

Figure 40) shows long range couplings for **5**. It gives couplings from 3-**H** to 141.96, 148.56 and 153.10 (**1)**, 1-**H** shows couplings to 124.34 (**2)**, 133.89 (**3)** and 148.56, 8-**H** to 127.60 and 141.33, and 2-**H** to 127.04 and 153.07 (**1)**.

Since both 1-**H** and 3-**H** correlates to the signal at 148.56, this must be from carbon **5.** It is the only unassigned carbon with a three-bond distance from both ptotons 1-**H** and 3-**H**. 2-**H** correlates to one unassigned peak 127.04. This must be from carbon **4** because it is the only carbon in a three-bond distance from 2-**H** and that are unassigned. 3-**H** correlates to the signal at 141.96 and the only candidate for this is carbon **6**. The signal at 141.33 must then be carbon **7** and 127.60 must be carbon **9**, because Br has a shielding effect and N has a deshielding effect on the ipso carbon. All the carbon

peaks have then been assigned as follows: 153.07 (**1**), 148.56 (**5**), 141.96 (**6**), 141.33 (**7**), 133.89 (**3**), 133.31 (**8**), 127.60 (**9**), 127.04 (**4**), 124.31 (**2**). The correlations are shown in Figure 41: $^{1}H - ^{13}C$ HMBC correlations for **5**.Figure 41.

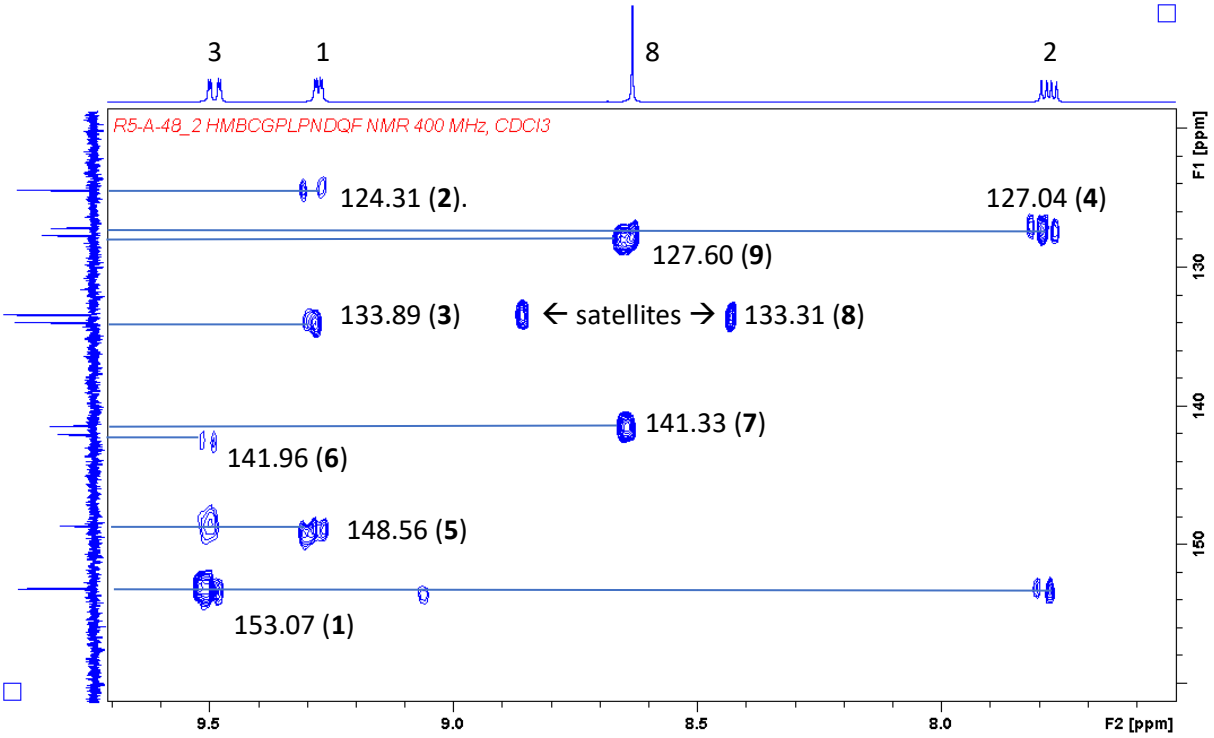


*Figure 40: $^{1}H - ^{13}C$ HMBC Long range ($^{2-4}J$) correlations for **5**. One-bond correlations are suppressed but can sometimes be seen as satellites. $^{3}J$ couplings follow the Karplus equation which means that if the dihedral angle is near to 90 degrees the intensity is nearly zero.*

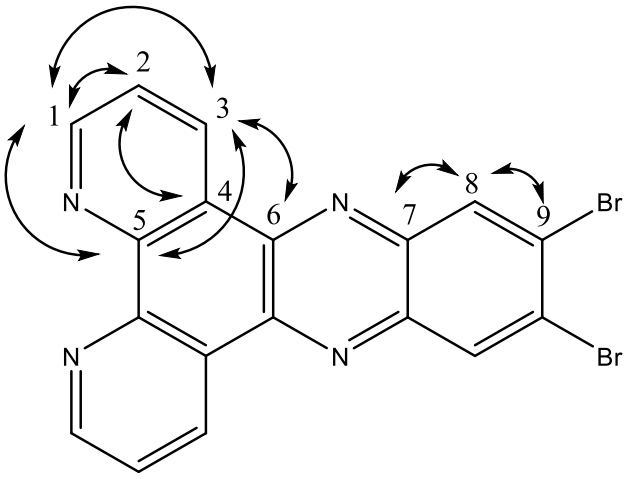


*Figure 41: $^{1}H - ^{13}C$ HMBC correlations for **5**.*

## 2.6 Synthesis of 4-ethynylbenzonitrile (6)

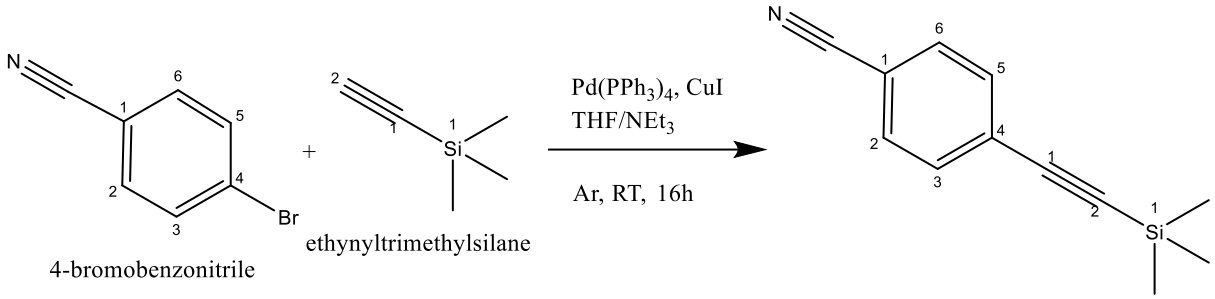


4-bromobenzonitrile + ethynyltrimethylsilane

4-((trimethylsilyl)ethynyl)benzonitrile

**6a**

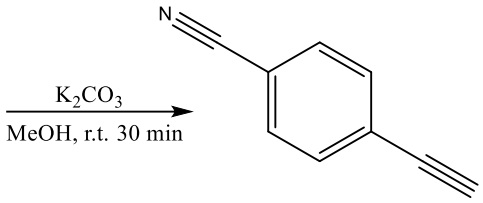


4-ethynylbenzonitrile

**6b**

The reaction was done in two steps according to literature[27] and experience from fellow student Atiqa Ansar for workup. Alternative workup to column chromatography was sublimation. We used a kugelrohr for sublimation at 70 °C for about 1 h but this gave a poor yield of only 32 % while column chromatography gave 69 % yield.

## Characterization of *6*.

The Proton NMR (400 MHz, $CDCl_3$, Figure 42) showed two peaks. The multiplet at 7.59 ppm (4H) resembles two doublets but is the results of an AA'BB' spin system on the para substituted phenyl ring. The singlet at 1.55 ppm (1H) is from the ethynyl proton.

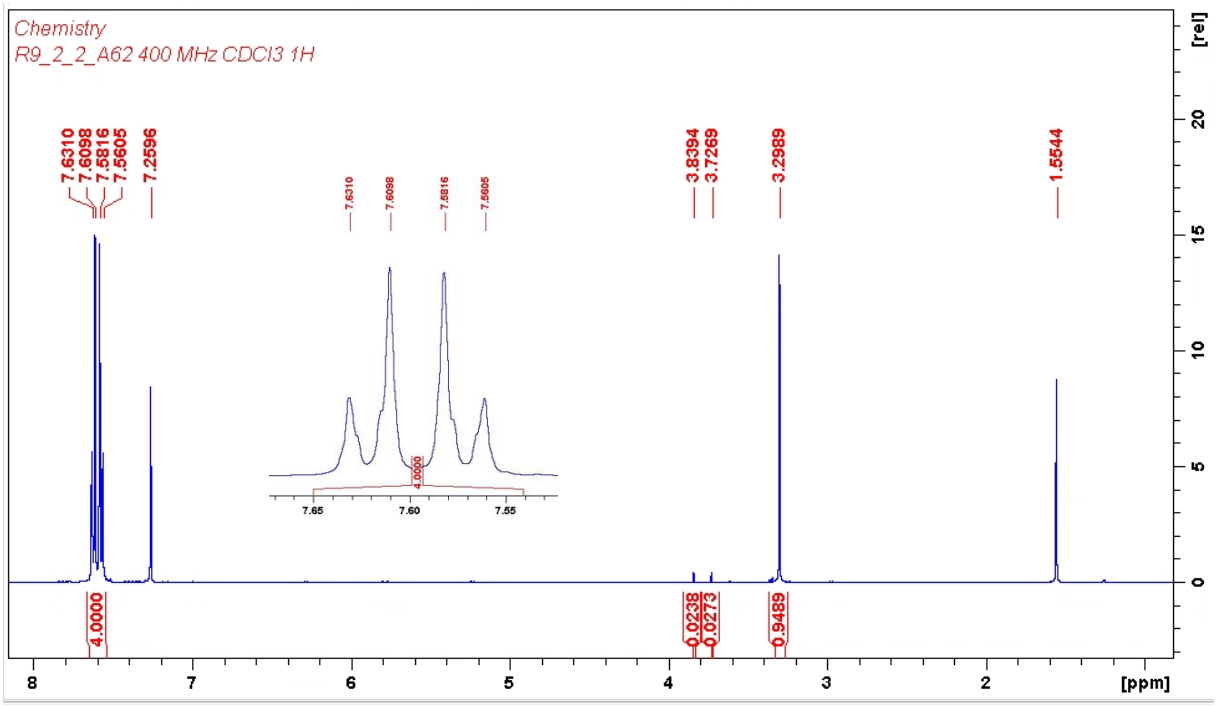


*Figure 42: $^{1}H$ NMR (400 MHz, $CDCl_3$) δ 7.62 (m, 7.59, 4H), 3.30 (s, 1H).*

The carbon NMR *(101 MHz, $CDCl_3$,* Figure 43*) shows seven peaks that correspond to the seven chemically inequivalent carbons in **6**. Three of them are larger and correspond to the C-H carbons, two in the aromatic region and one in the aliphatic region.*

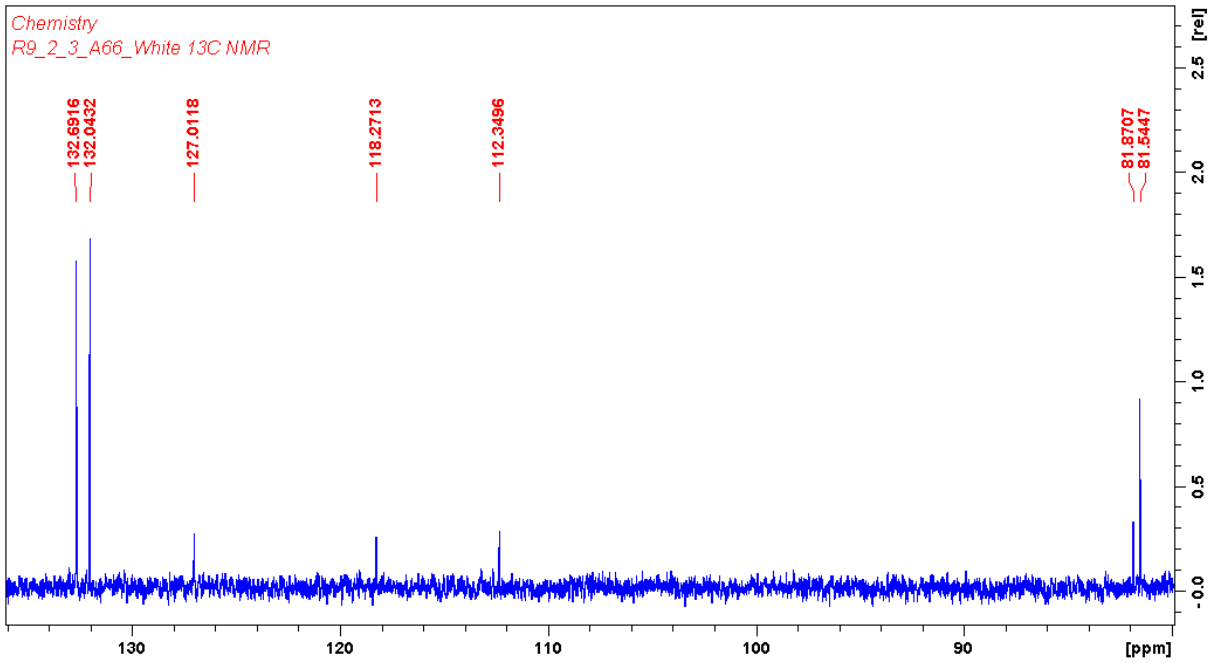


*Figure 43: $^{13}C$ NMR (101 MHz, $CDCl_3$) δ 132.69 (s, 2C), 132.04 (s, 2C), 127.01 (s, 1C), 118.27 (s, 1C), 112.35 (s, 1C), 81.87 (s, 1C), 81.55 (s, 1C).*

The $^{1}H$ - $^{13}C$ HSQC (400 - 101 MHz, CDCl3, Figure 44) of 6 shows 2 $^{1}J$ correlations, one for alkynyl proton and one for the phenyl protons.

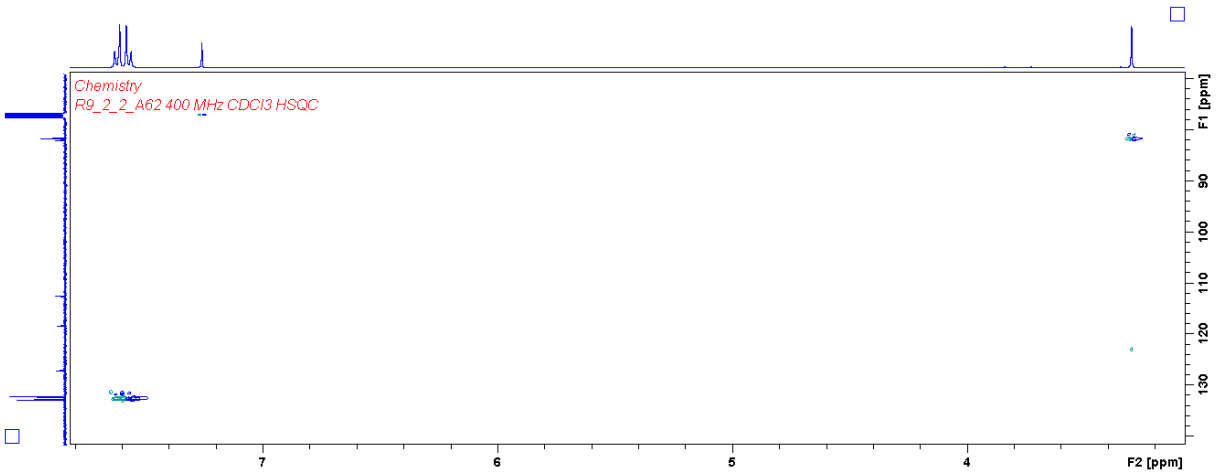


*Figure 44: $^{1}H$ - $^{13}C$ HSQC (400 - 101 MHz, $CDCl_3$) of 6.*

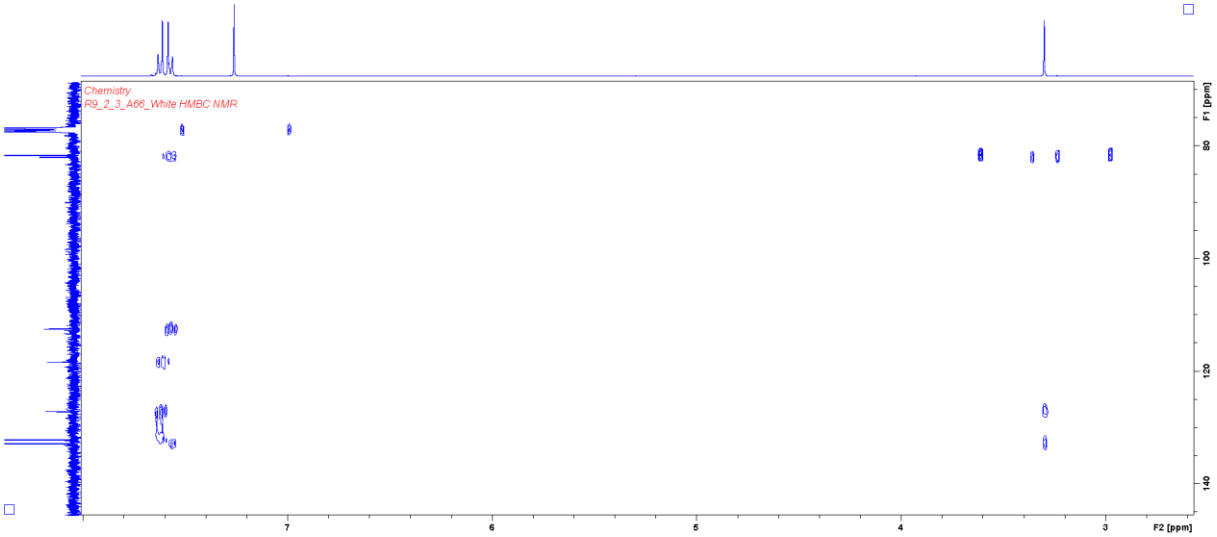


*Figure 45: $^{1}H$ - $^{13}C$ HMBC (400 - 101 MHz, $CDCl_3$) of 6.*

## 2.7 Synthesis of Dipyrido[3,2-a:2',3'-c]phenazine (dppz, **7**)

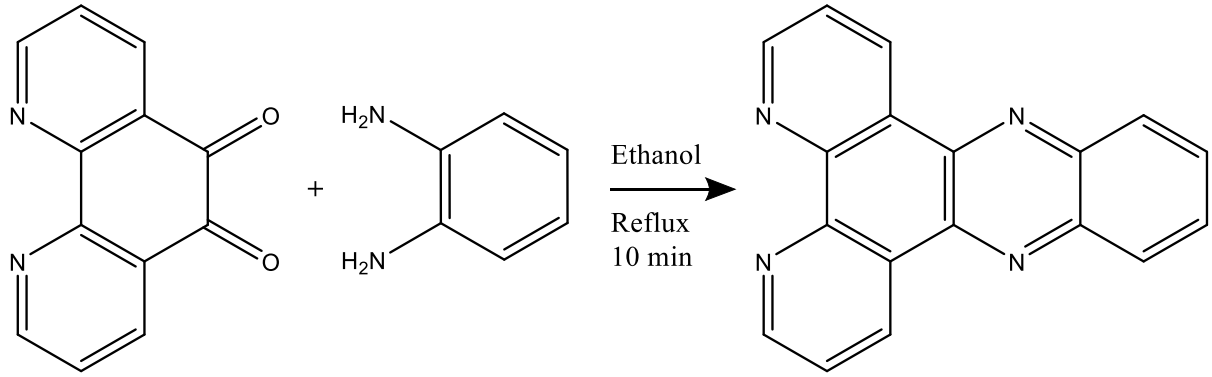


*Figure 46: Reaction scheme for **7**.*

The reaction was done according to literature[28] by refluxing phendione and o-phenylenediamine in absolute anhydrous ethanol for only 10 min. After removal of ethanol the solids was heated in water until dissolved, cooled down and the precipitates filtered off. Figure 47 shows **7** with numbering of chemically nonequivalent carbons.

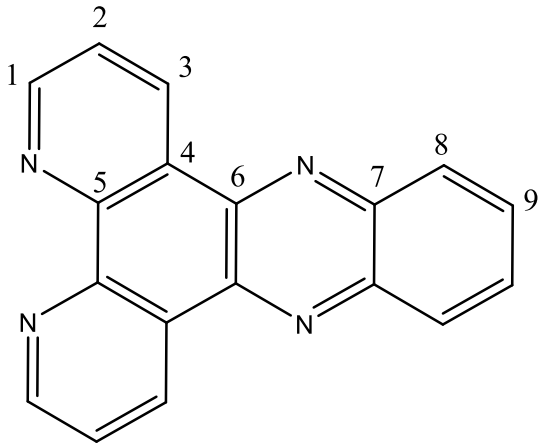


dipyrido[3,2-*a*:2',3'-*c*]phenazine

*Figure 47: 7 with numbering of chemically nonequivalent carbons.*

## Characterization of 7.

The proton NMR (400 MHz, $CDCl_3$, Figure 48) shows five double doublets, one for each chemically nonequivalent proton at position 1, 2, 3, 8 and 9.

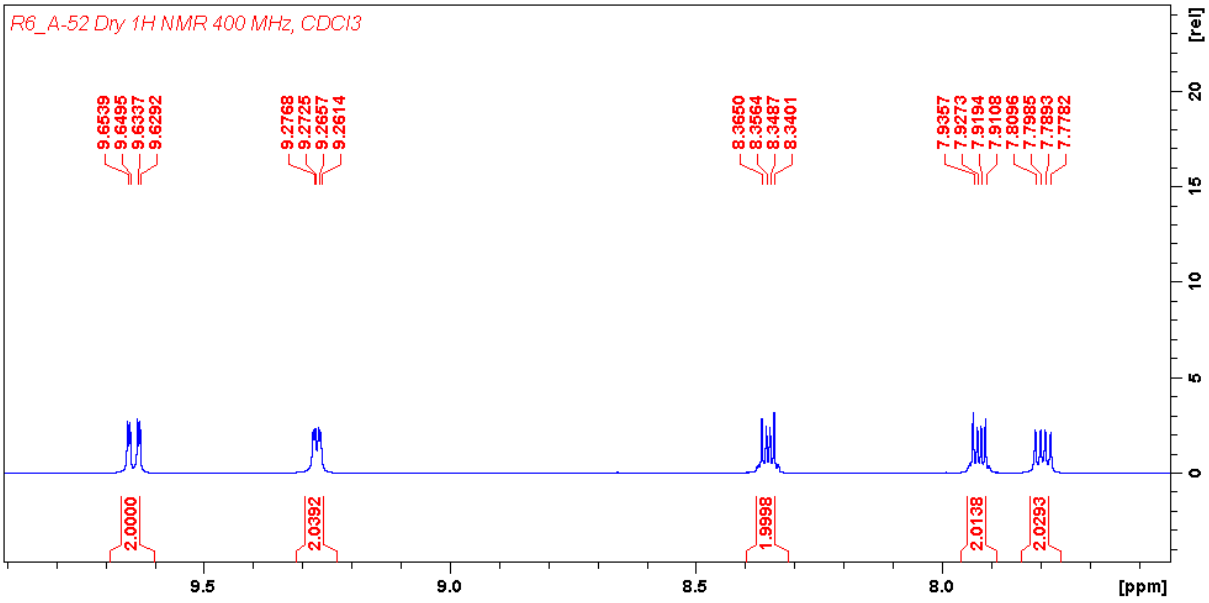


*Figure 48: $^1$H NMR (400 MHz, $CDCl_3$) of the aromatic region of **7**. δ 9.64 (dd, J = 1.8, 8.1 Hz, 2H), 9.27 (dd, J = 1.7, 4.4 Hz, 2H), 8.35 (dd, J = 3.4, 6.5 Hz, 2H), 7.92 (dd, J = 3.4, 6.6 Hz, 2H), 7.79 (dd, J = 4.4, 8.1 Hz, 2H).*

Carbon NMR (101 MHz, CDCl3, Figure 49) shows 9 peaks corresponding to the 9 chemically nonequivalent carbons (**1**-**9**). The five larger peaks correspond to the carbons with protons, as confirmed in DEPT135 spectrum (Figure 50) that shows all the C-H carbons.

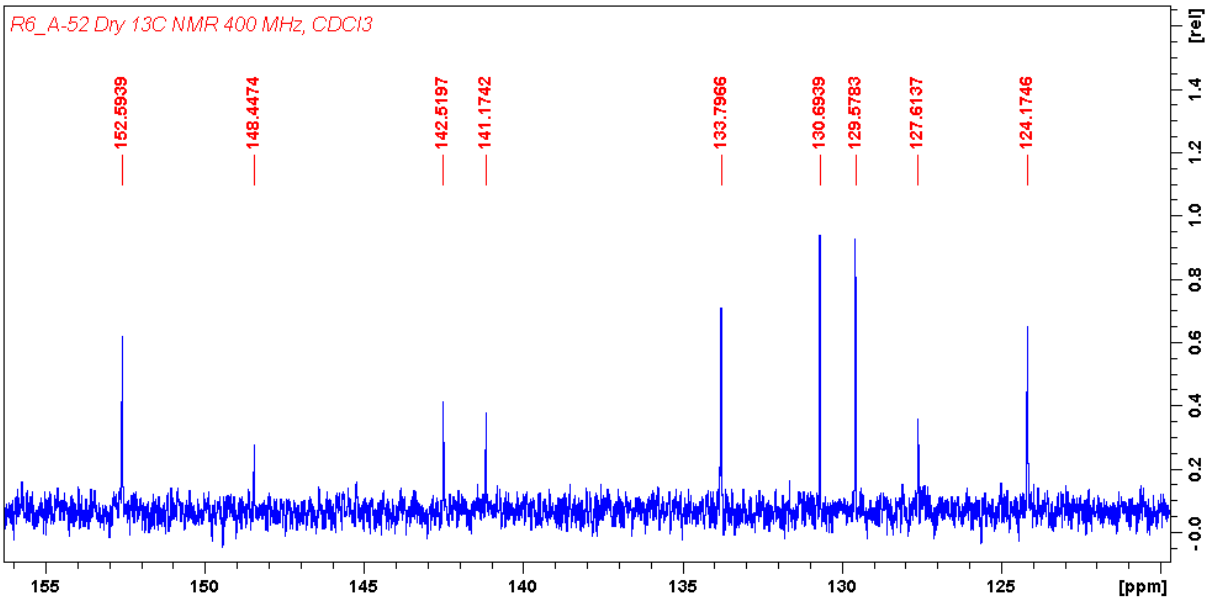


*Figure 49: $^{13}C$ NMR (101 MHz, $CDCl_3$) δ 152.59, 148.45, 142.52, 141.17, 133.80, 130.69, 129.58, 127.61, 124.17.*

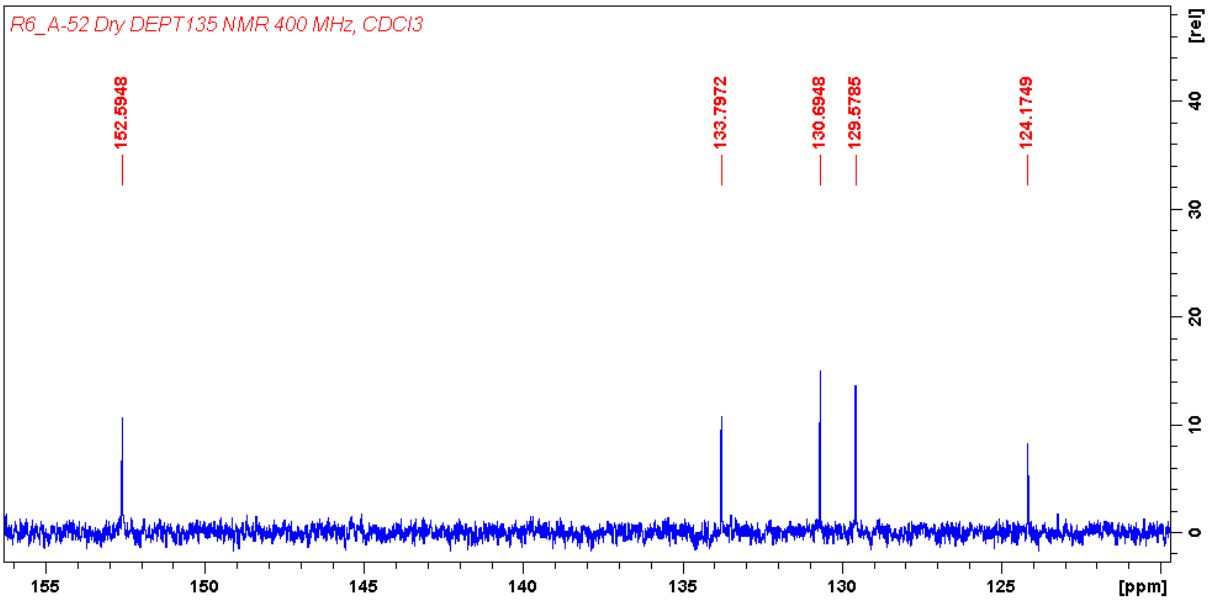


*Figure 50: $^{13}C$ DEPT135 NMR (101 MHz, $CDCl_3$) δ 152.59, 133.80, 130.69, 129.58, 124.17.*

The $^{1}H$ - $^{1}H$ COSY (400 MHz, $CDCl_3$, Figure 51) spectrum of 7 shows two π-systems, one for the protons at 1, 2 and 3 and one for 8 and 9.

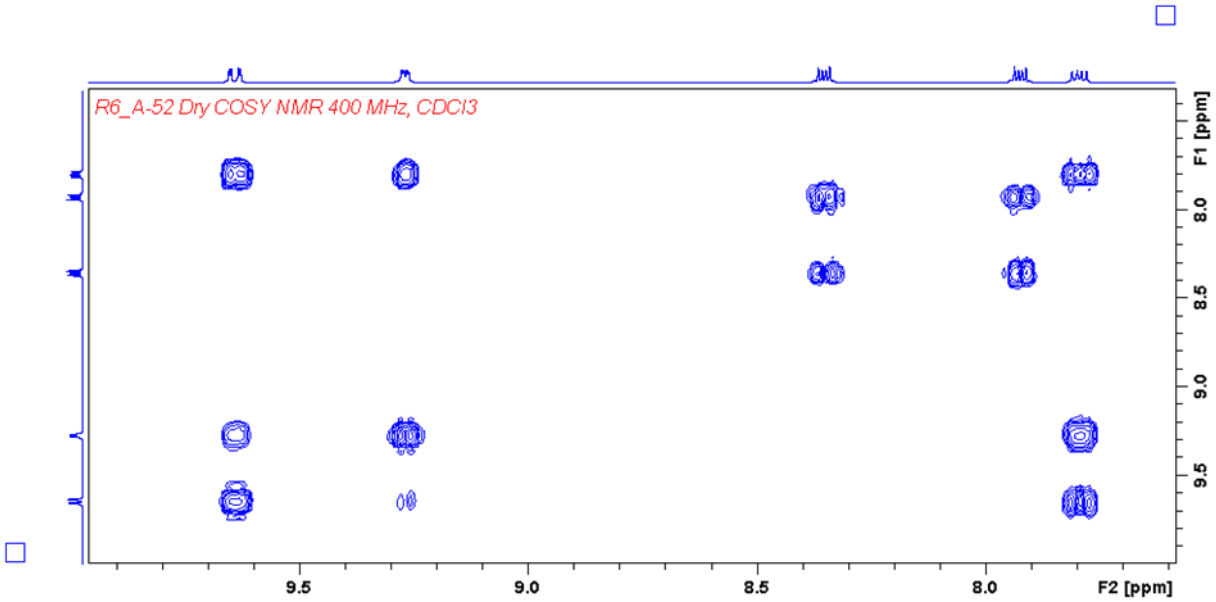


*Figure 51: $^{1}H$ - $^{1}H$ COSY (400 MHz, CDCl3) spectrum of 7.*

The $^{1}H$ - $^{13}C$ HSQC spectrum (Figure 52) shows five proton - carbon $^{1}J$ correlations and helps assign the carbon signals to the proton signals.

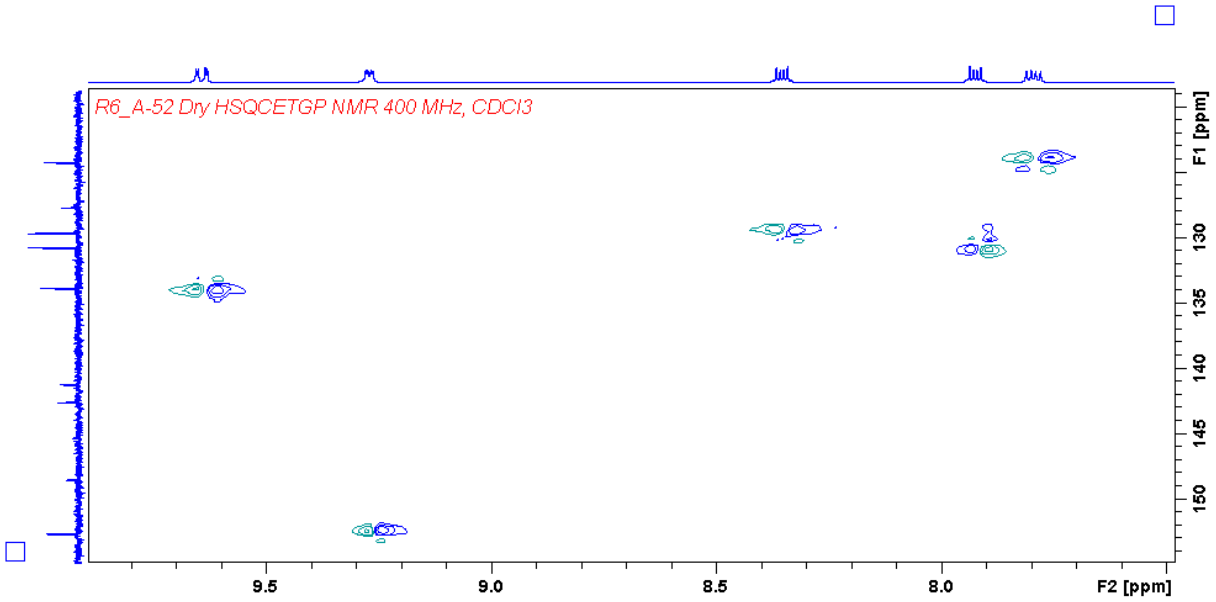


*Figure 52: $^{1}H$ - $^{13}C$ HSQC (400/101 MHz, $CDCl_3$) spectrum of **7**.*

The $^{1}H$ - $^{13}C$ HMBC (400/101 MHz, CDCl3, Figure 53) spectrum of 7 shows proton – carbon $^{2}J$ to $^{4}J$ correlations.

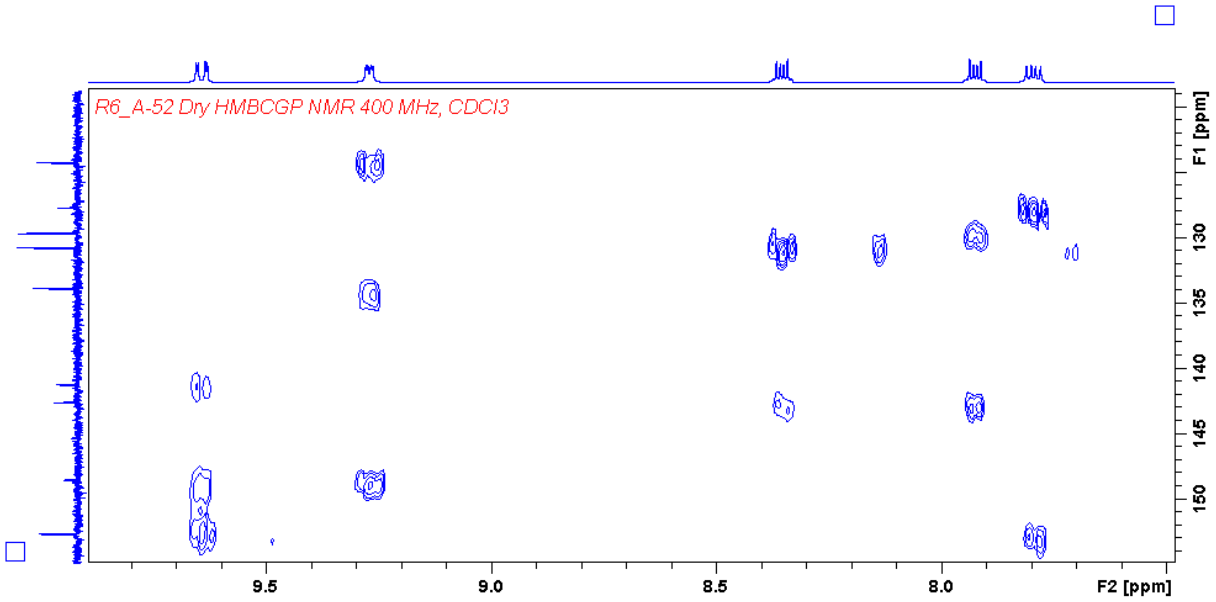


*Figure 53: $^{1}H$ - $^{13}C$ HMBC (400/101 MHz, CDCl3) spectrum of 7.*

## 2.8 Attempted synthesis of 4,4'-(dipyrido[3,2-a:2',3'-c]phenazine-11,12-diylbis(ethyne-2,1-diyl))dibenzonitrile (8)

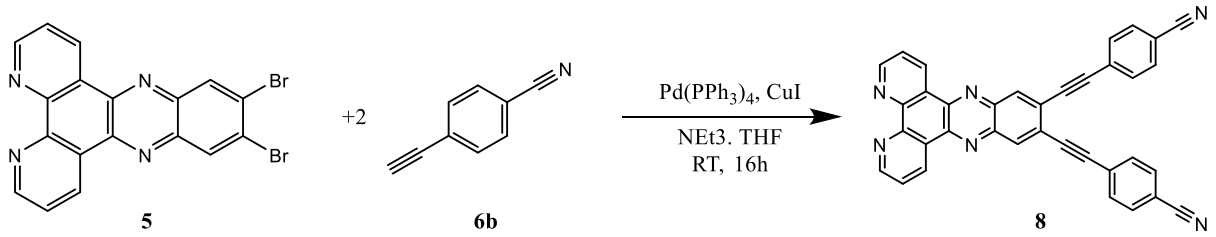


The reaction was done mostly according to literature[29, 30] but a different palladium catalyst ($Pd(PPh_3)_4$) were used. Because of the small amount of 5 available for the reaction it was tried to do the reaction by stirring at r.t. for 16 h as was done by Thorand and Krause [30]. This was not successful. It might be necessary to reflux the reaction mixture overnight as van der Salm et al.[29] did. This might require some more solvent and smaller reflux setup than was available. The crude did not show any product in $^{1}H$ NMR but mostly the reactant **6b** and the catalyst. No further purification was done.

Figure 54 and Figure 55 shows a comparison of the $^{1}H$ NMR (400 MHz, $CDCl_3$) spectra from crude of 8 (bottom), reactants **6b** and **5**, and top catalyst $Pd(PPh_3)_4$. There is no sign of **5** in the spectrum for **8**.

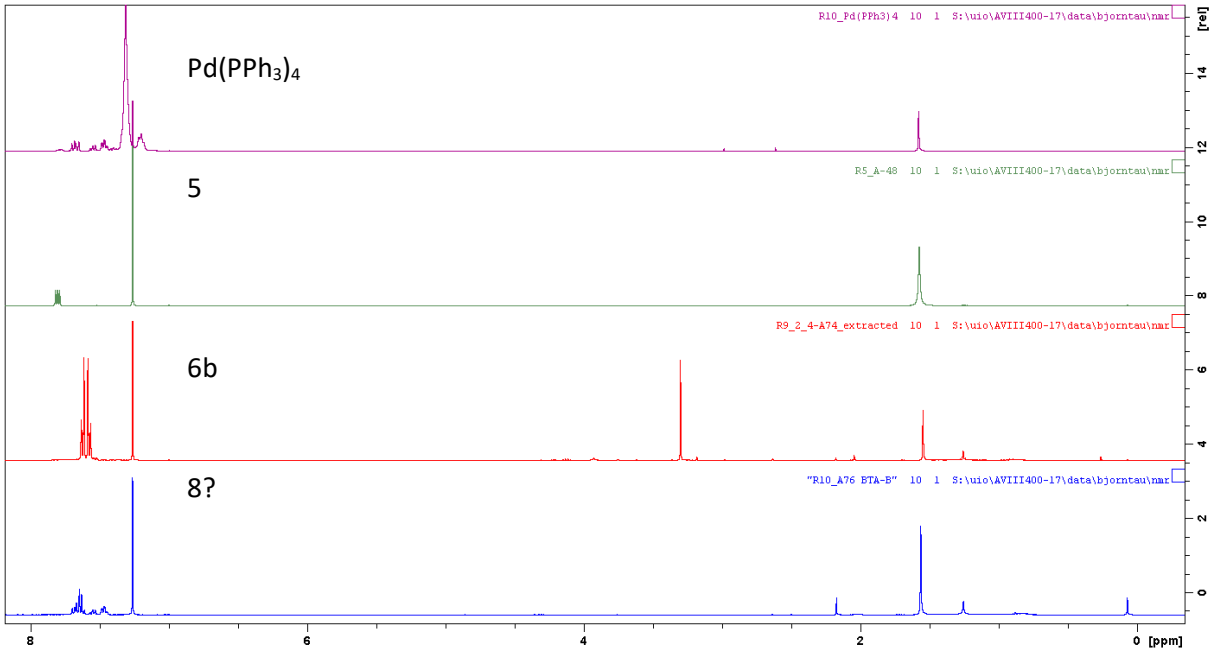


*Figure 54: $^{1}H$ NMR (400 MHz, $CDCl_3$) from bottom: crude from **8**, **6b**, **5** and top catalyst $Pd(PPh_3)_4$.*

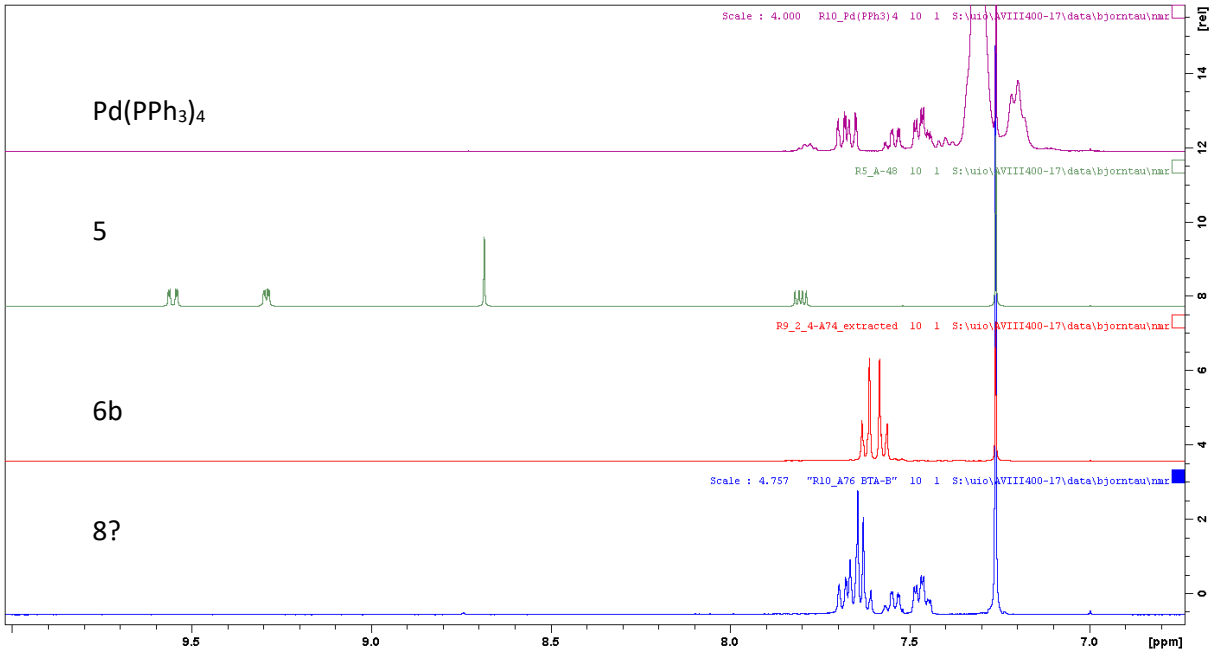


*Figure 55: Aromatic region of the same spectra as in Figure 54.*

# 3. Experimental

## General

NMR spectra were recorded using a Bruker AVIII HD 400 MHz NMR spectrometer at the Department of Chemistry at UiO. Deuterated chloroform were used as solvent and chemical shifts were referenced to signals at 7.26 for $^{1}H$ and 77.0 ppm for $^{13}C$, with TMS as the internal standard. Mass spectra were recorded on a maXis II instrument with electrospray ionization (ESI) or atmospheric pressure chemical ionization (APCI). High-resolution mass spectrometry (HRMS) with suggested molecular formula and simulated isotopic pattern was provided for most of the compounds. The analysis was done by the Mass Spectrometry Laboratory at the department of chemistry at UiO.

Melting points were determined with a Stuart SMP10 instrument. Starting materials, solvents and catalysts were from commercial sources and used without further purification.

## 3.1 Synthesis of 1

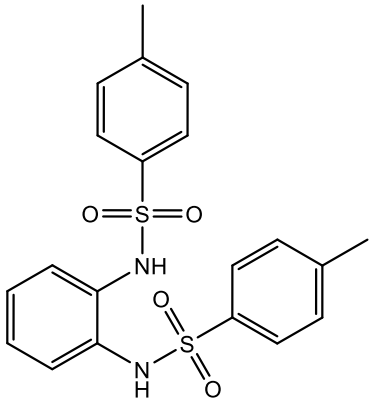

*N*,*N*'-(1,2-phenylene)bis(4-methylbenzenesulfonamide)

### Reaction in microwave.

The reaction was done according to literature[21] with some modifications for the workup. o-Phenylenediamine (37.36 mmol, 4.4 g) and p-Toluenesulfonyl chloride (2 eq, 74.72 mmol, 14.25 g) was added to a beaker with 16.5 mL pyridine while stirring. The solution got hot. The reaction was done in two baches in microwave for 4 min at 120 °C. Pyridine was removed from the combined batches by reduced pressure at 80 °C for 1 hour. A thick black or dark brownish liquid resulted. This was dissolved in chloroform (40 mL) and filtered on a 3 cm column of silica gel. Only some of the eluent came through before a black layer clogged the silica gel. The chloroform was removed from the filtrate by reduced pressure and the resulting white solid was dissolved in n-Hexane by heating. After cooling a precipitate was filtered of. This gave a white pinkish solid (0.3 g, yield = 2 %).

The rest of the eluent and the black/brownish layer in the column was then pulled through the column by applying vacuum suction and adding more eluent. A black/brownish solution resulted that did not dissolve in n-hexane after eluent was removed. An alternative work up procedure from Shao et al.[22] was then followed. The black thick liquid was dissolved in chloroform (50 mL) and extracted with 1M HCl (50 mL) and water (25 mL x 4). A precipitate in the chloroform phase was filtered. The white sluggish precipitate was washed with chloroform and water on the filter, then dissolved in ethanol, filtered and dried. A light pink solid resulted (6.0 g, yield = 36 %). This gave a total of 6.3 g with a yield of 38 %.

### Reaction at room temperature.

The reaction was done according to literature[22] with some modifications. p-Toluenesulfonyl chloride (2 eq, 114.87 mmol, 21.9 g) was added slowly to a solution of o-Phenylenediamine (1 eq, 57.86 mmol, 6.25 g) in dry pyridine (33 mL) which was cooled to -3 to -5 °C in a NaCl–ice bath. The resulting mixture was stirred at room temperature for 18 h. About 25 mL 15 % aqueous HCl was added to form a precipitate. The solids were filtered off, washed with some more 15 % HCl and water, dissolved in about 100 mL absolute ethanol and refluxed for 1 h. It was cooled overnight, and the solids were filtered off, washed with some EtOH and dried. The product was obtained as a pale solid (17.0 g, yield = 71 %).

$^1$H NMR (400 MHz, $CDCl_3$): δ ppm = 7.57 (d, J = 8.3 Hz, 4 H), 7.21 (d, J = 8.1 Hz, 4 H), 7.05–6,05 (m, 2 H), 6.98–6.92 (m, 4 H), 2.39 (s, 6 H).

$^{13}$C NMR (100 MHz, $CDCl_3$): δ ppm = 144.18, 135.39, 130.79, 129.60, 127.52, 127.31, 126.09, 21.58.

ESI-MS+ (m/z): Calculated for $C_{20}H_{20}N_2O_4S_2$: 416.08645 ([M]+); found 416.089 ([M]+, 100%) (error = 6,7 ppm)

Melting point: 205 – 206 °C. Lit.[31] 204-205 °C.

## 3.2 Synthesis of 2

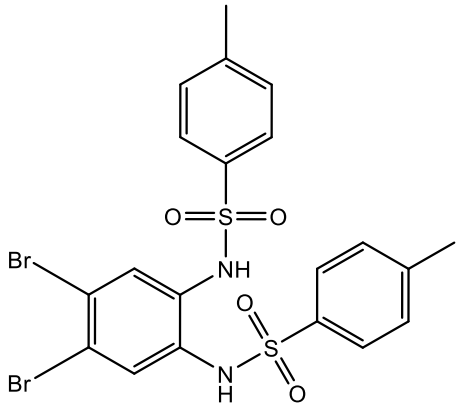


*N*,*N*'-(4,5-dibromo-1,2-phenylene)bis(4-methylbenzenesulfonamide)

### Method 1 with bromine.

The synthesis was done according to literature [22]. Bromine (3.25 g, 1.04 mL, 20.3 mmol, 2 eq) was added drop-wise with a syringe to an ice-cooled and stirred suspension of **1** (4.24 g, 10.2 mmol, 1 eq) and anhydrous NaOAc (4.43 g, 54.0 mmol, >2 eq) in glacial acetic acid (33 mL). The mixture was stirred and refluxed at 110 °C for 3 h, then cooled and poured into ice water (110 mL), and then stirred for an additional 1 h. The precipitate was filtered and dried overnight (70 °C). The solids were dissolved in EtOH (50 mL), filtered four times and dried (50 °C). It gave a white powder (3.74 g, yield = 64 %).

$^{1}$H NMR (400 MHz, $CDCl_3$): ppm = 7.60 (d, J=8.3, 4H), 7.28 (d, J=8.0, 4H), 7.20 (s, 2H), 6.79 (br, 2H), 2.42 (s, 6H).

$^{13}$C NMR (100 MHz, $CDCl_3$): ppm = 144.84, 134.82, 130.71, 130.04, 129.88, 127.55, 122.63, 21.63.

ESI-MS+ (m/z): calcd for $C_{20}H_{18}Br_2N_2O_4S_2$: 571.9075; found 571.9068. (error = −1.2 ppm).

### Method 2 with NaBr and $KBrO_3$

The method was based on literature [24]. Compound **1** (4.16 g, 10 mmol) and glacial acetic acid (22 mL) was added to a round bottom flask. A mixture of NaBr (3.39 g, 33 mmol) and $KBrO_3$ (1.12 g, 6.7 mmol) was added in portions at room temperature and stirred for 6 hours at °60 C. The mixture was cooled down over night and the precipitate was filtered off and washed with warm water, air dried and recrystallized in ethanol. It gave a white powder (4.2 g). NMR showed only partial conversion with a side product.

## 3.3 Synthesis of 3

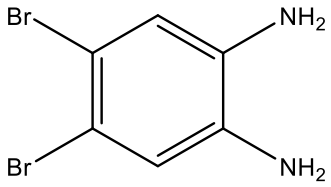


4,5-dibromobenzene-1,2-diamine

The reaction was done according to literature.[22] Compound **2** (0.946 g, 1.65 mmol) was heated on oil-bath in 2 mL concentrated sulphuric acid at 104-113 °C for 22 min. The solution changed to a dark purple color. After cooling to room temperature, it was poured into ice water (65 mL). A white precipitate formed immediately. It was neutralized with about 7 mL 50 % NaOH solution until basic and stirred for 5 minutes. The white precipitate was filtered off and cleaned three times with water on the filter. It was dried in oven at 80 °C for approximately 1 hour. A white powder resulted. Yield: 0.385 g, 88 %.

$^{1}$H NMR (400 MHz, $CDCl_3$) δ 6.93 (s, 2H, C**H**), 3.40 (br, 4H, N**H**$_2$).

$^{13}$C NMR (101 MHz, $CDCl_3$) δ 135.35 (**C**NH2), 120.46 (**C**H), 113.49 (**C**Br)

ESI-MS+ (m/z): calcd for $C_6H_6Br_2N_2H^+$: 264.89705; found: 264.897; (error = -0.04 ppm). The isotopic pattern matched the expected.

Melting point: 142-144 °C, lit.[32] 135-139 °C.

### 3.4 Synthesis of **4**

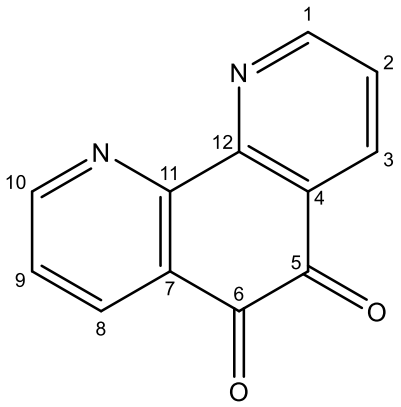


1,10-phenanthroline-5,6-dione

The reaction was done according to literature [25]. $H_2SO_4$ (40 mL, 95 %) and $HNO_3$ (20 mL, 68 %) was stirred and cooled in ice-water bath. This was added to A mixture of 1,10-phenanthroline (4.032 g, 22.37 mmol) and KBr (4.18 g, 35.13 mmol) in a 100 mL round bottom flask. It was then stirred on ice-bath for 10 min before heated to 90 °C for 2h. The crude product was let cool down over night and then poured into a beaker with ice (120 g) and neutralized with NaOH (120 mL, 50 %) to pH 6-7. The neutralized product was extracted with $CH_2Cl_2$ (8x50 mL). The solvent was evaporated at reduced pressure and an orange product was observed. It was recrystallized in EtOH (52.5 mL, 95 %) and yellow needles formed on top of a precipitate that was filtered out (2.46 g, yield = 52 %).

$^{1}$H NMR (400 MHz, $CDCl_3$): δ 9.12 (dd, J=4.7, 1.8 Hz, 2H, 1,10-**H**), 8.51 (dd, J=7.9, 1.8 Hz, 2H, 3,8-**H**), 7.59 (dd, 7.9, 4.7 Hz, 2H, 2,9-**H**)

$^{13}$C NMR (101 MHz, $CDCl_3$): δ 178.6768 (5,6), 156.4243, 152.9195, 137.3230, 128.0785, 125.6035

ESI-MS [M+Na]+ calcd 233.03270, found 233.032 (error -3.0 ppm)

Melting point 259-260 °C, lit.[33] 260 °C.

### 3.5 Synthesis of 5

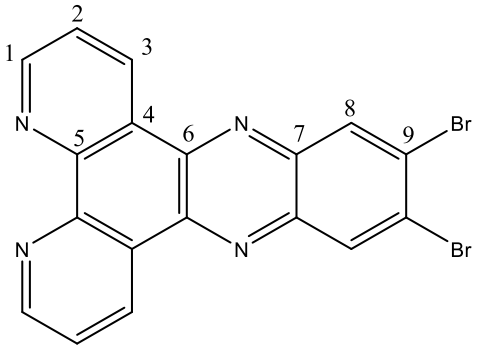


The reaction was performed according to literature[26] but no filtration was done. **3** (0.146 g, 0.549 mmol) and **4** (0.108 g, 0.514 mmol) was refluxed in 30 mL absolute ethanol overnight (15h). The solvent was evaporated under reduced pressure and the product dried at 60°C overnight. This gave an orange solid (0.120 g, Yield =53 %).

$^{1}$H NMR (400 MHz, $CDCl_3$): ppm = 9.55 (dd, J=8.1, 1.7, 2H, 3-**H**), 9.29 (dd, J=4.4, 1.7, 2H, 1-**H**), 8.68 (s, 2H, 8-**H**), 7.80 (dd, J=8.1, 4.4, 2H, 2-**H**).

$^{13}$C NMR (101 MHz, $CDCl_3$): ppm = 153.07 (**1**), 148.56 (**5**), 141.96 (**6**), 141.33 (**7**), 133.89 (**3**), 133.31 (**8**), 127.60 (**9**), 127.04 (**4**), 124.31 (**2**).

MS (ESI+): Calcd. $C_{18}H_8Br_2N_4Na$+ [M+Na+]: 460.9008, Observed: 460.9007, err [ppm] 0.2. The isotopic pattern matches the expected.

Melting point: Above 310 °C

### 3.6 Synthesis of 6

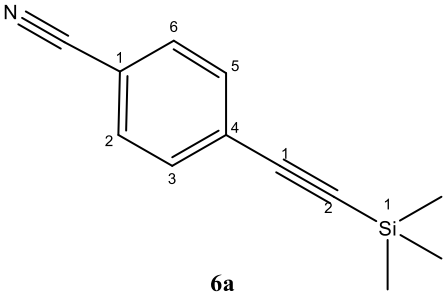


**6a**

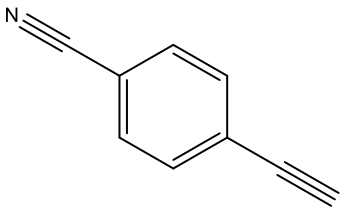


**6b**

The reaction was done in two steps according to literature [27]. First a sonogashira cross coupling was done to make **6a** and then a removal of the protecting trimethylsilyl group to make **6b**.

**6a:** To a 50 mL round bottom flask it was added 4-bromobenzonitril (0.623 g, 3.4 mmol, 1.0 eq.), $Pd(PPh_3)_4$, (93 mg, 2.4 mol %) and CuI (50 mg, 8 mol %). The atmosphere was changed to argon before dry THF (6 mL) and diisopropylamin (2 mL) was added with a syringe. The mixture was cooled down on ice bath and trimethylsilylacetylene (0.50 mL, 3.5 mmol, 1.03 eq.) was added dropwise over 5 min. It was then stirred in room temperature overnight. The solvent in the resulting brown mixture was then removed by rotavapor and the solids dissolved in Hexane (50 mL) and acetone (20 mL). The

mixture was washed with water and the organic layer filtered over celite, dried with $N_2SO_4$ and solvents removed by rotavapor. The product was a white, flaky solid, 682 mg.

**6b:** In a 50 mL round bottom flask **6a** (682 mg, 3.4 mmol, 1 eq.) was dissolved in MeOH (17 mL), followed by addition of $K_2CO_3$ (0.6 g, 4.3 mmol, 1.3 eq.). The reaction mixture was then stirred at room temperature for 1.5 h. MeOH was removed by reduced pressure at 30 °C. The crude was purified by column chromatography on silica gel with CH2Cl2 – Hexane (1:3) as eluent. A white product was isolated (300 mg, yield = 69 %).

$^1$H NMR (400 MHz, $CDCl_3$) δ 7.62 (d, *J* = 8.6 Hz, 2H), 7.57 (d, *J* = 8.6 Hz, 2H), 3.30 (s, 1H).

$^{13}$C NMR (101 MHz, $CDCl_3$) δ 132.70, 132.05, 127.02, 118.27, 112.35, 81.88, 81.55.

HRMS (APCI) calcd for $C_9H_5N_1H^+$ [M+H$^+$]: 128.0496, Found: m/z = 128.0495, err [ppm] -0.9.

Melting point: 157-158 °C, Lit.[34] 156-160 °C

### 3.7 Synthesis of 7

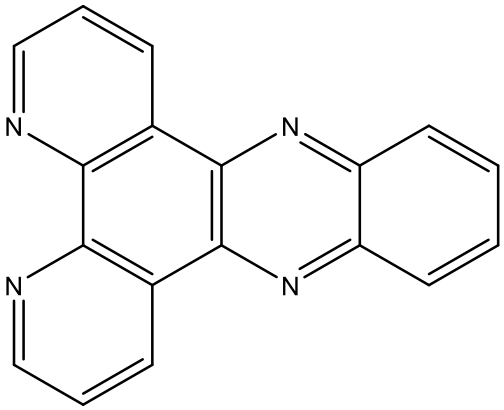

The synthesis was done according to literature [28]. Phendione (0.160 g, 1.43 mmol) and o-phenylenediamine (0.155 g, 0.761 mmol) were dissolved in anhydrous absolute ethanol (30 mL) and refluxed for 10 min. The ethanol was removed by evaporation and the solids dissolved in water (30 mL) and heated. After cooling a white precipitate was filtered off (0.21 g, yield = 98%).

$^1$H NMR (400 MHz, $CDCl_3$) δ 9.64 (dd, J = 1.8, 8.1 Hz, 2H), 9.27 (dd, J = 1.7, 4.4 Hz, 2H), 8.35 (dd, J = 3.4, 6.5 Hz, 2H), 7.92 (dd, J = 3.4, 6.6 Hz, 2H), 7.79 (dd, J = 4.4, 8.1 Hz, 2H).

$^{13}$C NMR (101 MHz, $CDCl_3$) δ 152.59, 148.45, 142.52, 141.17, 133.80, 130.69, 129.58, 127.61, 124.17.

HRMS (ESI+) cald. $C_{18}H_{10}N_4Na$+ [M+Na+] 305.0798, found m/z = 305.0804, err [ppm] -1.9.

Melting point: 262 °C. Lit.[35] 248 °C.

### 3.8 Attempted synthesis of 8

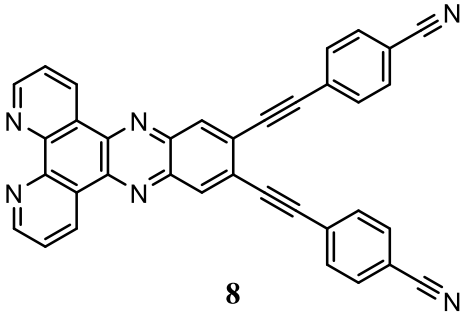

**8**

The reaction was done mostly according to literature[29, 30] but a different palladium catalyst ($Pd(PPh_3)_4$) were used. A mixture of **5** (58 mg, 0.13 mmol, 1 eq.) and **6b** (41 mg, 0,32 mmol, 2.4 eq.) in $NEt_3$ (6 mL) was bubbled with argon for 15 min. CuI (9 mg, 0.05 mmol) and $Pd(PPh_3)_4$ (14 mg, 0.01 mmol) were added and the mixture stirred at r.t. overnight. The crude did not show any product in $^1H$ NMR, mostly the reactant **6b** and the catalyst. No further purification was done.

# 4. Appendix

## Spectra of **1**

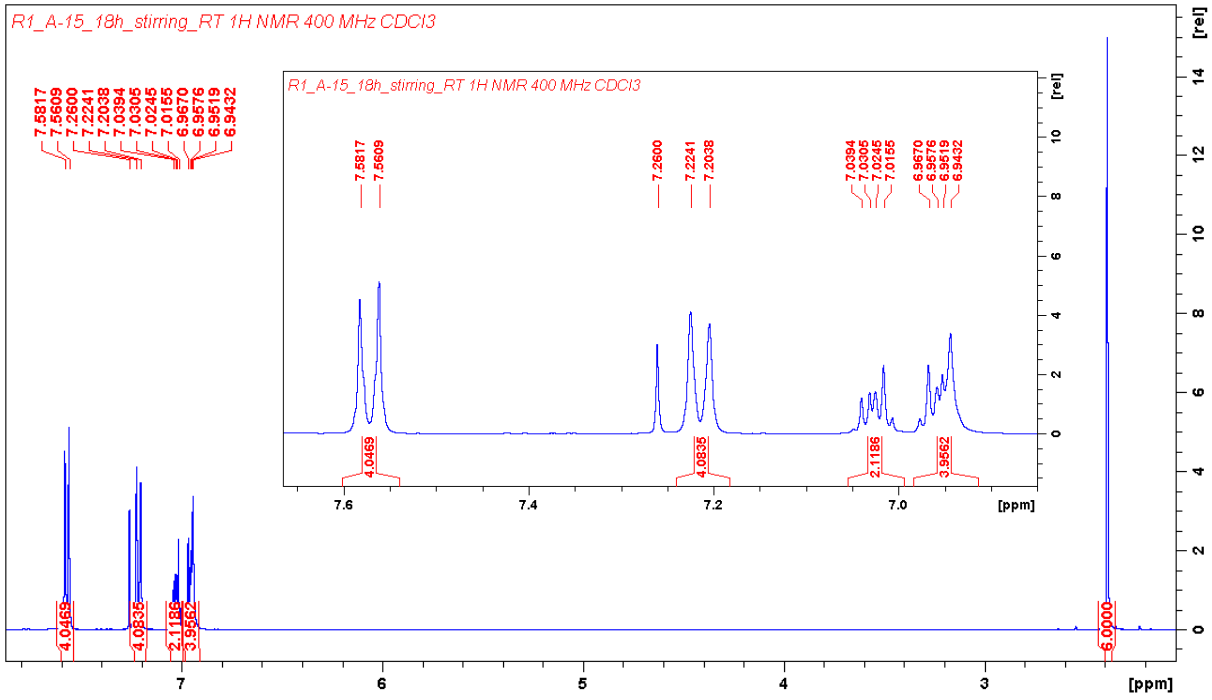


*Figure 56: $^1H$ NMR (400 MHz, $CDCl_3$) of **1**: δ ppm = 7.57 (d, J = 8.3 Hz, 4 H), 7.21 (d, J = 8.1 Hz, 4 H), 7.05–6,05 (m, 2 H), 6.98–6.92 (m, 4 H), 2.39 (s, 6 H).*

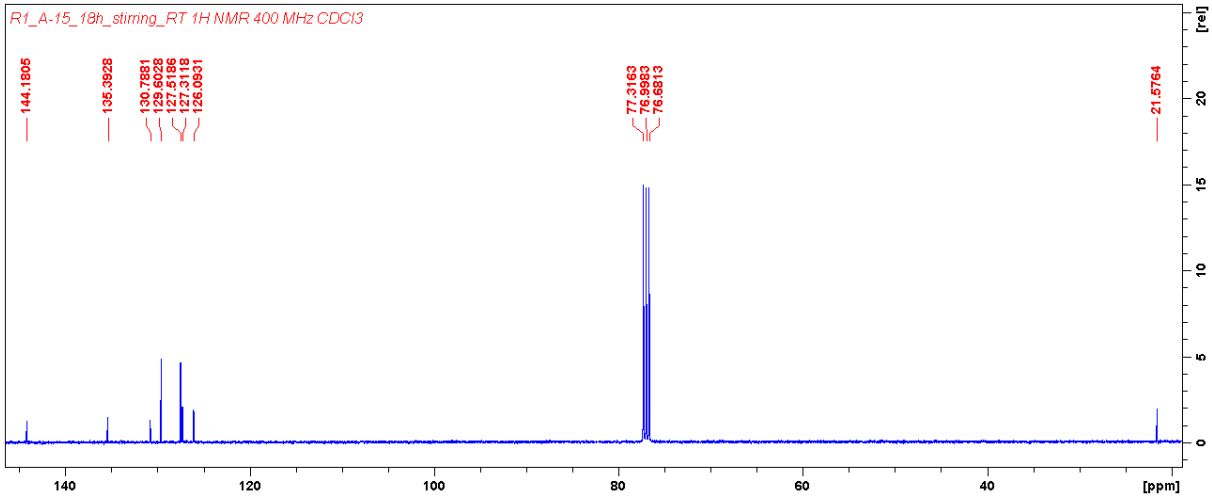


*Figure 57: $^{13}C$ NMR (101 MHz, $CDCl_3$) of **1**: δ ppm = 144,18, 135.39, 130.79, 129.60, 127.52, 127.31, 126.09, 21.58.*

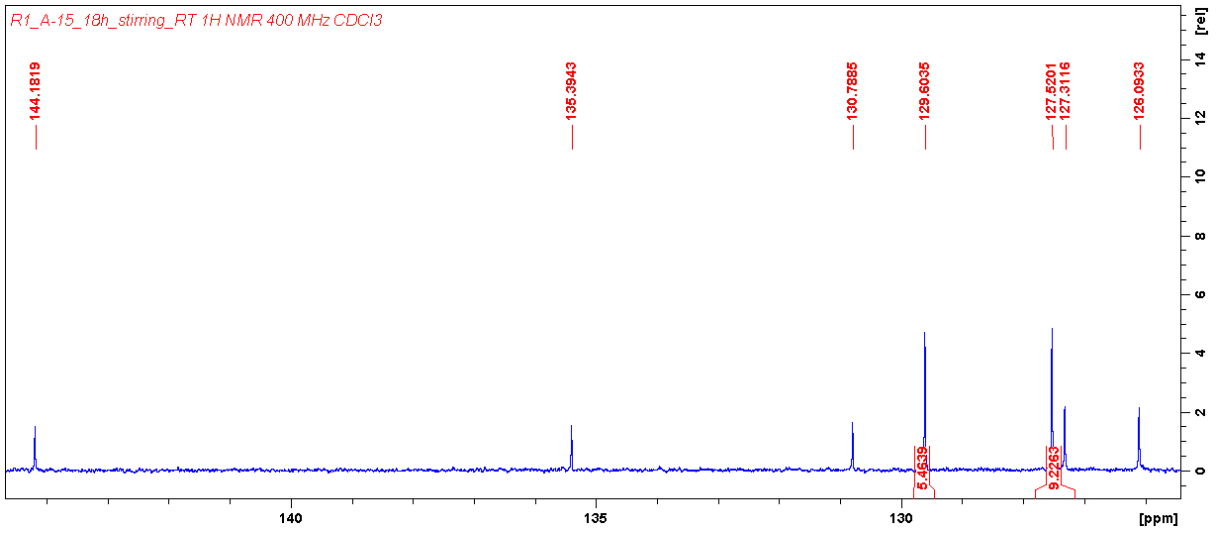


*Figure 58: $^{13}C$ NMR (100 MHz, $CDCl_3$) of the aromatic region of **1**: δ ppm = 144,18, 135.39, 130.79, 129.60, 127.52, 127.31, 126.09.*

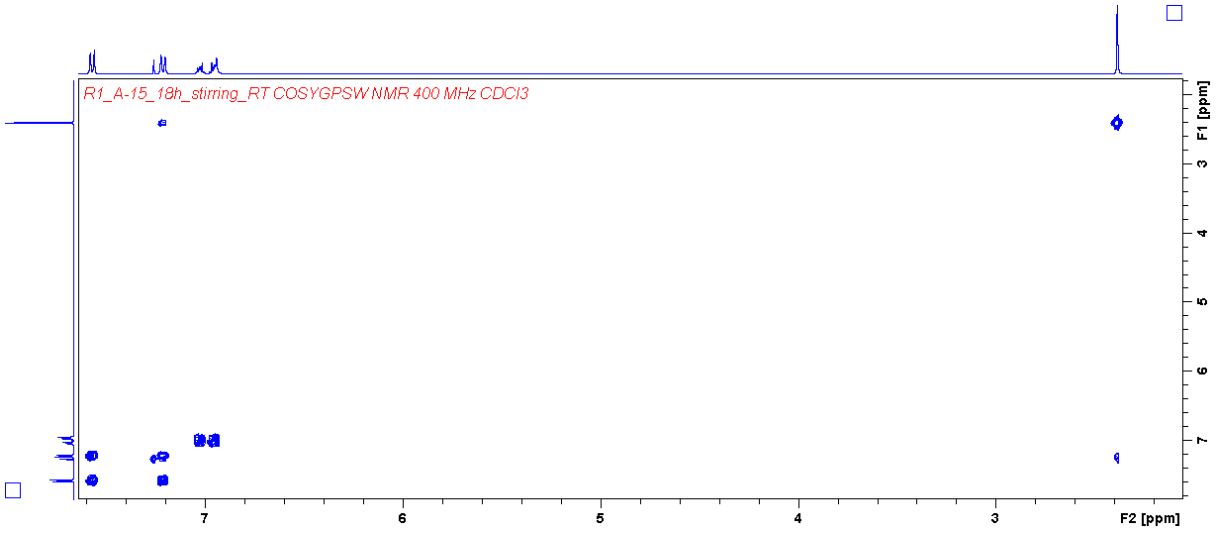


*Figure 59: COSY NMR (400 MHz, $CDCl_3$) of **1** with $^{1}H$-$^{1}H$ correlations.*

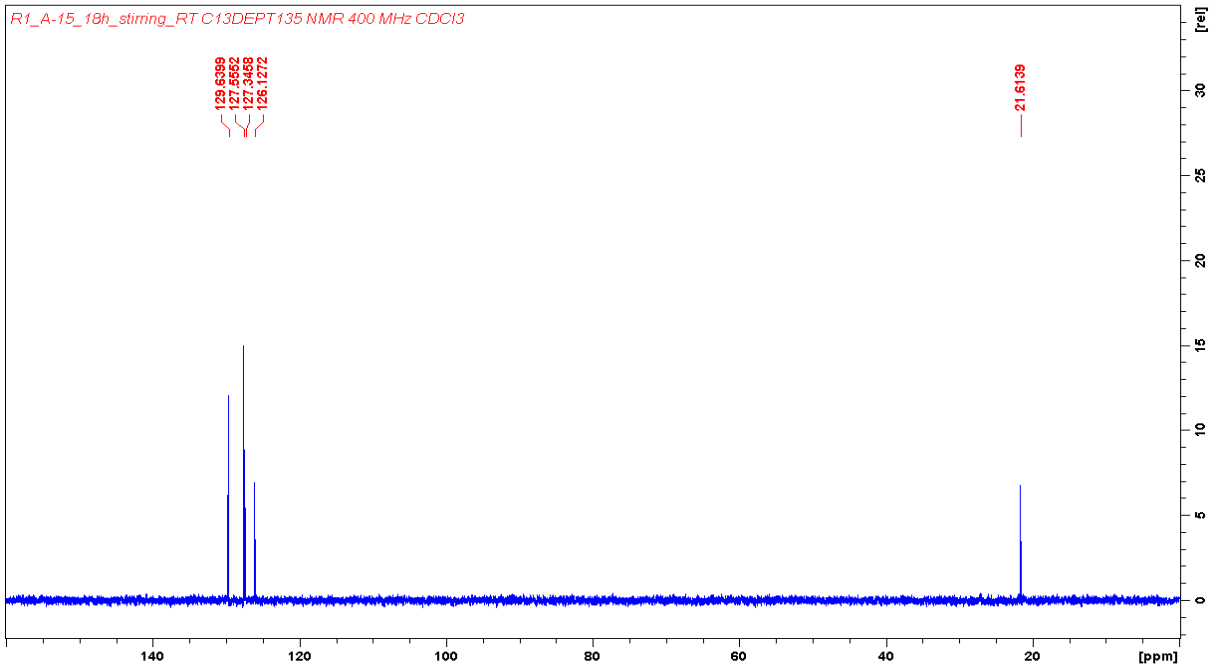


*Figure 60: $^{13}C$ DEPT 135 NMR (100 MHz, $CDCl_3$) of **1**. Spectrum shows carbons with CH or CH3 groups up. Carbons with no protons are not shown. δ ppm = 129.64, 127.56, 127.35, 126.13, 21.61.*

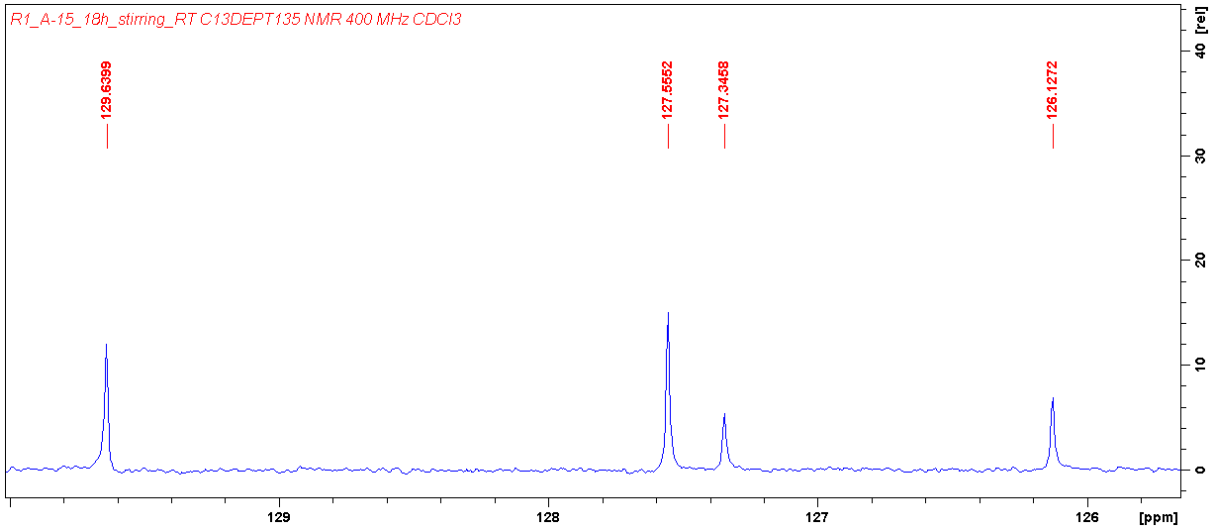


*Figure 61: $^{13}C$ DEPT 135 (101 MHz, $CDCl_3$) of **1** of the aromatic region of carbons with protons attached. δ ppm = 129.64, 127.56, 127.35, 126.13.*

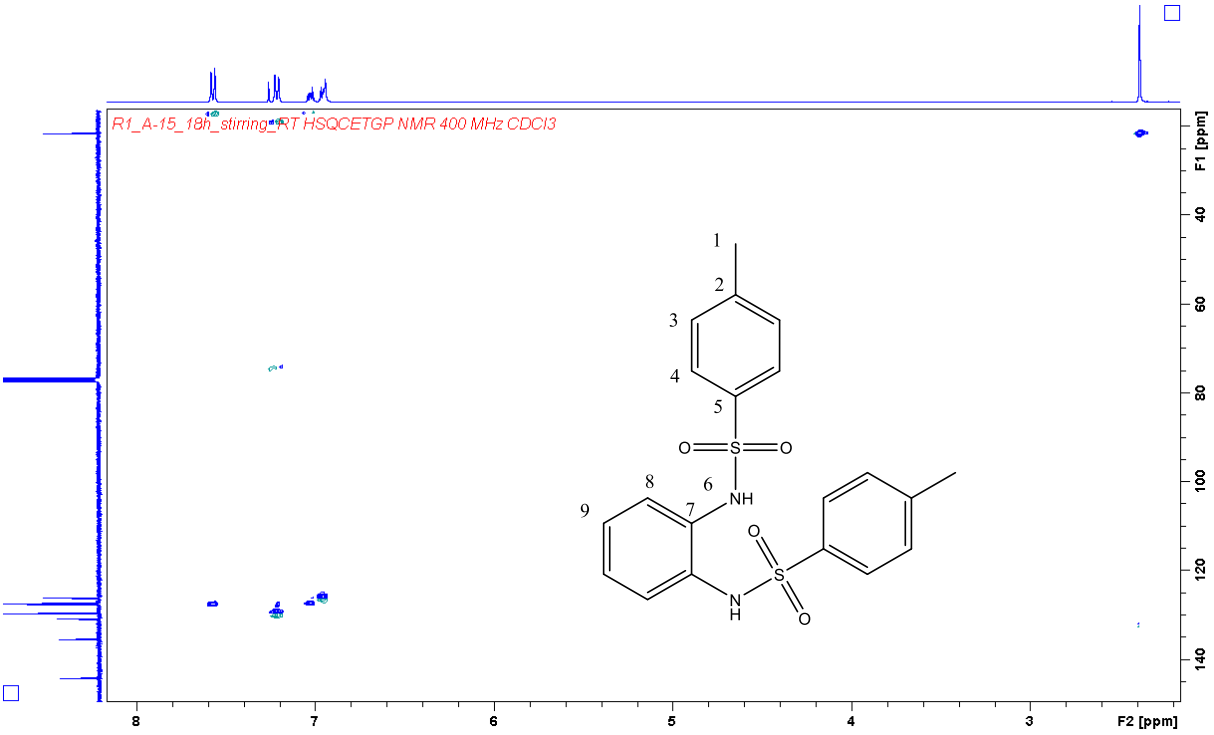


*Figure 62: $^{1}H$ - $^{13}C$ HSQC (400/101 MHz, $CDCl_3$) of **1**.*

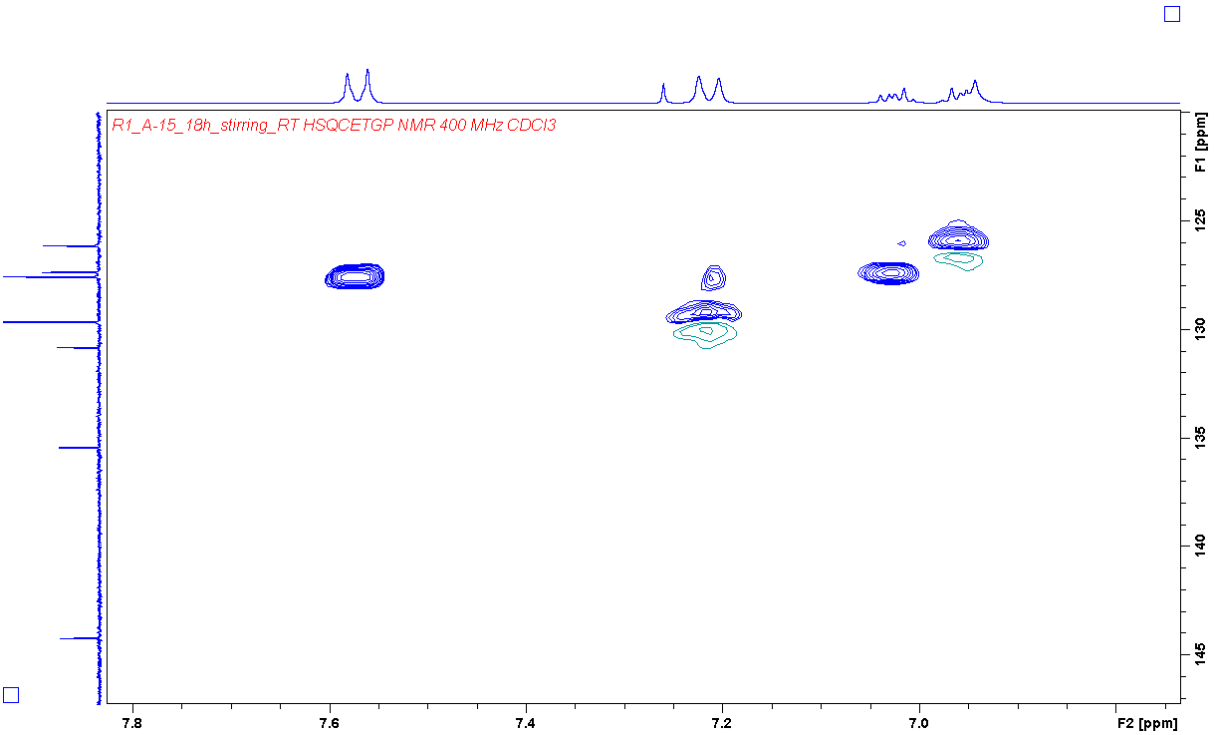


*Figure 63: $^{1}H$ - $^{13}C$ HSQC (400/101 MHz, $CDCl_3$) of aromatic region of **1**.*

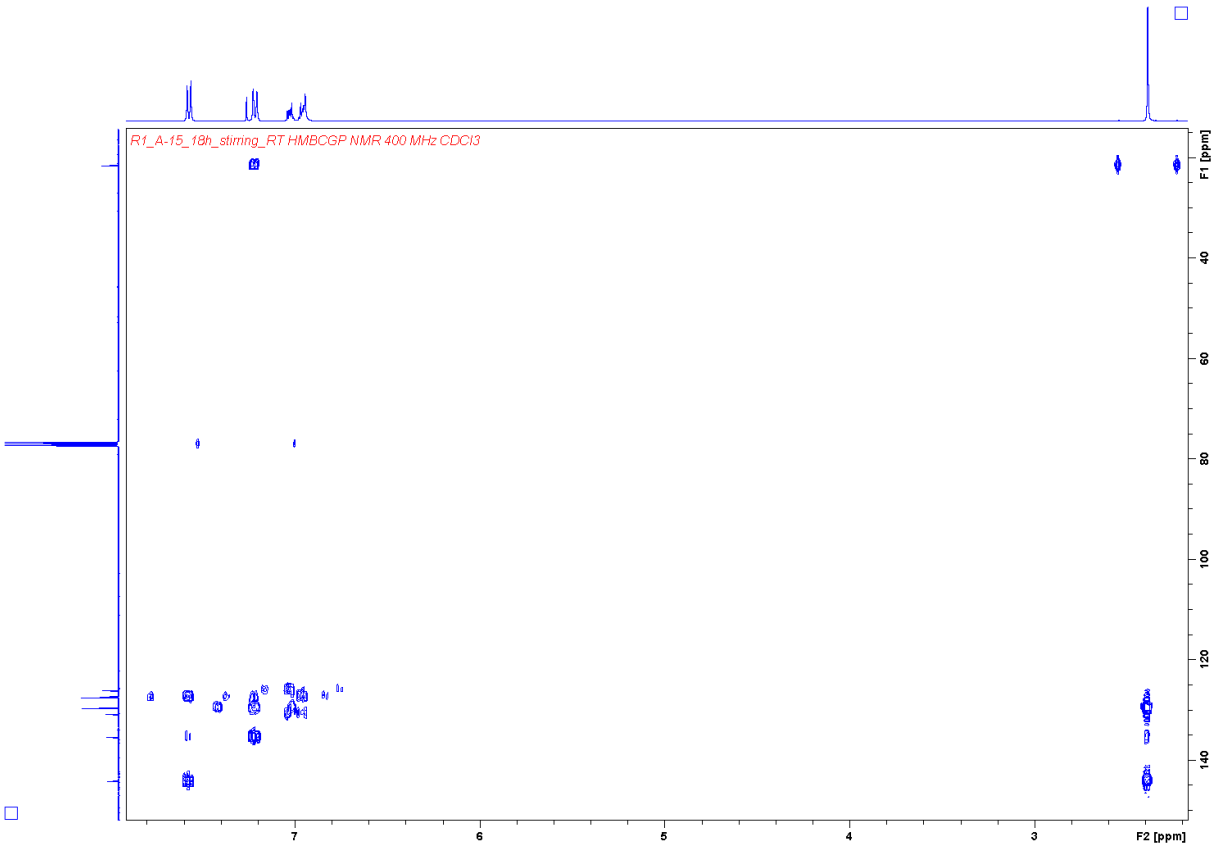


*Figure 64: $^{1}H$ - $^{13}C$ HMBC (400-101 MHz, $CDCl_3$) of **1**.*

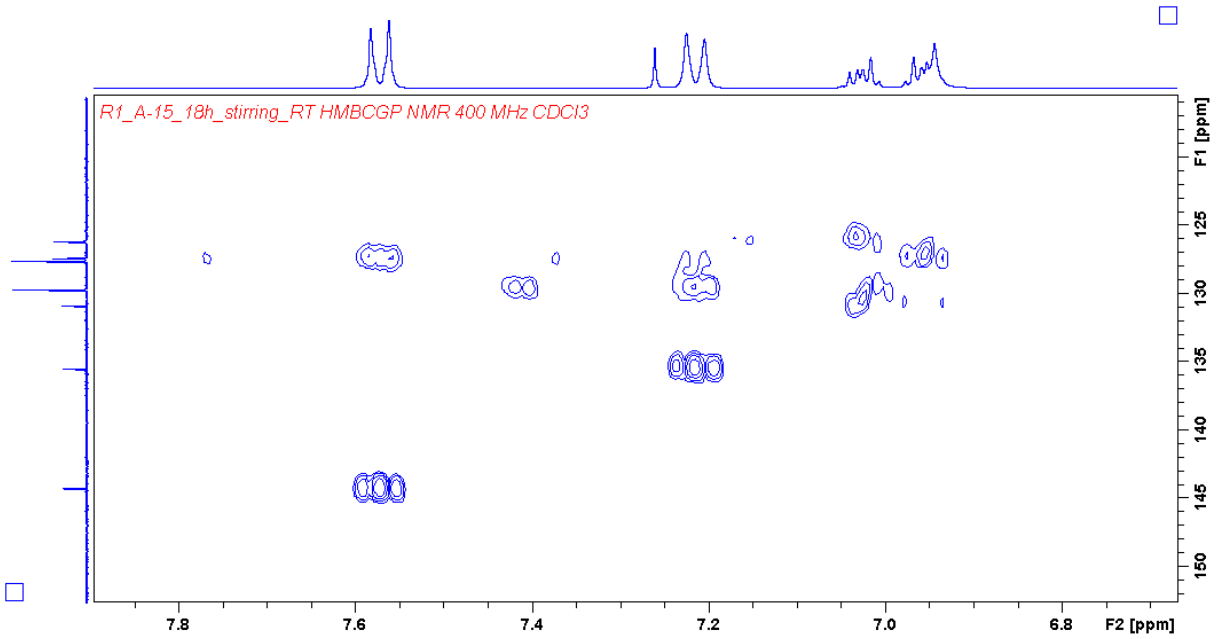


*Figure 65: $^{1}H$ - $^{13}C$ HMBC (400-101 MHz, $CDCl_3$) of aromatic region (weak) of **1**.*

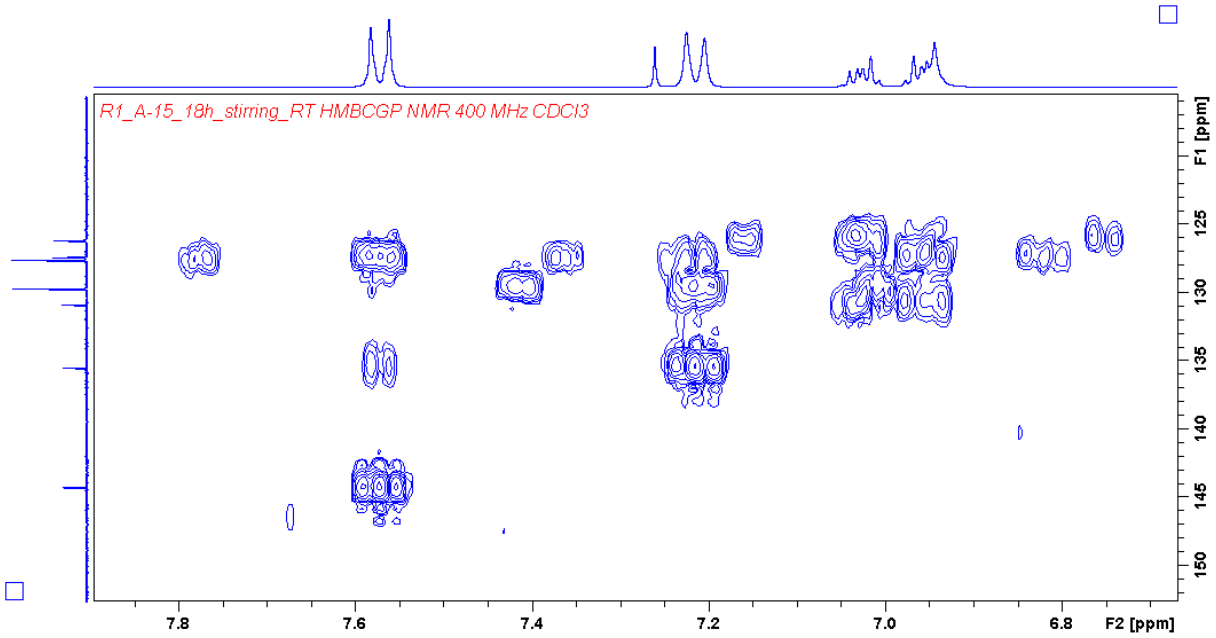


*Figure 66: $^{1}H$ - $^{13}C$ HMBC (400-101 MHz, $CDCl_3$) of aromatic region (strong) of **1**.*

## Spectra of **2**

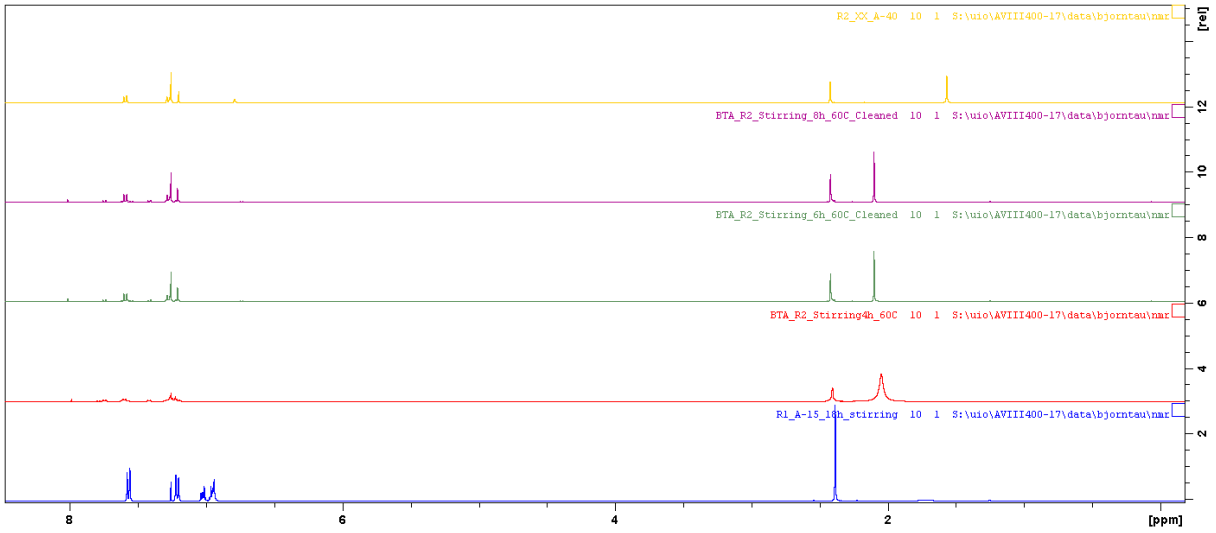


*Figure 67: The figure shows the full $^{1}H$ NMR (400 MHz, $CDCl_3$)spectra for the conversion of **2** for the method with NaBr and $KBrO_3$. From bottom: starting material **1**, conversion after 4 h, 6 h, 8 h and top compound **2** from the reaction with $Br_2$.*

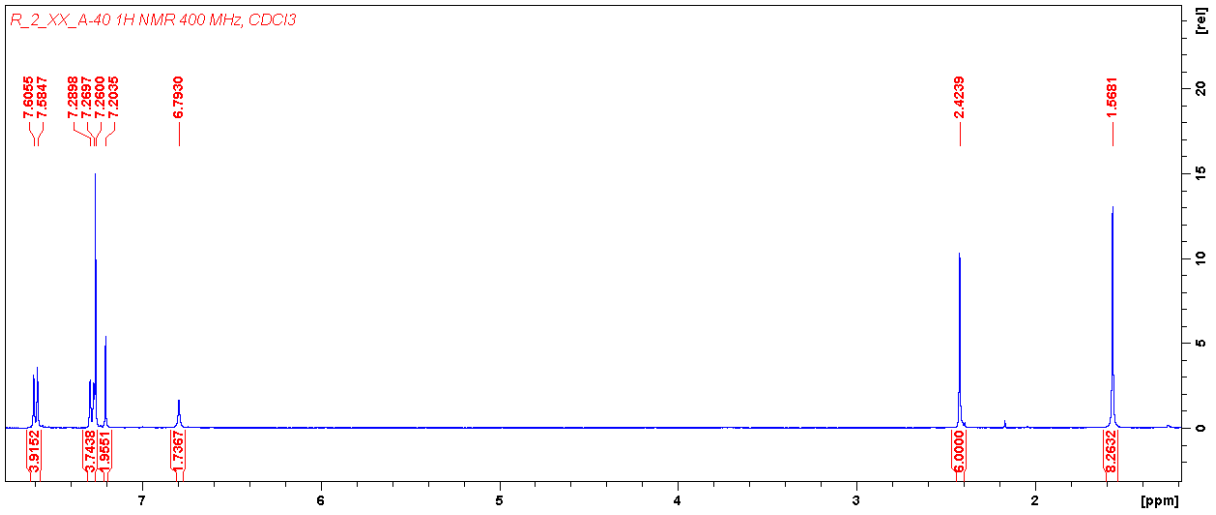


*Figure 68: $^{1}$H NMR (400 MHz, $CDCl_3$) of **2**: ppm = 7.60 (d, J=8.3, 4H), 7.28 (d, J=8.0, 4H), 7.20 (s, 2H), 6.79 (br, 2H), 2.42 (s, 6H).*

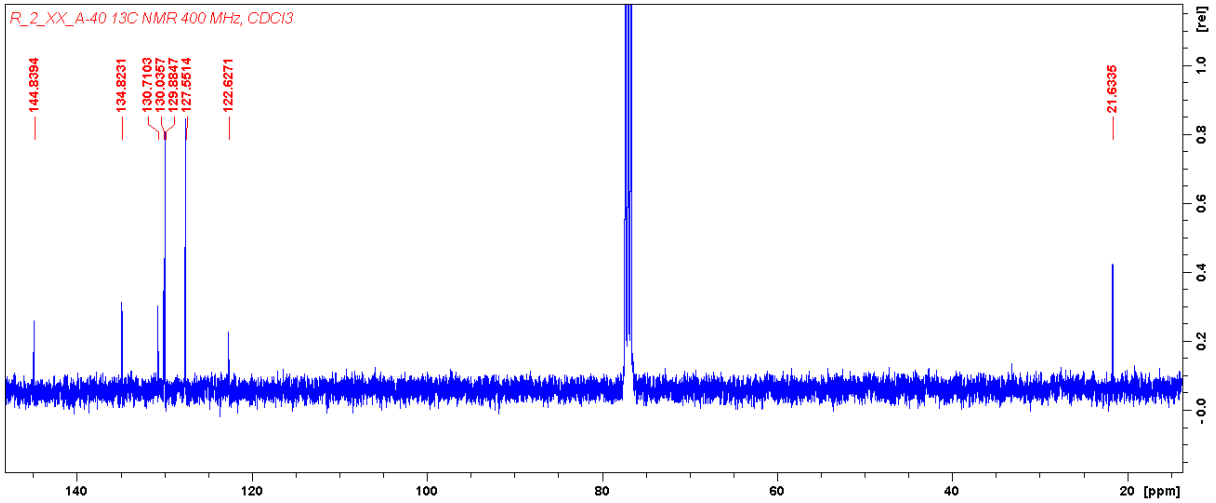


*Figure 69: $^{13}$C NMR (101 MHz, $CDCl_3$) of **2**: ppm = 144.84, 134.82, 130.71, 130.04, 129.88, 127.55, 122.63, 21.63.*

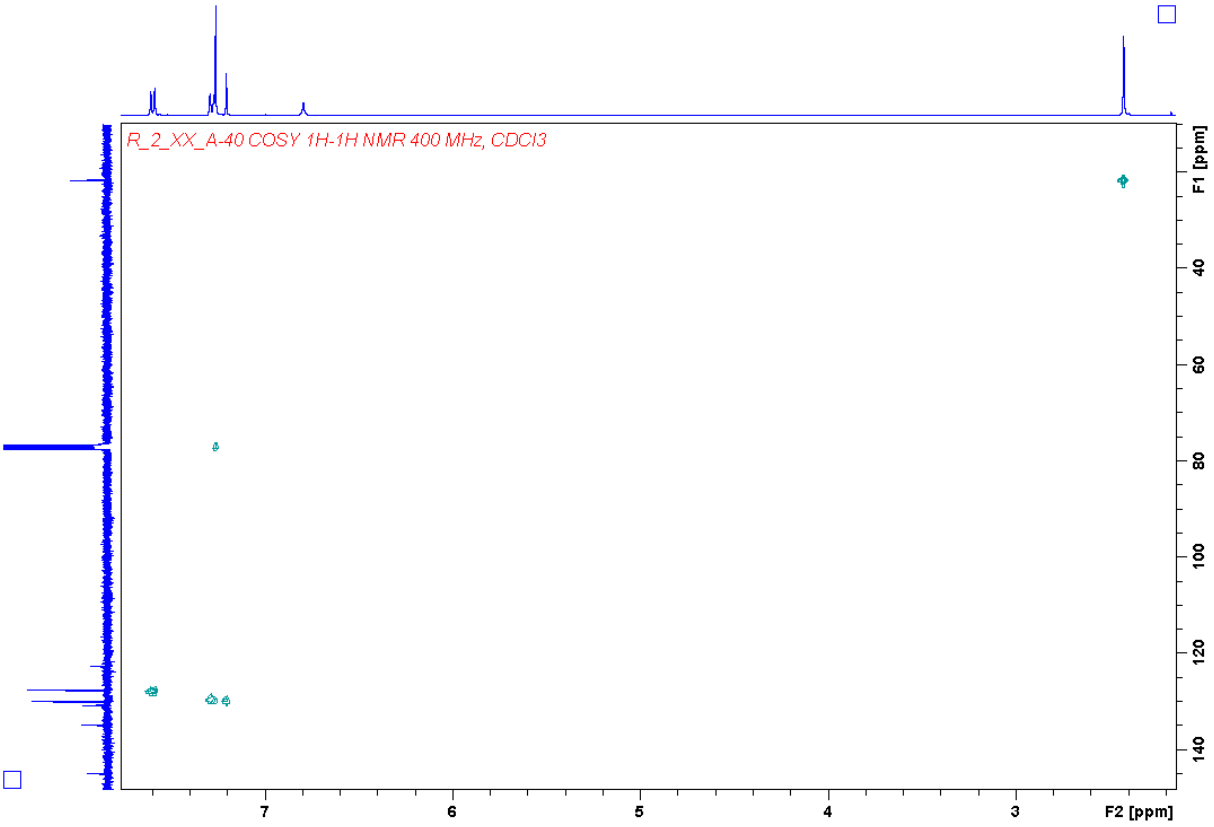


*Figure 70: $^{1}H$ - $^{13}C$ HSQC (400-101 MHz, $CDCl_3$) $^{1}J$ couplings of **2**.*

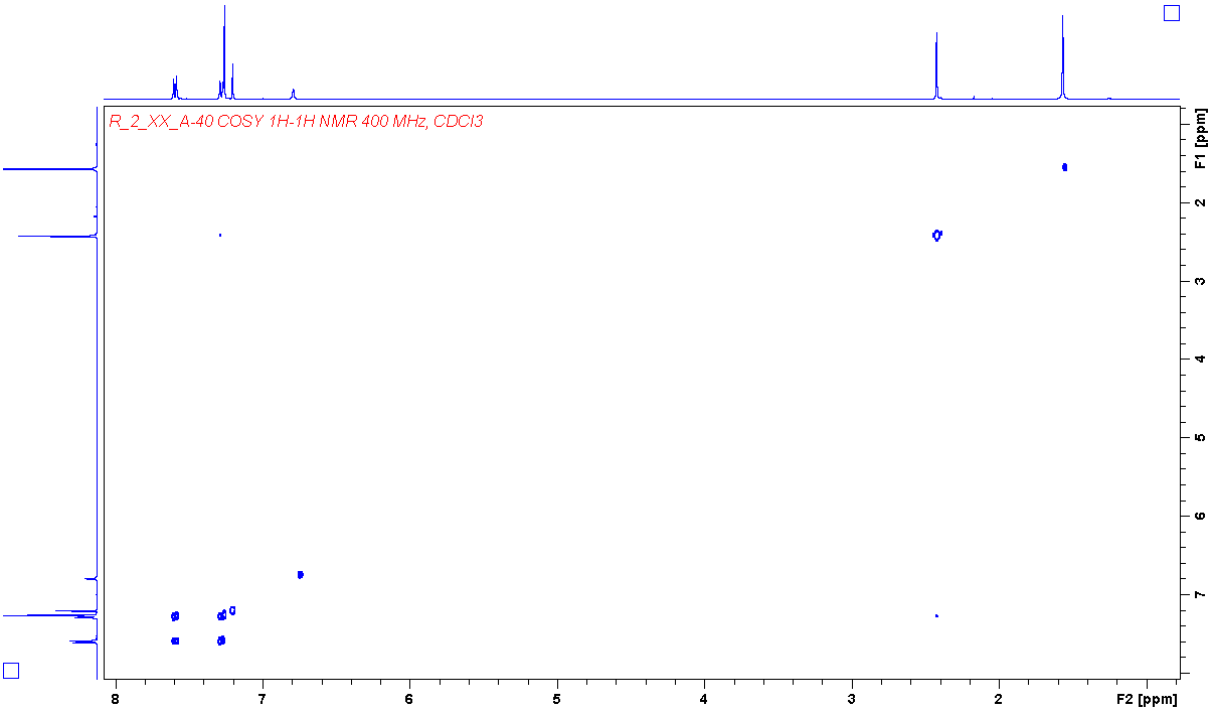


*Figure 71: $^{1}H$ - $^{1}H$ COSY NMR (400 MHz CDCl3) of **2**.*

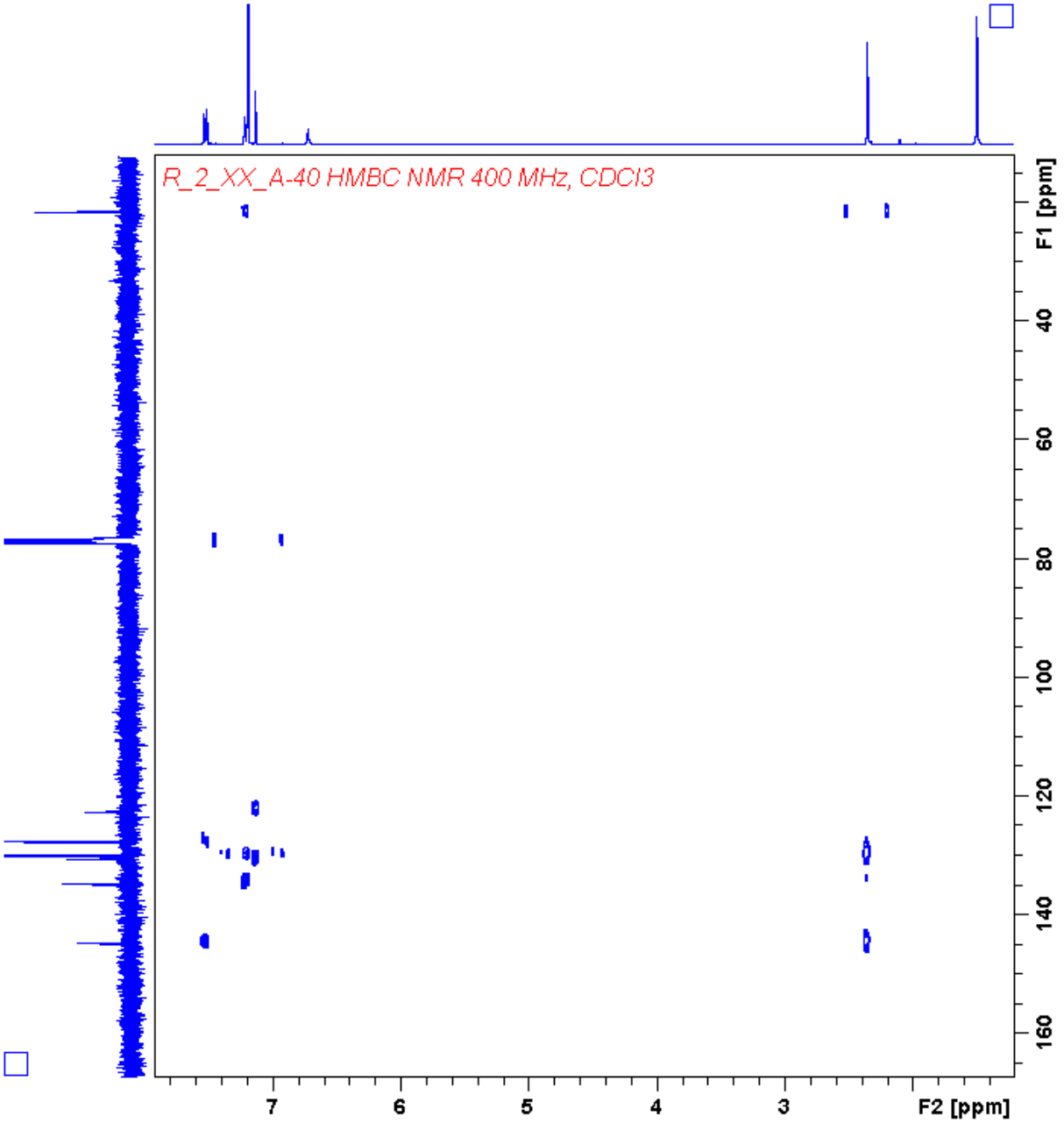


*Figure 72: $^{1}H$-$^{13}C$ HMBC (400-101 MHz, $CDCl_3$) of **2**. The spectrum shows $^{2}J$ to $^{4}J$ couplings but $^{1}J$ couplings can also be observed as satellites.*

## Spectra of **3**

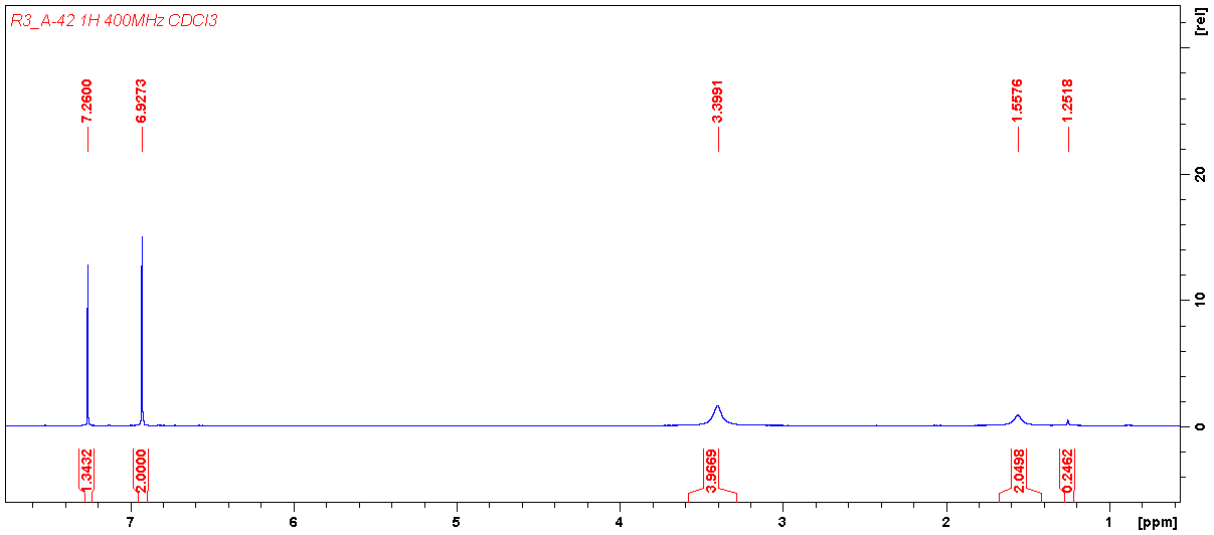


*Figure 73: $^{1}H$ NMR (400 MHz, $CDCl_3$) of **3** (4,5-dibromobenzene-1,2-diamine). ppm = 6.93 (s, 2H), 3.40 (br, 4H).*

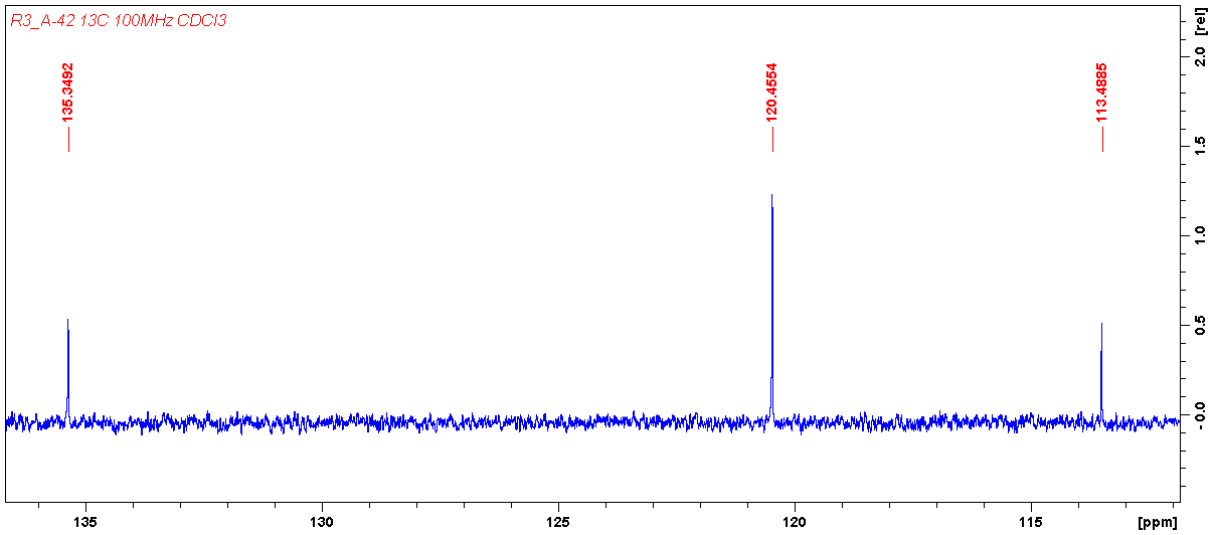


*Figure 74: $^{13}C$ NMR (101 MHz, $CDCl_3$) of **3.** ppm = 135.35, 120.46, 113.49.*

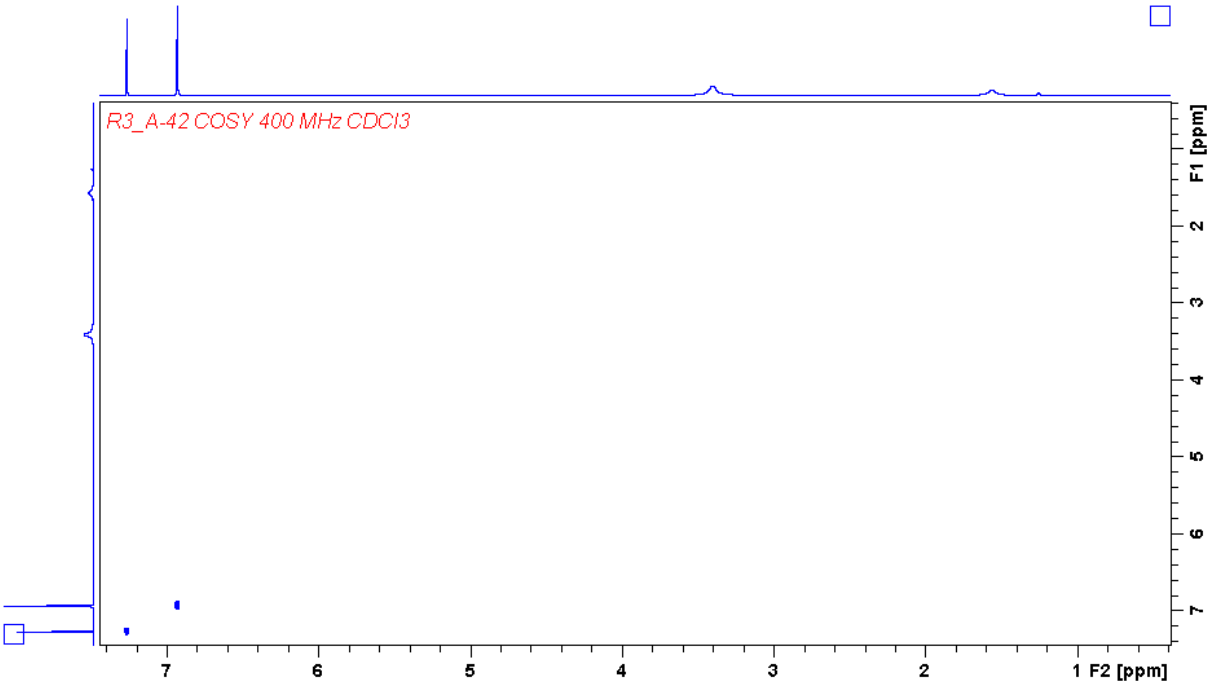


*Figure 75: $^{1}H$ - $^{1}H$ COSY (400MHz, $CDCl_3$) NMR spectrum of **3** shows no correlating peaks as expected.*

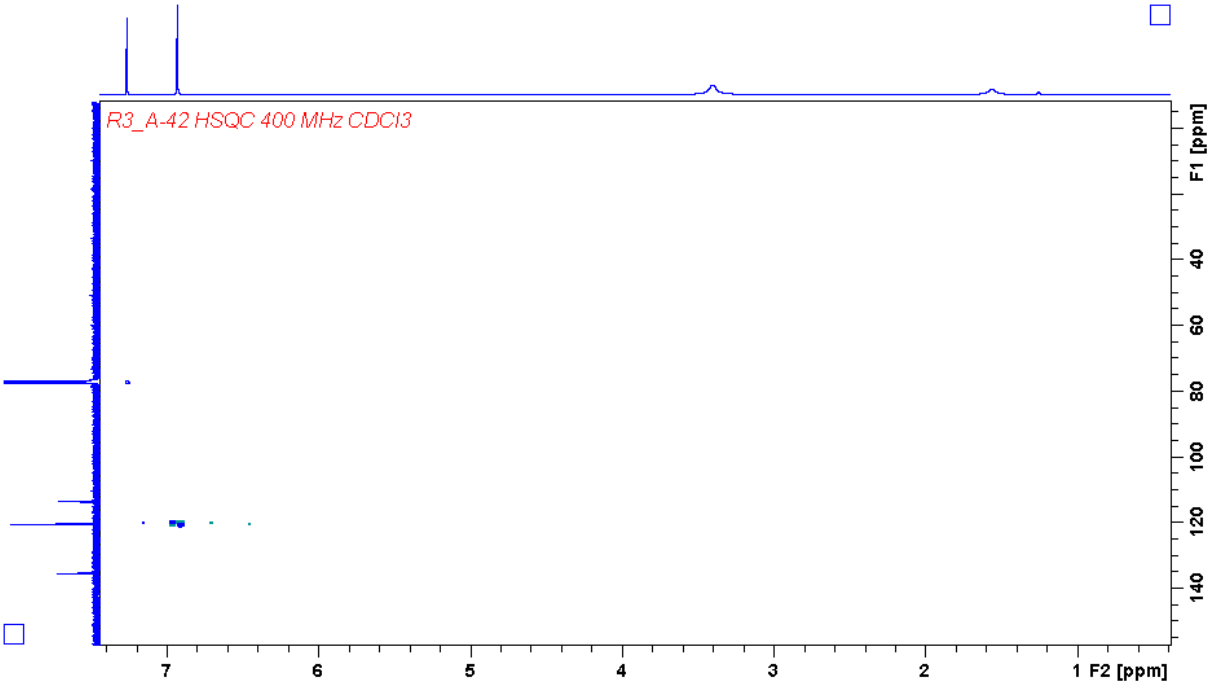


*Figure 76: $^{1}H$ – $^{13}C$ HSQC (400-101 MHz, $CDCl_3$) NMR spectrum of **3**. $^{1}H$ - $^{13}C$ correlation between 6.93 ppm $^{1}H$ peak and 120.46 ppm $^{13}C$ peak.*

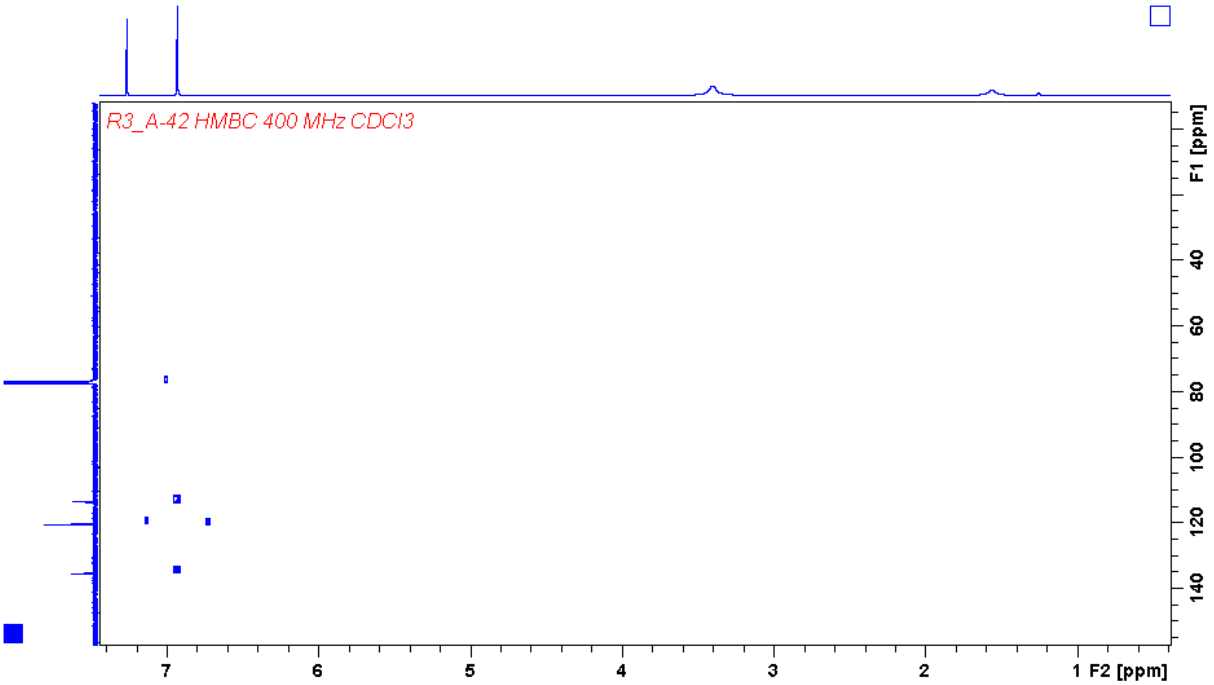


*Figure 77: $^{1}H$ – $^{13}C$ HMBC (400-101 MHz, $CDCl_3$) spectrum of **3** shows long range couplings ($^{2}J$ - $^{4}J$) from 6.93 ppm $^{1}H$ peak to 135.35 and 113.49 13C peaks. It also shows satellite peaks for a $^{1}J$ coupling from 6.93 $^{1}H$ peak to 120.46 $^{13}C$ peak shown in the HSQC spectrum.*

## Spectra of **4**

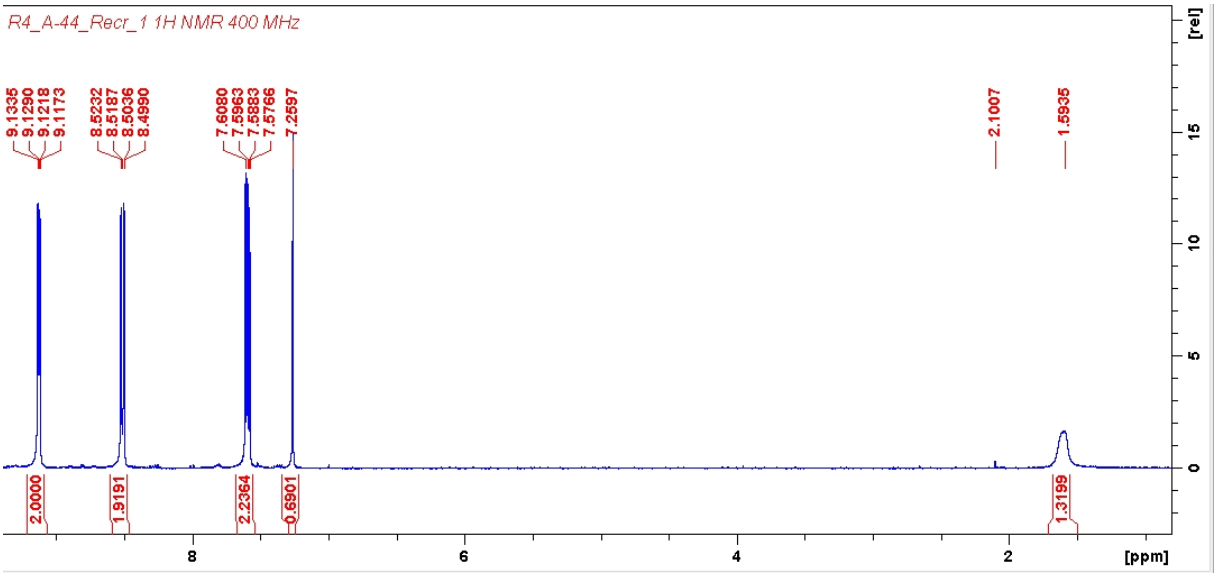


*Figure 78: $^{1}H$ NMR (400 MHz, $CDCl_3$) of **4**: ppm = 9.12 (dd, J=4.7, 1.8 Hz, 2H), 8.51 (dd, J=7.9, 1.8 Hz, 2H), 7.59 (dd, 7.9, 4.7 Hz, 2H). Some water is present at 1.59 ppm.*

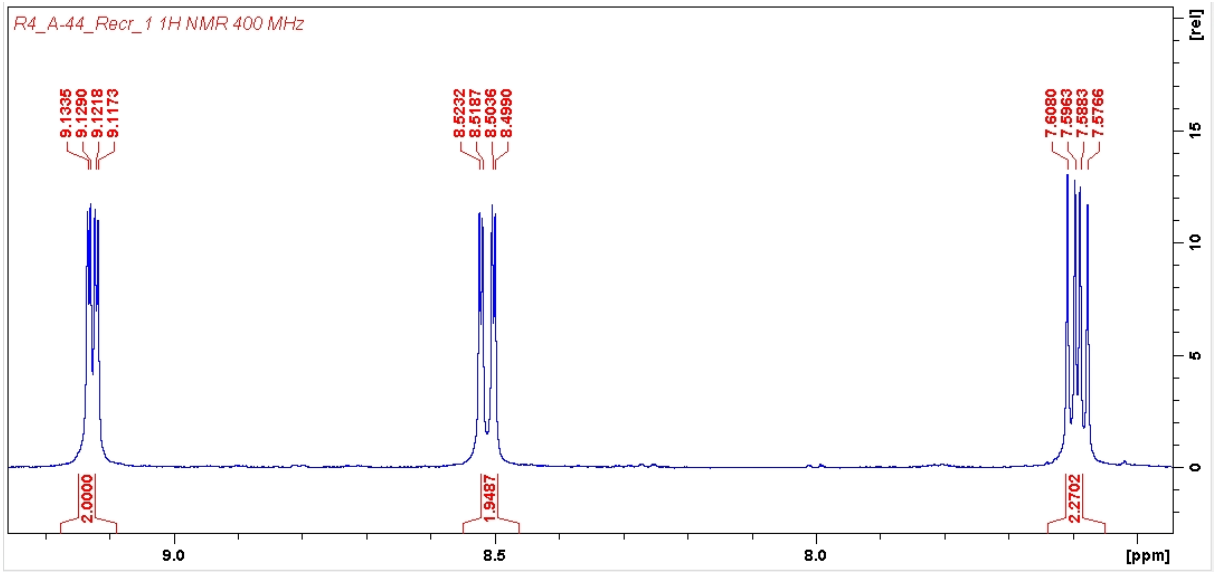


*Figure 79: $^{1}$H NMR (400 MHz, $CDCl_3$) of **4**, excerpt of region with product peaks. ppm = 9.12 (dd, J=4.7, 1.8 Hz, 2H), 8.51 (dd, J=7.9, 1.8 Hz, 2H), 7.59 (dd, 7.9, 4.7 Hz, 2H).*

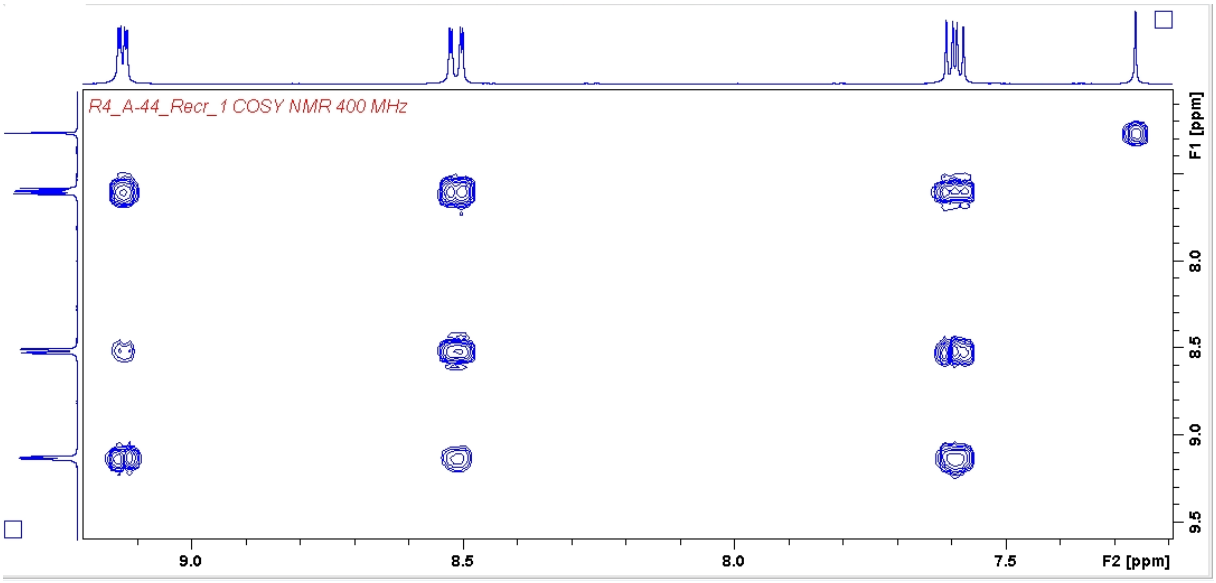


*Figure 80: COSY 2D NMR (400 MHz, $CDCl_3$) of **4**.*

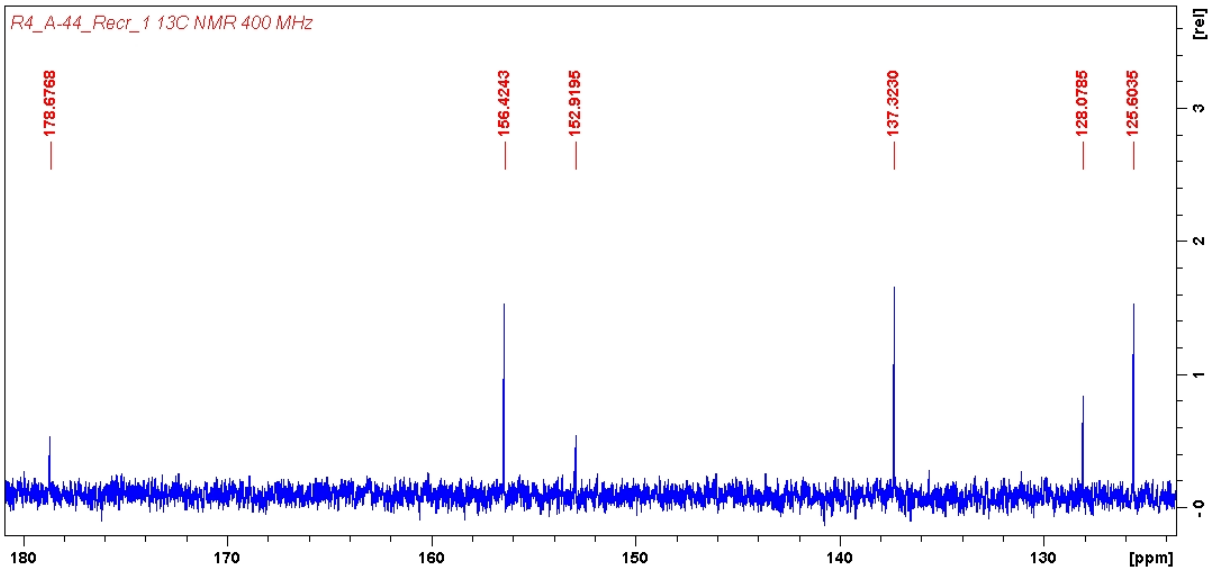


*Figure 81: $^{13}C$ NMR (101 MHz, $CDCl_3$) of **4**: ppm = 178,67, 156.42, 152.91, 137.32, 128.08.*

## Spectra of 5

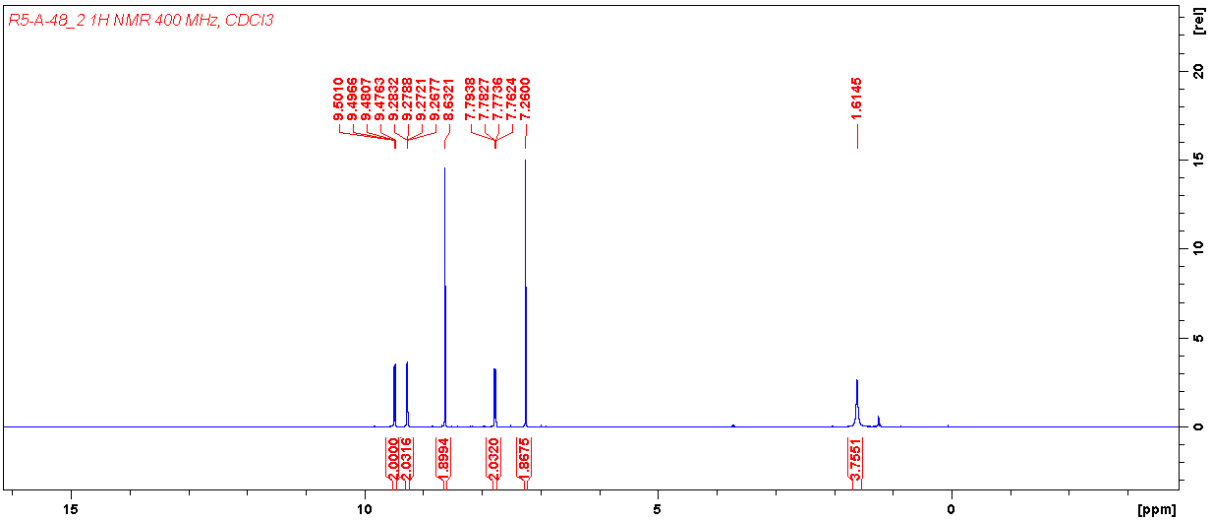


*Figure 82: $^{1}H$ NMR (400 MHz, $CDCl_3$) of **5**: ppm = 9.55 (dd, J=8.1, 1.7, 2H), 9.29 (dd, J=4.4, 1.7, 2H), 8.68 (s, 2H), 7.80 (dd, J=8.1, 4.4, 2H).*

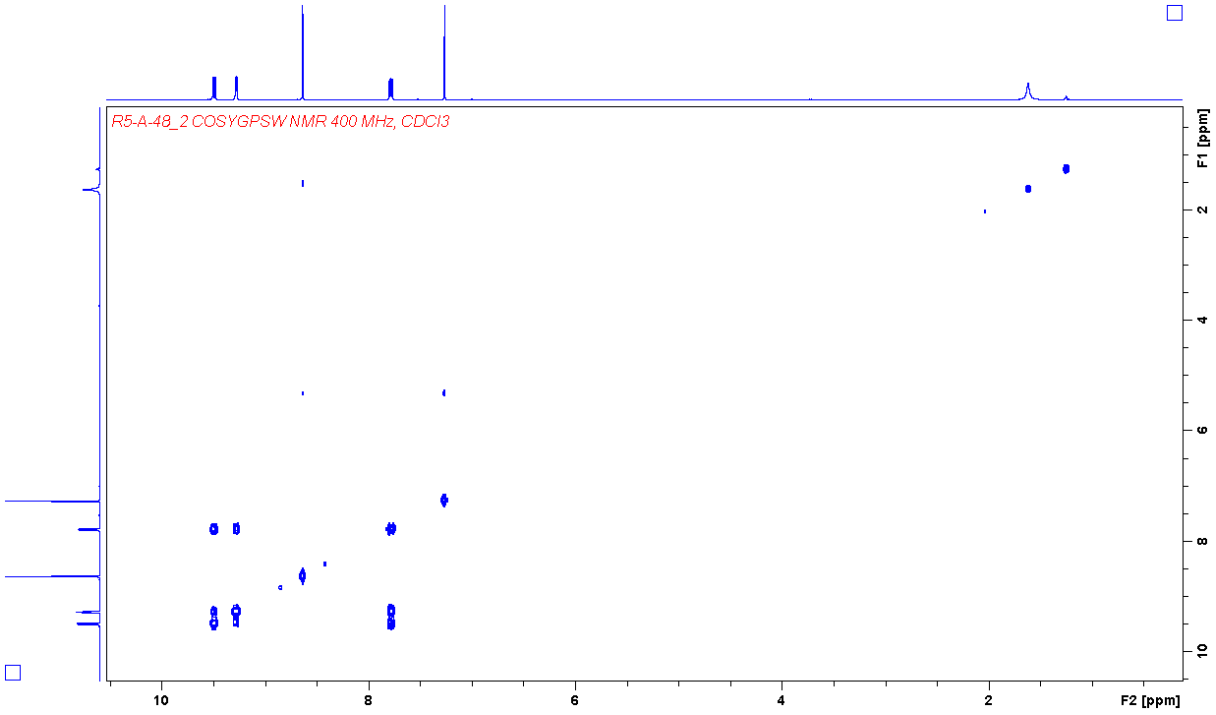


*Figure 83: $^{1}H - ^{1}H$ COSY NMR (400 MHz, $CDCl_3$) of **5**.*

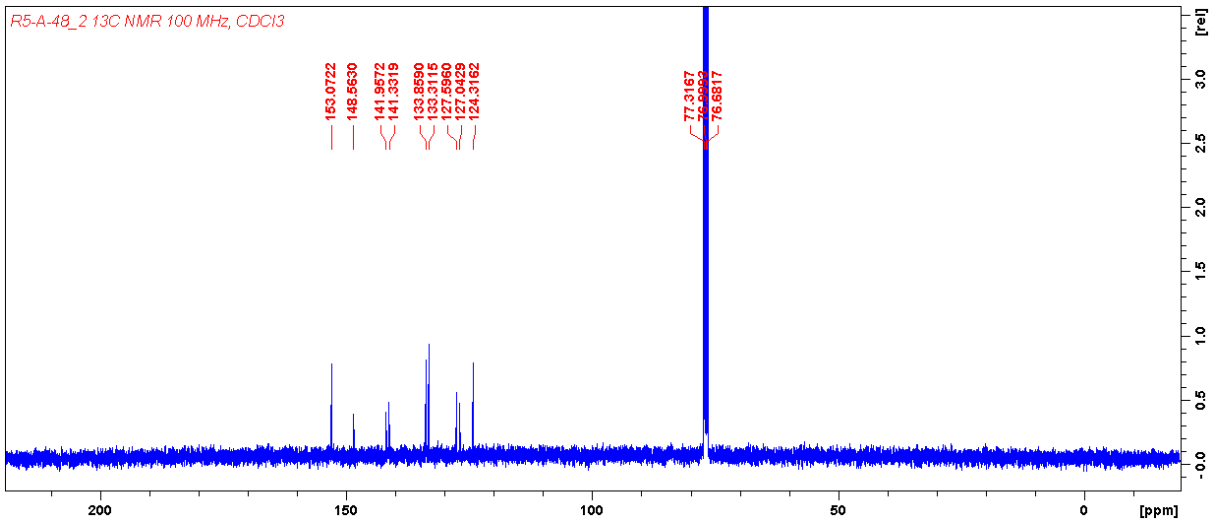


*Figure 84: $^{13}C$ NMR spectra of **5** (100 MHz, $CDCl_3$): δ 153.07, 148.56, 141.96, 141.33, 133.86, 133.31, 127.60, 127.04, 124.31.*

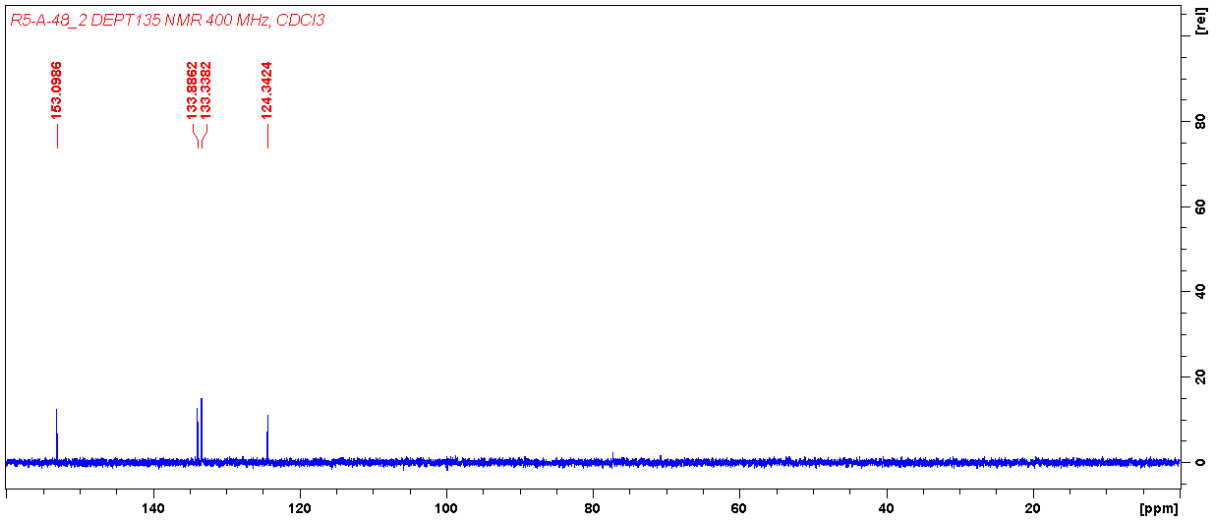


*Figure 85: $^{13}C$ DEPT135 of **5** (101 MHz, $CDCl_3$). C-H carbons: δ 153.10, 133.89, 133.34 and 124.34.*

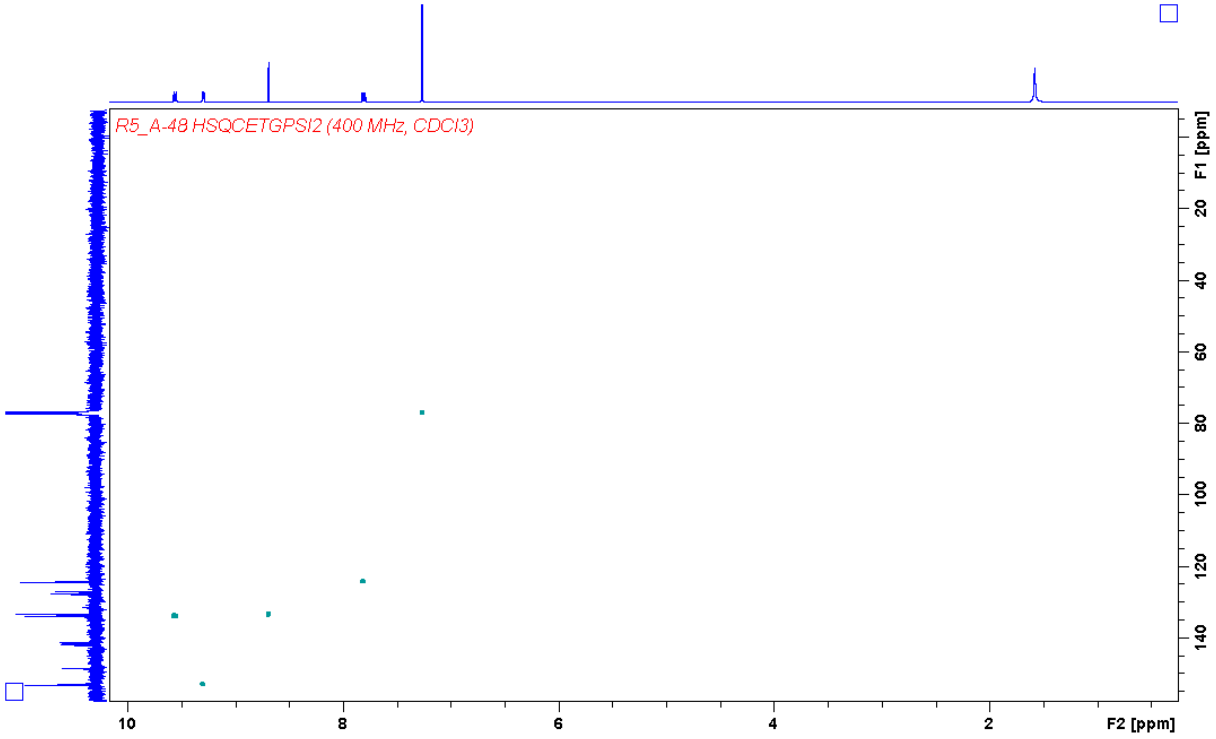


*Figure 86: $^{1}H$-$^{13}C$ HSQC (400-101 MHz, $CDCl_3$) of 5.*

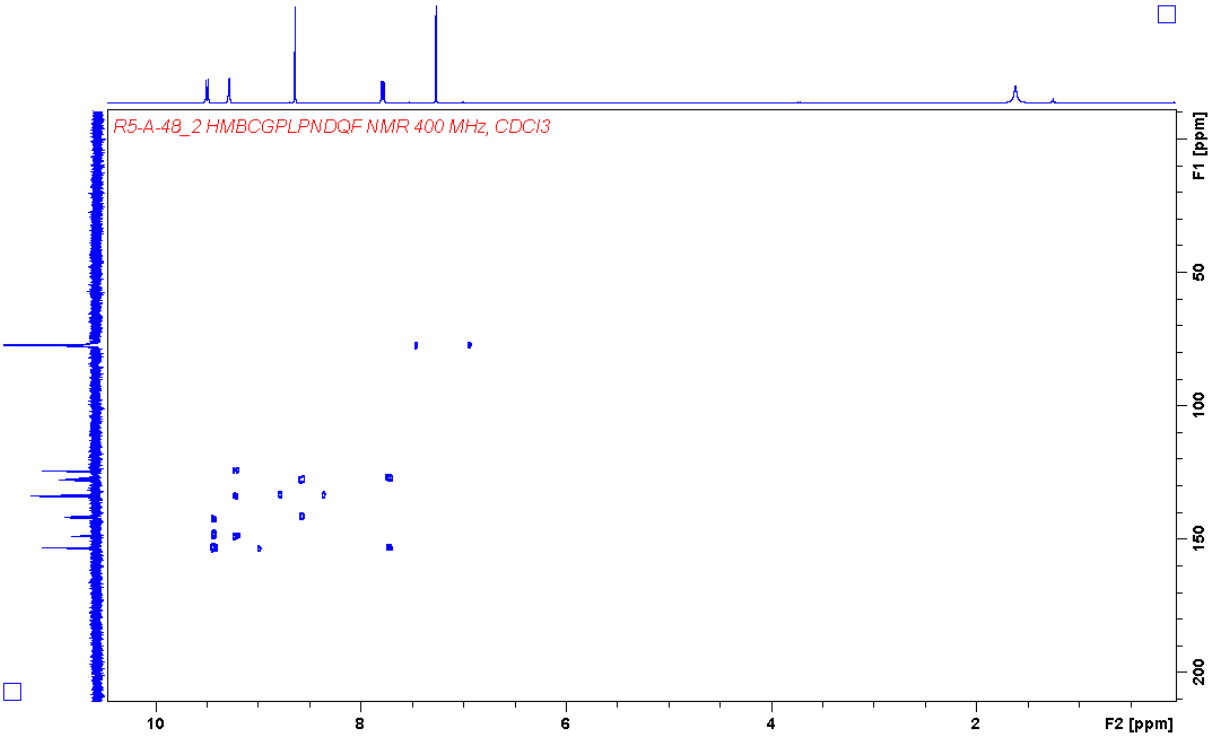


*Figure 87: $^{1}H$ – $^{13}C$ HMBC of **5** (400 MHz, $CDCl_3$).*

## Spectra of 6b

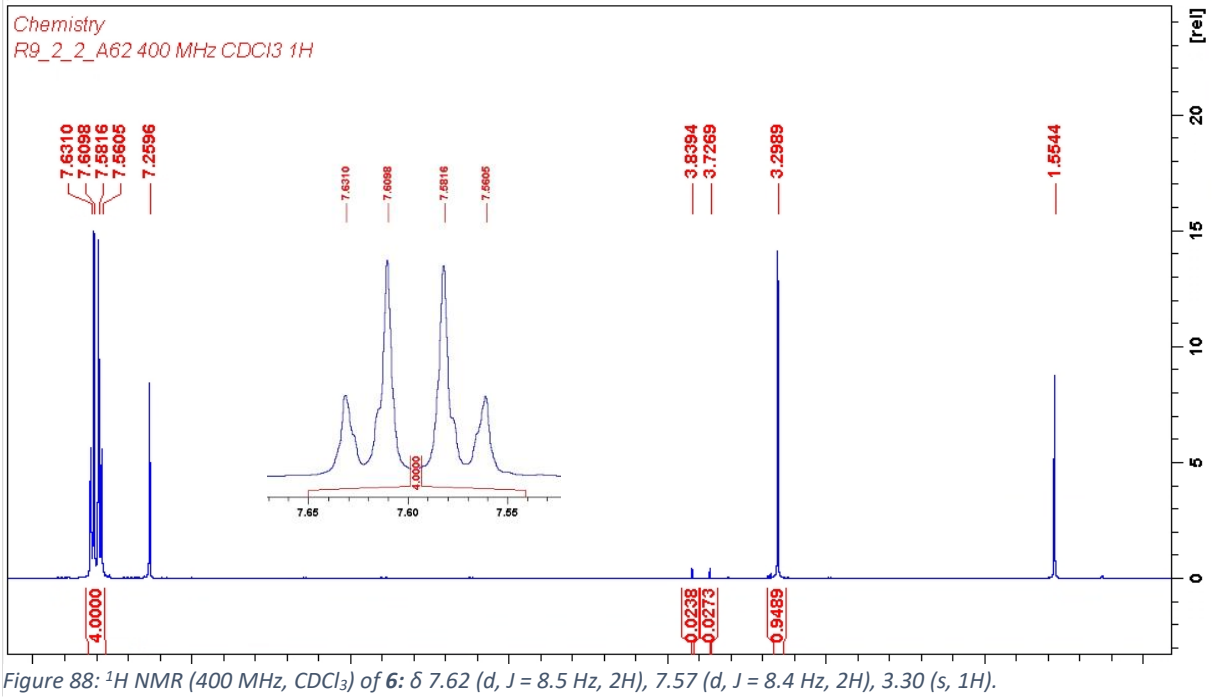


*Figure 88: $^{1}H$ NMR (400 MHz, $CDCl_3$) of **6:** δ 7.62 (d, J = 8.5 Hz, 2H), 7.57 (d, J = 8.4 Hz, 2H), 3.30 (s, 1H).*

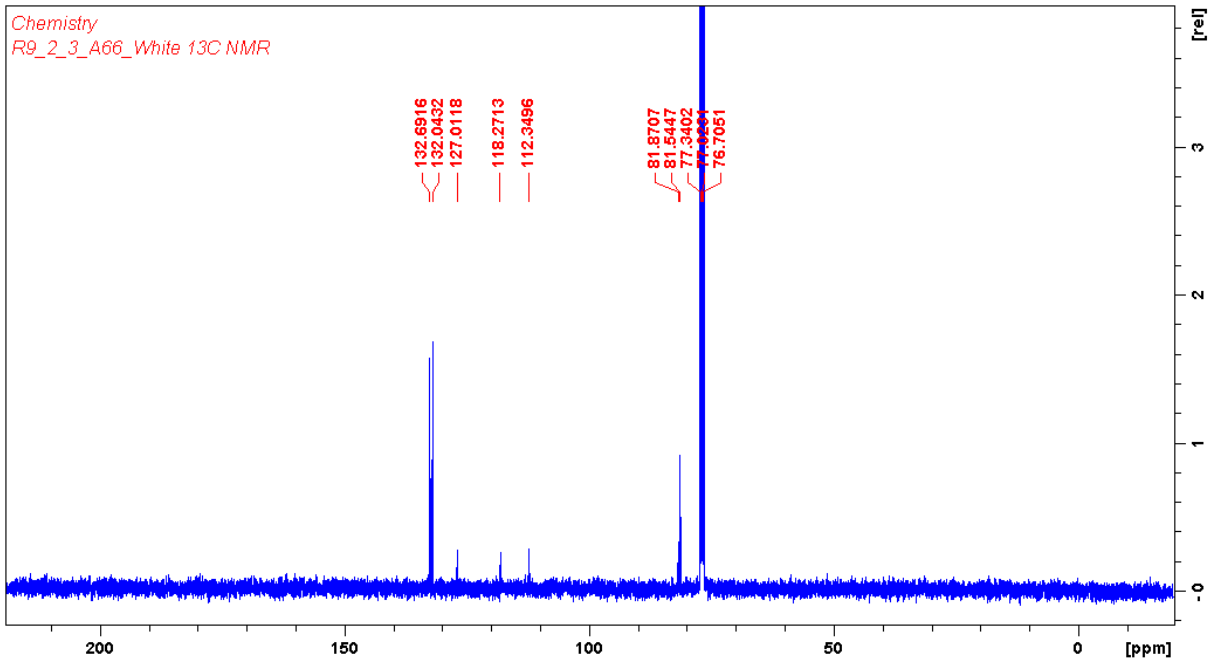


*Figure 89: $^{13}C$ NMR (101 MHz, $CDCl_3$) of **6b**.*

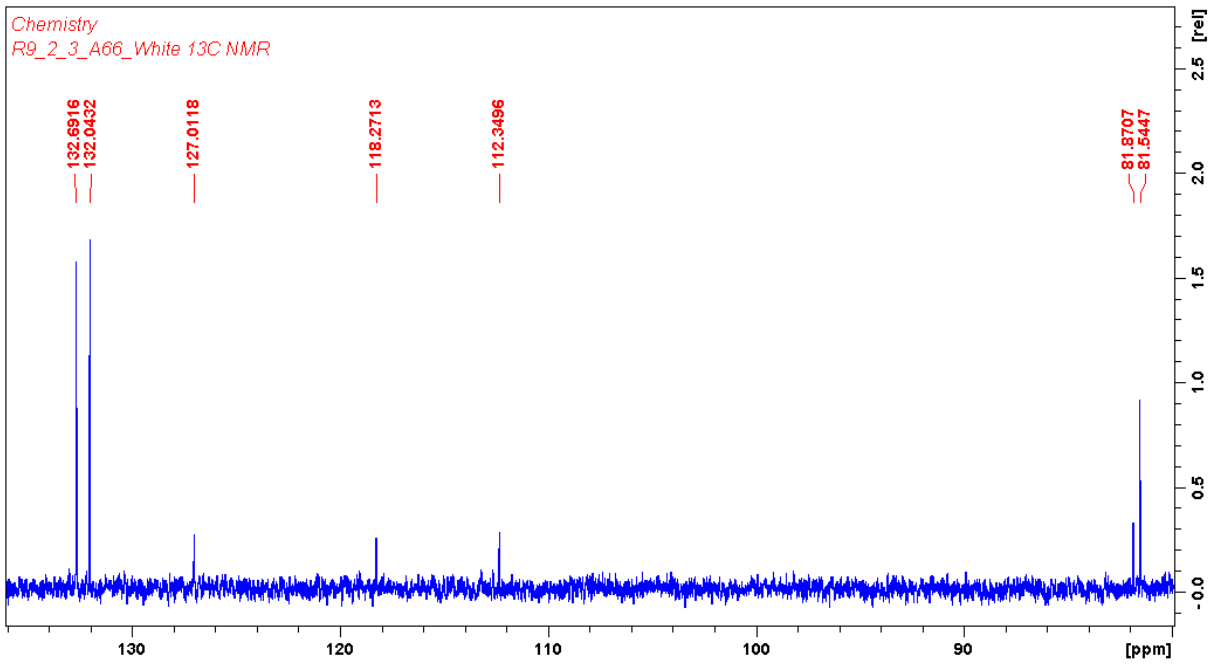


*Figure 90: $^{13}C$ NMR (101 MHz, $CDCl_3$) δ 132.69 (s, 2C), 132.04 (s, 2C), 127.01 (s, 1C), 118.27 (s, 1C), 112.35 (s, 1C), 81.87 (s, 1C), 81.55 (s, 1C).*

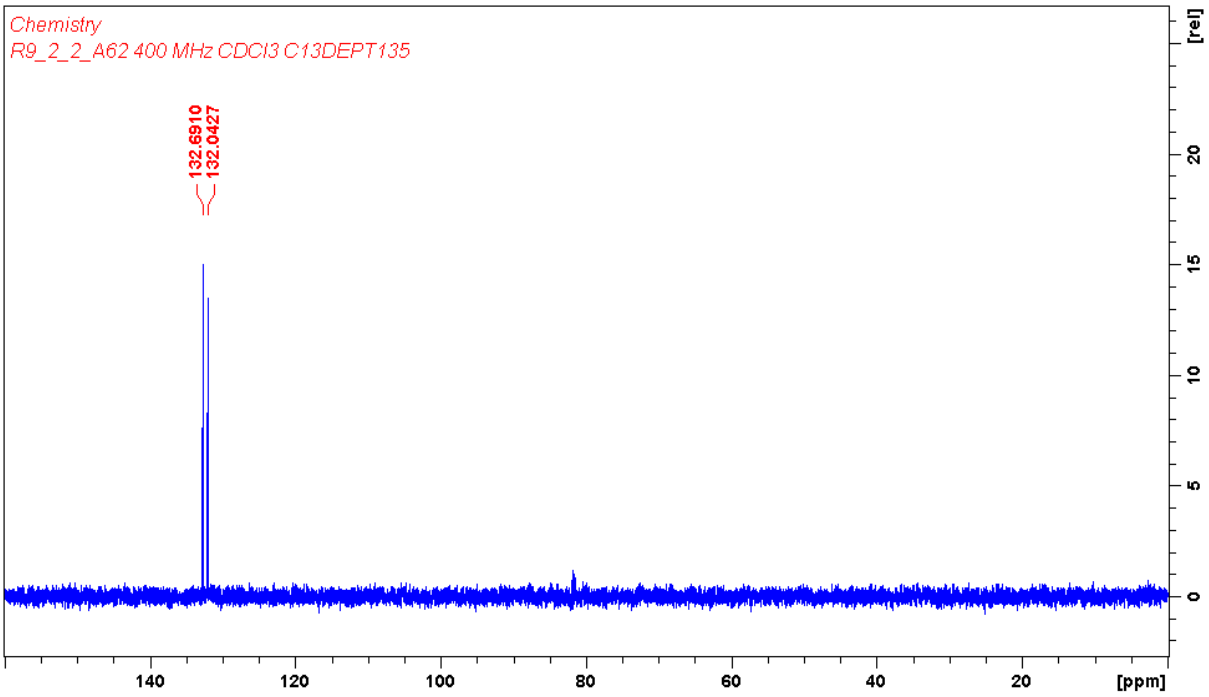


*Figure 91: $^{13}C$ DEPT135 NMR (101 MHz, $CDCl_3$) δ 132.69 (s, 2C), 132.04 (s, 2C).*

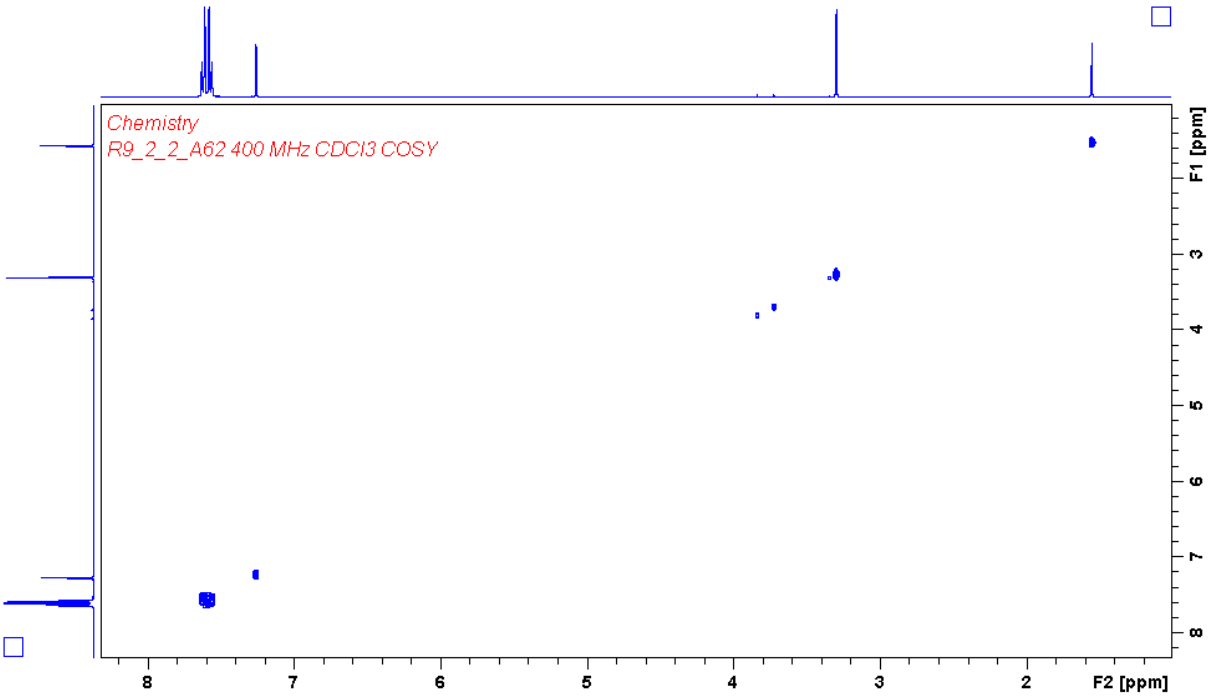


*Figure 92: $^{1}H$-$^{1}H$ COSY (400 MHz, $CDCl_3$) of **6b**.*

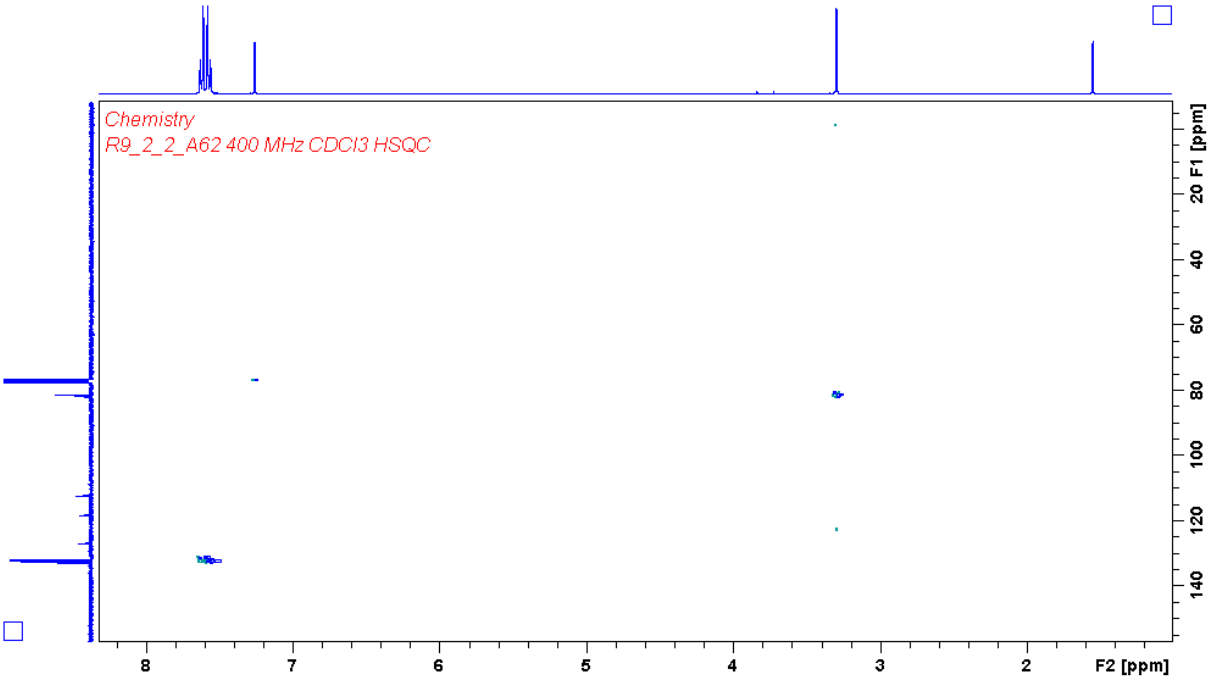


*Figure 93: $^{1}H$ - $^{13}C$ HSQC (400 – 101 MHz, CDCl3) of **6b**.*

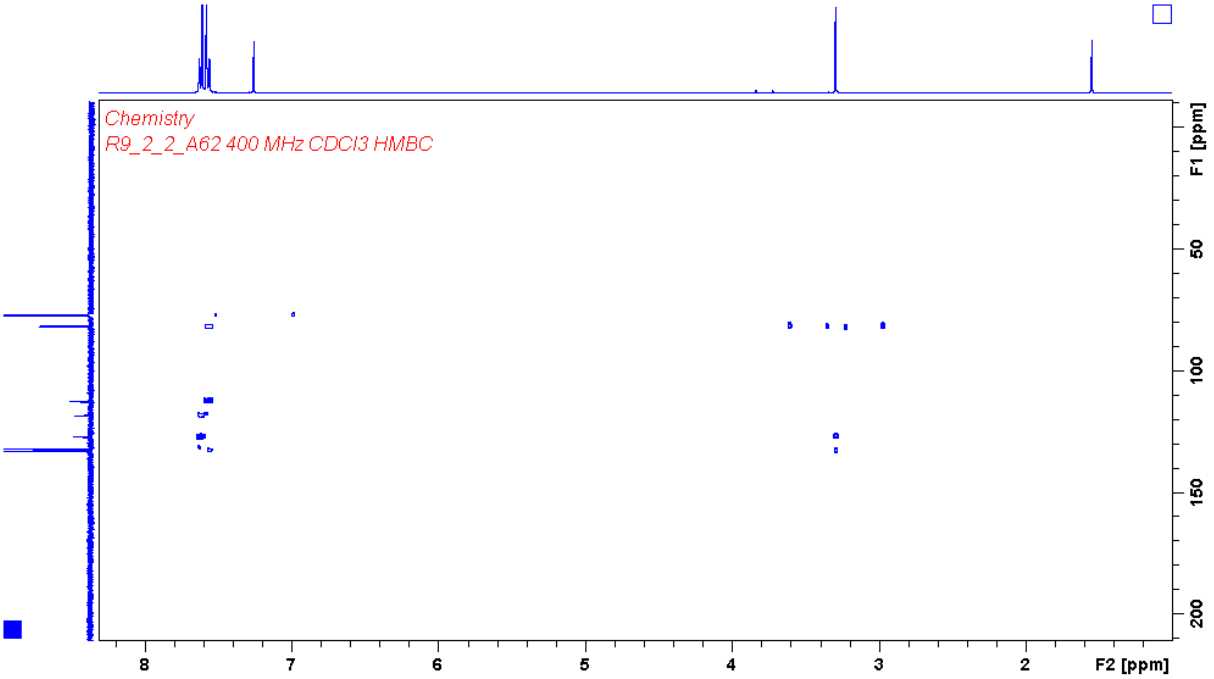


*Figure 94: $^{1}H$ – $^{13}C$ HMBC (400 – 101 MHz, CDCl3) of **6b**.*

## Spectra of 7

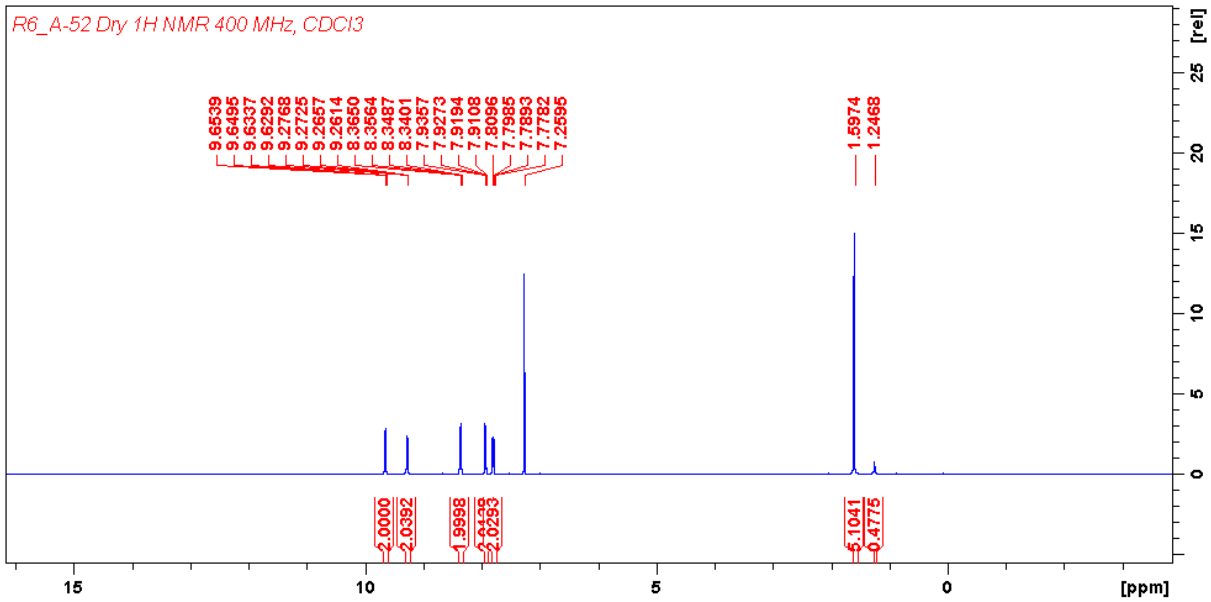


*Figure 95: $^{1}$H NMR (400 MHz, $CDCl_3$) of **7**. δ 9.64 (dd, J = 1.8, 8.1 Hz, 2H), 9.27 (dd, J = 1.7, 4.4 Hz, 2H), 8.35 (dd, J = 3.4, 6.5 Hz, 2H), 7.92 (dd, J = 3.4, 6.6 Hz, 2H), 7.79 (dd, J = 4.4, 8.1 Hz, 2H).*

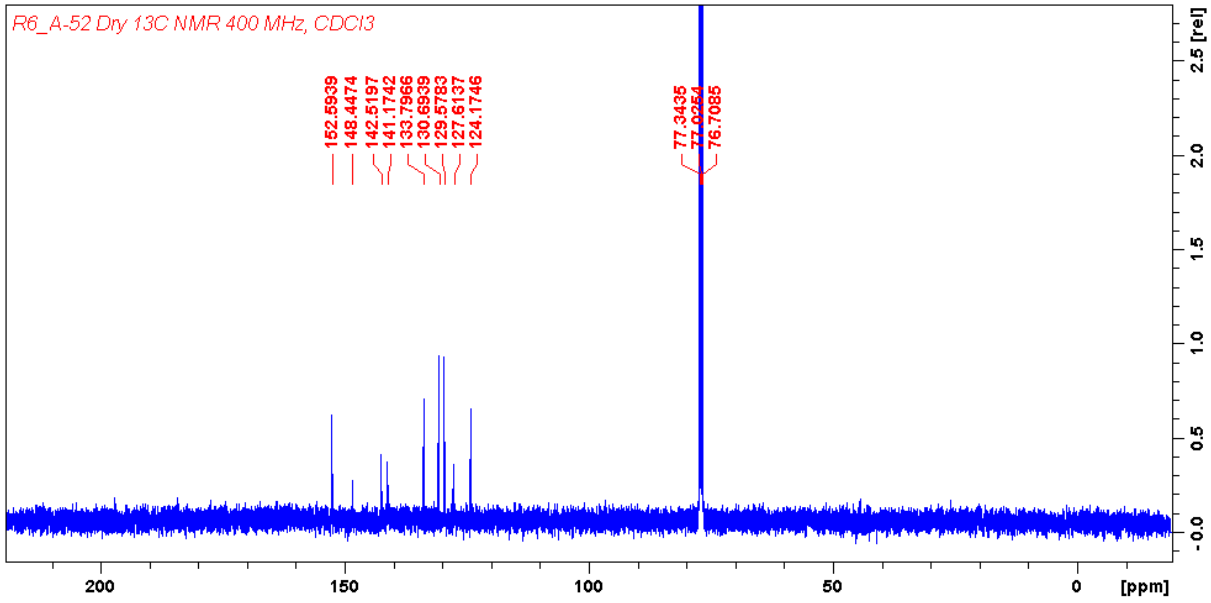


*Figure 96: $^{13}$C NMR (101 MHz, $CDCl_3$) δ 152.59, 148.45, 142.52, 141.17, 133.80, 130.69, 129.58, 127.61, 124.17.*

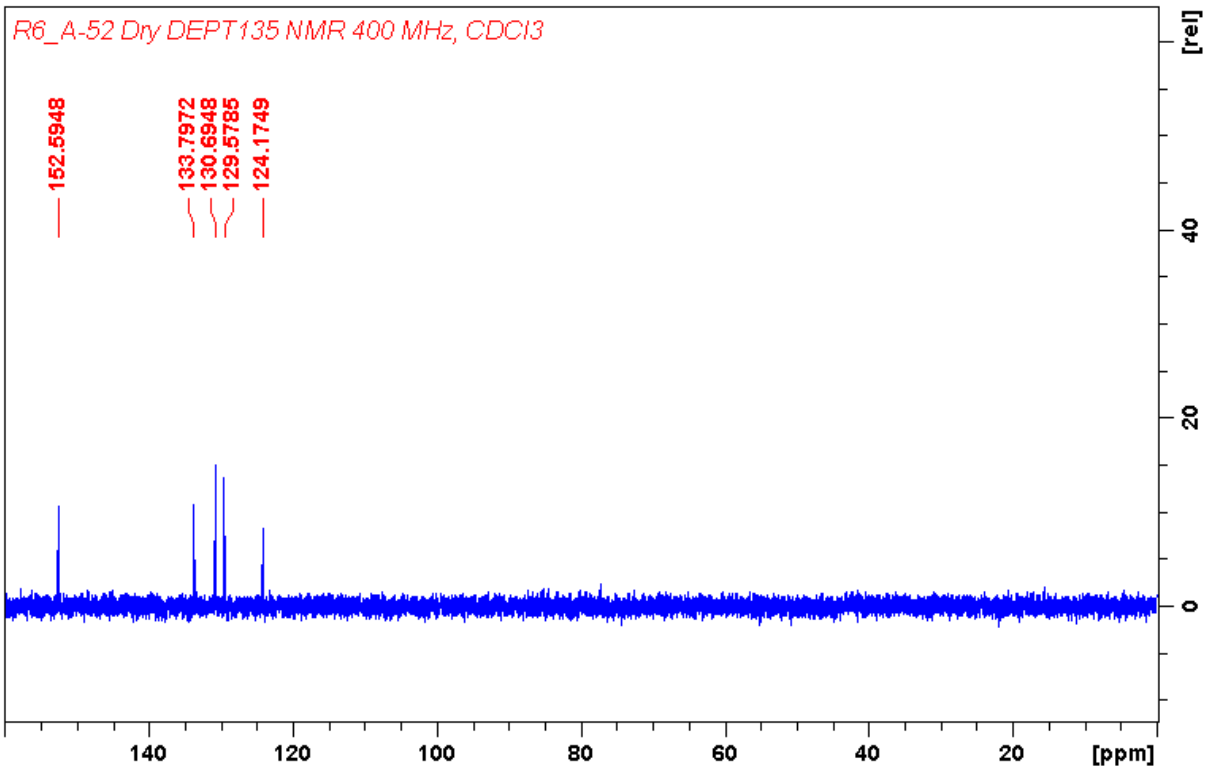


*Figure 97: Figure 48: 13C DEPT135 NMR (101 MHz, CDCl3) δ 152.59, 133.80, 130.69, 129.58, 124.17.*

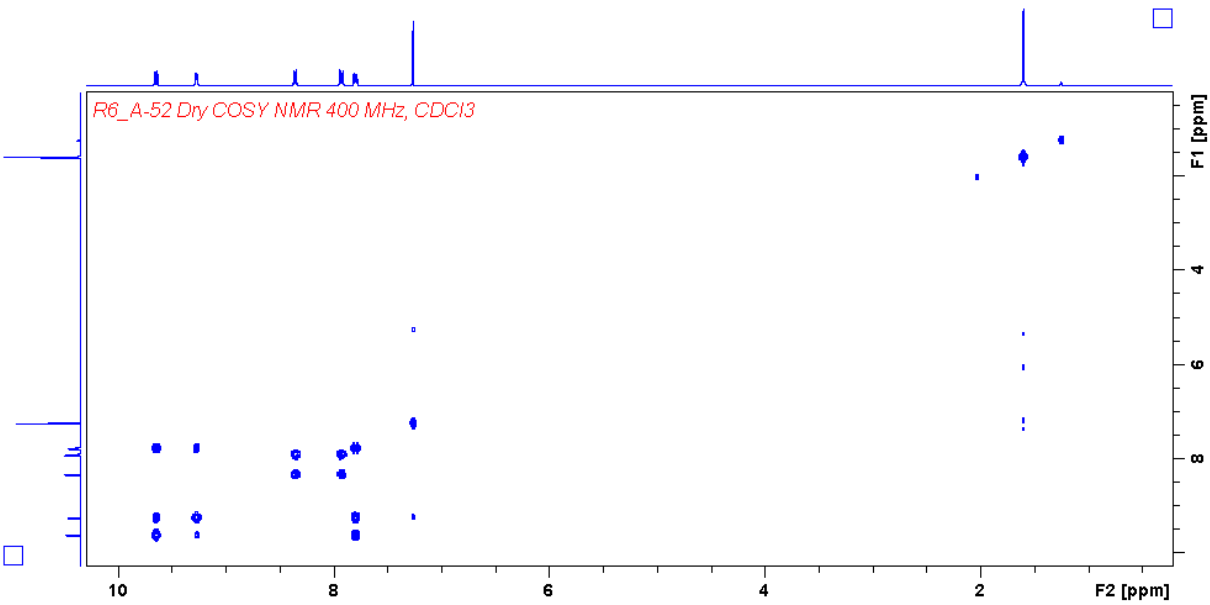


*Figure 98: $^{1}H$ - $^{1}H$ COSY (400 MHz, CDCl3) spectrum of **7**.*

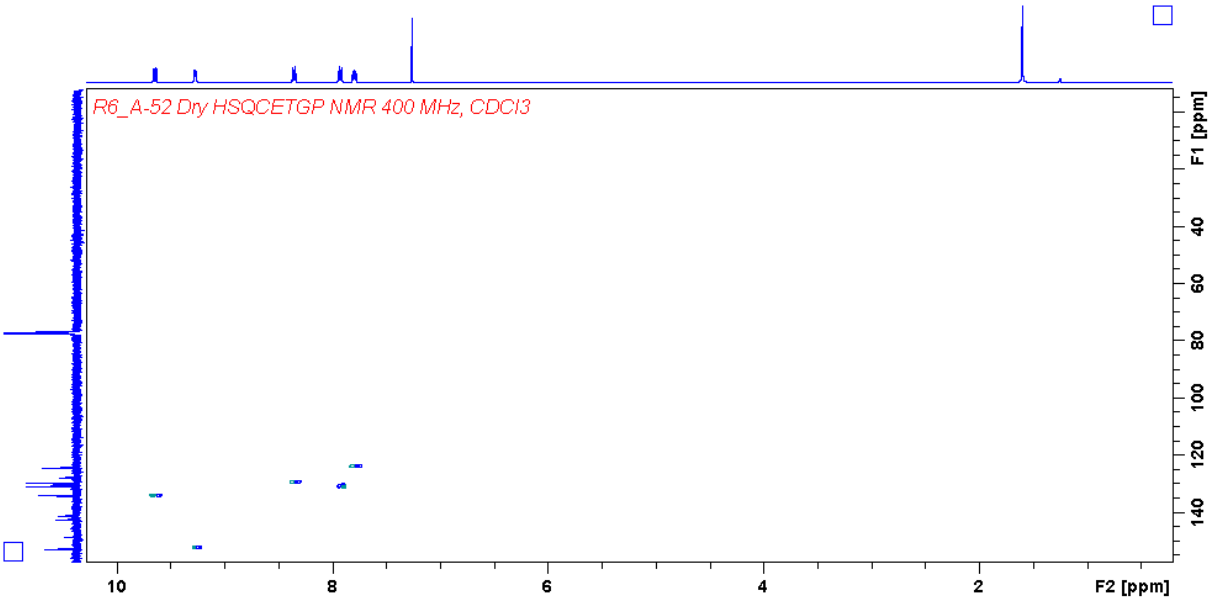


*Figure 99: $^{1}H$ - $^{13}C$ HSQC (400/101 MHz, $CDCl_3$) spectrum of **7**.*

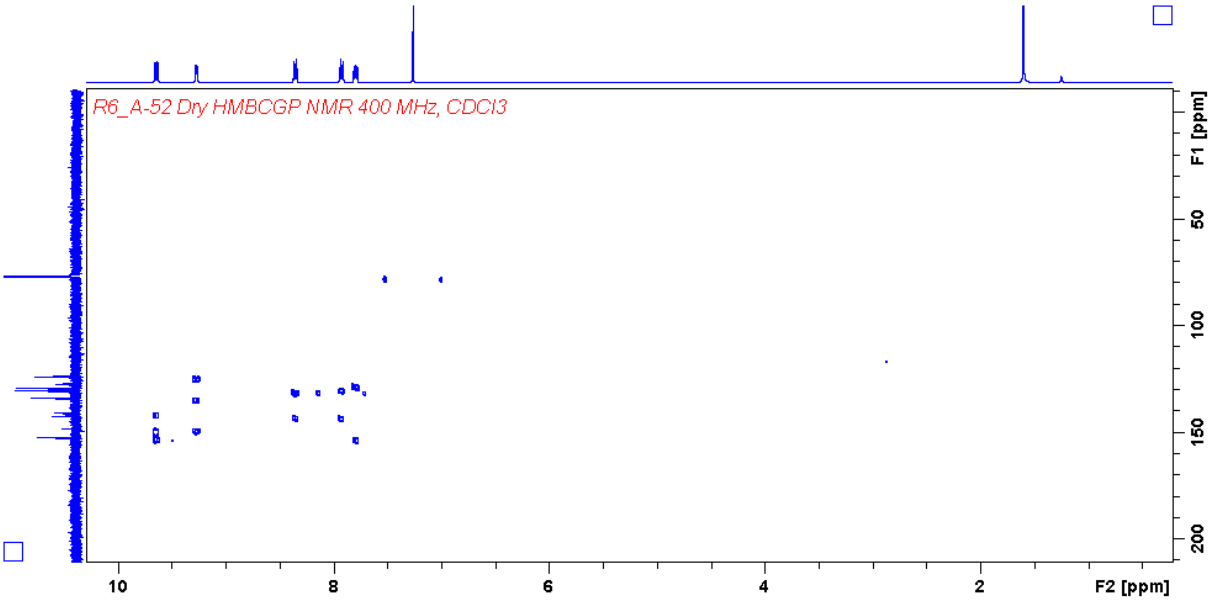


*Figure 100: $^{1}H$ - $^{13}C$ HMBC (400/101 MHz, $CDCl_3$) spectrum of **7**.*

## Spectrum of crude from reaction to synthesize 8

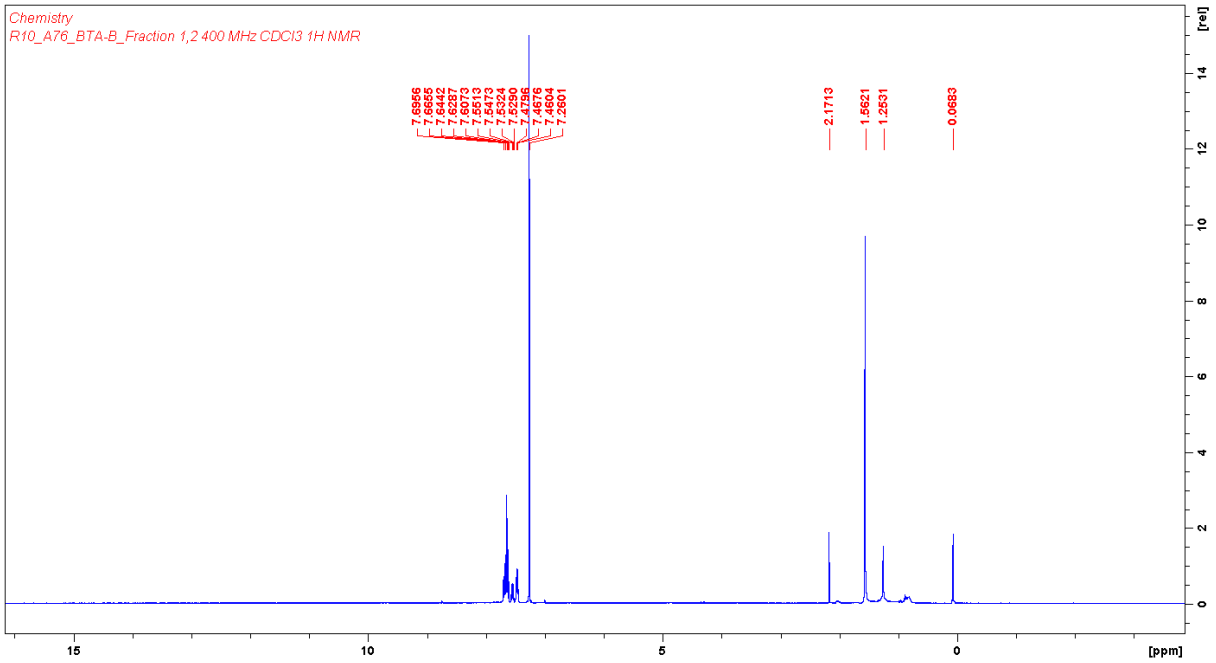


*Figure 101: $^1$H NMR (400 MHz, $CDCl_3$) of crude from reaction for synthesize **8**.*

# 5. Bibliography


1. Tucker, J.W. and C.R.J. Stephenson, *Shining Light on Photoredox Catalysis: Theory and Synthetic Applications.* The Journal of Organic Chemistry, 2012. **77**(4): p. 1617-1622.
2. Sun, Y., et al., *Effect of Ligands with Extended π-System on the Photophysical Properties of Ru(II) Complexes.* The Journal of Physical Chemistry B, 2010. **114**(45): p. 14664-14670.
3. Shimizu, A., et al., *HOMO–LUMO Energy-Gap Tuning of π-Conjugated Zwitterions Composed of Electron-Donating Anion and Electron-Accepting Cation.* The Journal of Organic Chemistry, 2021. **86**(1): p. 770-781.
4. Thoresen, E.M., et al., *Strongly visible light-absorbing metal–organic frameworks functionalized by cyclometalated ruthenium(ii) complexes.* RSC Advances, 2020. **10**(15): p. 9052-9062.
5. Wilkinson., A.D.M.a.A., *IUPAC Compendium of Chemical Terminology, 2nd ed. (the "Gold Book").* . 1997, Blackwell Scientific Publications, Oxford (1997). : Online version (2019-) created by S. J. Chalk.
6. Wang, Y., et al., *Construction of Robust Iridium(III) Complex-Based Photosensitizer for Boosting Hydrogen Evolution.* Inorganic Chemistry, 2023. **62**(19): p. 7212-7219.
7. Thoresen, E.M., et al., *Cyclometalated ruthenium complexes with carboxylated ligands from a combined experimental/computational perspective.* Dalton Transactions, 2018. **47**(8): p. 2589-2601.
8. Machuca, A., et al., *Rhodium Nanoparticles as a Novel Photosensitizing Agent in Photodynamic Therapy against Cancer.* Chemistry – A European Journal, 2020. **26**(34): p. 7685-7691.
9. Hao, S., et al., *Natural dyes as photosensitizers for dye-sensitized solar cell.* Solar Energy, 2006. **80**(2): p. 209-214.
10. Takeda, H., et al., *Development of Visible-Light Driven Cu(I) Complex Photosensitizers for Photocatalytic CO(2) Reduction.* Front Chem, 2019. **7**: p. 418.
11. Zhang, Y., et al., *Visible-light-mediated copper photocatalysis for organic syntheses.* Beilstein Journal of Organic Chemistry, 2021. **17**: p. 2520-2542.
12. LibreTexts. *6.1: Structures of Metal Complexes*. Inorganic Chemistry (Saito) 2023 Jun 16, 2023]; Available from: https://chem.libretexts.org/@go/page/125406.

13. LibreTexts. *1.19: Electron Counting and the 18 Electron Rule*. Advanced Inorganic Chemistry (Wikibook) 2023; Available from: https://chem.libretexts.org/@go/page/204720.
14. Atkins, P. and J. de Paula, *Physical Chemistry (WH Freeman 2006)*. ISBN 0-7167-8759-8. p. 494.
15. Wang, C., et al., *Increasing the triplet lifetime and extending the ground-state absorption of biscyclometalated Ir(<scp>iii</scp>) complexes for reverse saturable absorption and photodynamic therapy applications.* Dalton Transactions, 2016. **45**(41): p. 16366-16378.
16. McMurry, J., *Organic Chemistry*. 2012, Brooks/Cole Cengage Learning.
17. Reutenauer, L. *DEPT C-13 NMR Spectroscopy*. 2023 June 19, 2023]; Available from: https://chem.libretexts.org/@go/page/432205.
18. Claridge, T.D.W., *Chapter 6 - Correlations Through the Chemical Bond I: Homonuclear Shift Correlation*, in *High-Resolution NMR Techniques in Organic Chemistry (Third Edition)*, T.D.W. Claridge, Editor. 2016, Elsevier: Boston. p. 203-241.
19. Claridge, T.D.W., *Chapter 7 - Correlations Through the Chemical Bond II: Heteronuclear Shift Correlation*, in *High-Resolution NMR Techniques in Organic Chemistry (Third Edition)*, T.D.W. Claridge, Editor. 2016, Elsevier: Boston.
20. Claridge, T.D.W., *Chapter 9 - Correlations Through Space: The Nuclear Overhauser Effect*, in *High-Resolution NMR Techniques in Organic Chemistry (Third Edition)*, T.D.W. Claridge, Editor. 2016, Elsevier: Boston. p. 315-380.
21. Oloyede, H.O., et al., *New cobalt coordination designs and the influence of varying chelate characters, ligand charges and incorporated group I metal ions on enzyme-like oxidative coupling activity.* New Journal of Chemistry, 2020. **44**(35): p. 14849-14858.
22. Shao, J., J. Chang, and C. Chi, *Linear and star-shaped pyrazine-containing acene dicarboximides with high electron-affinity.* Organic & Biomolecular Chemistry, 2012. **10**(35): p. 7045.
23. Pople, J.A., W.G. Schneider, and H.J. Bernstein, *THE ANALYSIS OF NUCLEAR MAGNETIC RESONANCE SPECTRA: II. TWO PAIRS OF TWO EQUIVALENT NUCLEI.* Canadian Journal of Chemistry, 1957. **35**(9): p. 1060-1072.
24. Khrustalev, D., et al., *A New Method for the Synthesis of Bromine-Containing Heterocyclic Compounds for Photovoltaic Polymers.* Eurasian Chemico-Technological Journal, 2019(1): p. 41.
25. Paw, W. and R. Eisenberg, *Synthesis, Characterization, and Spectroscopy of Dipyridocatecholate Complexes of Platinum.* Inorganic Chemistry, 1997. **36**(11): p. 2287-2293.
26. Schäfer, B., et al., *Derivatives of dipyrido[3,2-a:2′,3′-c]phenazine and its ruthenium complexes, influence of arylic substitution on photophysical properties.* Dalton Trans., 2006(18): p. 2225-2231.
27. Richardson, C. and C.A. Reed, *Synthesis of meso-Extended Tetraarylporphyrins.* The Journal of Organic Chemistry, 2007. **72**(13): p. 4750-4755.
28. Li, X., et al., *Protein Nanocages for Delivery and Release of Luminescent Ruthenium(II) Polypyridyl Complexes.* ACS Applied Materials & Interfaces, 2016. **8**(35): p. 22756-22761.
29. Van Der Salm, H., et al., *Stretching the phenazine MO in dppz: the effect of phenyl and phenyl–ethynyl groups on the photophysics of Re(i) dppz complexes.* Dalton Trans., 2014. **43**(47): p. 17775-17785.
30. Thorand, S. and N. Krause, *Improved Procedures for the Palladium-Catalyzed Coupling of Terminal Alkynes with Aryl Bromides (Sonogashira Coupling).* The Journal of Organic Chemistry, 1998. **63**(23): p. 8551-8553.
31. Kato, T., et al., *Four different types of hydrogen bonds observed in 1,2-bis(N-benzenesulfonylamino)benzenes due to conformational properties of the sulfonamide moiety.* Tetrahedron, 2006. **62**(36): p. 8458-8462.
32. AKScientific. *4,5-Dibromobenzene-1,2-diamine* 2023; CAS Number: 49764-63-8]. Available from: https://aksci.com/item_detail.php?cat=W6528.
33. Sigmaaldrich. *1,10-Phenanthroline-5,6-dione*. 2023; CAS Number: 27318-90-7]. Available from: https://www.sigmaaldrich.com/NO/en/product/aldrich/496383.

34. Sigmaaldrich. *4-Ethynylbenzonitrile*. 2023; CAS Number: 3032-92-6]. Available from: https://www.sigmaaldrich.com/.
35. FischerScientific. *Dipyrido[3,2-a:2',3'-c]phenazine*. 2023 jun 16, 2023]; CAS 19535-47-8]. Available from: https://www.fishersci.com/shop/products/dipyrido-3-2-a-2-3-c-phenazine-tci-america-2/D4379200MG.